Alma Mater Studiorum – Università di Bologna

DOTTORATO DI RICERCA

COLTURE ARBOREE ED AGROSISTEMI FORESTALI ORNAMENTALI E PAESAGGISTICI

Ciclo XX

Settore/i scientifico disciplinari di afferenza: *AGR 03*

TITOLO TESI

LIGHT ENERGY MANAGEMENT IN PEACH: UTILIZATION, PHOTOPROTECTION, PHOTODAMAGE AND RECOVERY. MAXIMIZING LIGHT ABSORPTION IN ORCHARD IS NOT ALWAYS THE BEST SOLUTION

Presentata da: **dott. PASQUALE LOSCIALE**

Coordinatore Dottorato
Chiar.mo prof. SILVIERO SANSAVINI

Relatore
Chiar.mo prof. LUCA CORELLI GRAPPADELLI

Esame finale anno 2008

TABLE OF CONTENTS

Chapter I

LITERATURE REVIEW

The energetic basis of orchard productivity lies in the interaction between the tree and sunlight. The light intercepted by a plant is linearly related to the amount of dry matter it produces (Monteith, 1977; Lakso, 1994). This concept drew the evolution of the new, intensive orchard planting systems (Corelli Grappadelli and Lakso, 2007). The goal is to cover as soon as possible the ground with a photosynthetic surface in order to increase light interception while maintaining good light distribution, for improving productivity (Palmer, 1980). Orchard light interception is related to 2 main factors: light intensity and planting density. Hypothetically, the same orchard light interception could be reached decreasing the number of trees and increasing irradiance, with an attending change in orchard yield, which was not always detected in orchard efficiency studies. For example, no differences in orchard yield were recorded in the peach cv Ross trained as Cordon and Kearney Agricultural Center Perpendicular V (KAC-V) at 1196 trees per hectare each, even though the Cordon training system intercepted more light than the KAC-V (Grossman and DeJong, 1998). At the single tree level, the Open vase (299 pt ha^{-1}), Cordon and KAC-V training systems had similar crop efficiency (expressed as fruit dry weight on trunk diameter), even if the Open vase intercepted less light than the KAC-V and the Cordon, respectively (Grossman and DeJong, 1998).

Plants are unable to use more than 5-10% of the total absorbed energy for net carboxylation (Long et al.,1994), which is not very much, while the remaining amount is used by alternative mechanisms or lost via light reflection and transmission. Therefore, small changes in carboxylation

efficiency and phtosyntate allocation could modify the primary net and commercial plant productivity (Flore and Lakso, 1988). For this reason the relationship between plant photosynthetic performance and the environmental parameters arouses great interest among scientists.

Photosynthetic Photon Flux Density (PPFD) is the fuel for the electron transport generating ATP and reducing power used in the Calvin-Benson cycle for carboxylation. Leaf net photosynthesis increases with PPFD until no improvement is found for increasing light irradiance (Bohing and Burnside, 1956). The light intensity above which the response become flat is called the saturation point. This could be different for plant species, plant nutritional and water status, light growth environment and leaf age (Kappel and Flore, 1983; Gaudillere and Moing, 1992; Escalona et al., 1999; Iacono and Sommer, 1999; Cheng et al., 2000; Cheng et al., 2001; Greer, 2001; Greer and Halligan, 2001). In several parts of the world, under clear sky the PPFD reaches commonly 2000 μmol $m^{-2}s^{-1}$ or above (Nobel, 1983), and about 50% of the incoming light is enough for reaching the saturating point in most plant species (Lakso, 1994). On the other hand, about half of the available light may be in excess(Corelli Grappadelli and Lakso, 2007). Plants can't avoid to intercept the excessive photon pressure, thus Photosystems are over excited and may be subjected to photoinhibition risks. These could be further improved by contingent thermal, water and nutritional stresses (Powels, 1984; Miller et al., 1995; Evans, 1996; Lee et al., 1999; Baker and Rosenqvist, 2004).

1.1. THE PHOTOINIBITION PROCESS

Photoinhibition could be defined as the loss of photosystem ability to evolve oxygen accomplished by the formation of Reactive oxygen Species (ROS) at a critical level due to the plant inability to use all the incoming absorbed energy. ROS development occurs at the level of the PSII light

harvesting complex (LHCII) and the PSII and PSI core complex (Niyogi, 1999). In PSII (LHCII and core complex), a higher life time of chlorophyll (Chl) in the excited state drives ROS formation. In normal conditions a chlorophyll molecule is excited by a photon of wavelength between 400-700 nm. One of the external electrons is shifted to a more energetic orbital. chlorophyll passes from the fundamental state to the first or second excited singlet estate (^{1}Chl or ^{2}Chl) depending on whether the photon has wavelength of 700 or 400 nm, respectively (Fig. 1). ^{2}Chl however decades to first singlet estate quenching its absorbed energy as heat (Sauer, 1975). ^{1}Chl is very unstable, therefore its life time is quite short and it returns to the fundamental state while it gives off its energy to the contiguous chlorophylls evolving in ^{1}Chl. With this mechanism light energy is channeled through the light harvesting complex to P_{680}, a special chlorophyll molecule in the PSII core complex. When P_{680} is excited, one of its electrons is transferred to pheophytin (Ph), with ensuing charge separation (P_{680}^+/Ph^-). The electron transport across the Z-scheme is thus triggered, leading to ATP synthesis and reducing power production (Blankenship and Prince, 1985). In conditions of excessive light, or generally when the energetic and electronic transport rate is slower than the incoming photon pressure, chlorophylls (included P_{680}) are over-reduced and not available to receive more energy or electrons (Foyer e Harbinson, 1994). ^{1}Chl, being unstable, decades to a lower energy state: the excited triplet state (^{3}Chl). ^{3}Chl life time is longer than ^{1}Chl; therefore it can react with oxygen forming the first dangerous reactive oxygen species, the singlet oxygen ($^1O_2$). This molecule is a strong oxidizer, capable of reacting with all the present molecules, destroying them (Aro et al., 1993; Ohad et al., 1994; Anderson and Barber, 1996). Some research reported that the first dangerous reactive species is P_{680}^+. In intact PSII, the core complex seems to be sealed and oxygen could not react with $^3P_{680}$ (Anderson, 2001). The P_{680}^+ molecule is the most powerful oxidant agent in photosynthesis, thus could it substitute the $^1O_2$ and drain electrons from contiguous molecules.

P_{680}^{+} could trigger radical formation breaking the oxygen proof structure (Anderson, 1999; Anderson and Chow, 2002). After this event, the reaction between $^{3}P_{680}$ and singlet oxygen is allowed. The hypothesis that the first dangerous oxidant molecule could be the P_{680}^{+} was sustained by several experiments where damage was shown despite the anaerobic conditions (Park et al., 1997). Singlet oxygen species were not found in LHCI since the ^{1}Chl life time is very short, furthermore in the PSI core complex $^{1}P_{700}$ returns to the fundamental state, dissipating the energy as heat rather than turning into excited triplet (Dau, 1994; Owens, 1996; Barth et al., 2001). In PSI, ROS production is promoted by the ability of ferredoxin to give electrons alternatively to $NADP^{+}$ or to oxygen. When the $NADP^{+}$ regeneration rate is not able to cope with the photon exposure ferredoxin gives electrons to oxygen producing the Superoxide ion (O_2^{-}) according to the Meheler reaction (Asada, 1999). Photo-oxidative damage depends on ROS formation sites. In LHCII, antennae pigments and thylakoidal proteins are oxidized (Knox and Dodge, 1985), while in the core complex the reaction centre proteins are the first to be compromised and the D1 protein seems to be the preferential target for photodamage. In severe photoinhibition conditions even the lipids are oxidized and complete inactivation of the reaction centre occurs (Barber and Anderson, 1992; Aro et al., 1993). In PSI the reactive oxygen species excess promotes damage to the Fe-S centres and the inactivation of several enzymes. Photo-damage at PSI level was mainly recorded at low temperature when the enzymatic activities decrease and the electron transport becomes lower than the incoming photon pressure (Kaiser, 1979). Finally the free iron derived by altered proteins could interact with ROS forming the Fe-O radicals, highly dangerous for Rubisco (Halliwell and Gutteridge, 1984). The direct consequence of photo-oxidation can be the reduction of photosynthetic performance (Ort, 2001). In *Vitis berlandieri* Planch. leaves, the D1 amount and net photosynthesis decreased when irradiance of 1900 μmol $m^{-2}s^{-1}$ was imposed for 60 minutes. Photosystems were completely repaired after 60

minutes in the dark (Bertamini and Nedunchezhian, 2004). In grapefruit (*Citrus paradisi* L.) reducing the incoming irradiance by spraying kaolin on leaves increased net photosynthesis while photoinhibition was reduced (Jifon and Syvertsen, 2003).

1.2. ADAPTATION AND PROTECTIVE MECHANISMS

Given the serious consequences of the imbalance between the incoming energy and its utilization for carbon fixation, plants developed a pool of adaptive and protective mechanisms able to operate at several levels (Niyogi, 1999).

1.2.1. Light interception reduction

In high irradiance conditions some plant species are able to orient leaves and chloroplasts in order to expose less photosynthetic surface to full light, thus reducing the absorbed light (Anderson, 1986; Pastenes et al., 2003; Oguchi et al., 2005). This mechanism is shared by only a few species. In apple (*Malus* x *domestica* Borkh) for example, leaves are not able to prevent excessive light since their movement is slow (Koller, 1999). The transition state is another mechanism to equilibrate the photon pressure incoming on leaves. When light excess over-reduces the Quinol pool some kinases are activated. These are able to split and shift PSII antennae monomers on LHCI in order to balance the light pressure on both photosystems (Allen, 1995).

1.2.2. Improving exiting energetic flux

The main strategy plants adopt for limiting photodamage is to balance the incoming light excess improving the energetic and electronic fluxes exiting from photosystems. The purpose of these mechanisms is to maintain the energy/electron acceptors available to receive new energy

reducing the ^{1}Chl lifetime and increasing the $NADP^+$ regeneration (Niyogi, 1999). Plants dissipate light excess at different levels along the photosynthetic system. The two main strategies involved are thermal quenching and photochemistry (Foyer, 1995).

1.2.2.1. Thermal dissipation (Non Photochemical Quenching)

Thermal dissipation can be divided in three principal factors: energetic quenching (qE), transition quenching (qT) and inhibitory quenching (qI). The former represents the most important dissipative strategy for plants as it is able to quench up to 75% of the total incoming energy (Demming-Adams et al., 1996). The pigments (Xanthophylls) involved in this pathway are strictly connected to the light harvesting complex, particularly to the Lhc4 and Lhc5 monomers (Ort, 2001). The xanthophyll cycle is able to de-excite the ^{1}Chl reducing its life time and the potential ROS development in LHCII. Furthermore, the rapid thermal re-emission prevents the lumen over-acidification. In over-acid environment the electron transport from the oxygen evolving complex (OEC) to P_{680}^+ is inhibited and the long life time of the chlorophyll in an excited state could promote the $^1O_2$ formation (Niyogi, 1999), or could be dangerous per se (Anderson, 2001). When the incoming light is not excessive the thylakoidal lumen pH is about 6.5 - 7 (Foyer, 1995). violaxanthin (V), a xanthophyll carotenoid of ,is bound at the V1 site on LHCII. At the same time the PsbS, a low molecular weight protein (22kDa) linking the LHCII and the PSII core complex, is in a de-protonated state with a particular structure. At this lumen pH, violaxanthin de-epoxidase (VDE), the key enzyme of the xanthophyll cycle is de-protonated and detached (Fig. 2A) from the thylakoidal membrane (Ort, 2001). The photon pressure increase drives the lumen H^+ concentration to rise because H^+ production rate is higher than its utilization rate (Niyogi, 2004). Furthermore in tobacco (*Nicotiana tabaci* L.), as thermal dissipation occurred, a reduction in proton conductivity through the ATPase pump was recorded. Probably the H^+ conductivity

decrease would avoid to reduce again the lumen H^+ concentration. (Avenson et al., 2004). In the first instance the lumen acidification drives the PsbS protonation that changes its structure (Fig. 2B) enabling it to steal energy from ^{1}Chl, re-emitting heat (first NPQ stage, Morosinotto, 2003). A further trans-thylakoidal ΔpH increase promotes the protonation of VDE which, in this activated state, is bound to the thylakoid membrane. violaxanthin de-epoxidase catalyzes two subsequent violaxanthin de-epoxidation forming antheraxanthin (A) and zeaxanthin (Z). The electrons for these reduction reactions come from ascorbic acid (AsA) oxidation, which yields mono-dehydroascorbate (MDA). Some Authors reported that the VDE Km for ascorbic acid is strictly pH dependent and is achieved when lumen pH is lower than 6.5 (Bratt et al., 1995). The newly formed xanthophylls (A and Z) can replace violaxanthin in the V1 site re-emitting thermal energy. However the highest thermal dissipation is accomplished when A and/or Z are connected to the activated PsbS protein (Fig. 2C) forming a quenching super-complex (second NPQ stage; Ort, 2001). When the photon pressure decreases, zeaxanthin epoxidase (ZE) regenerates V using reducing equivalents (Fig. 3). This enzyme is bound to the thylakoid membrane on the stromatic side and it is always fully activated, therefore the xanthophyll cycle depends exclusively on VDE activity and PsbS structure; i.e. it depends on trans-thylakoidal ΔpH (Bouvier et al.,1996). Each event capable to increase the ΔpH contributes to trigger or support the energetic quenching (Björkman and Demming Adams, 1994; Horton el al., 1996; Gilmore, 1997). In several species the xanthophyll cycle has a pivotal role. In apple for example, the incoming photon flux increase determines violaxanthin reduction in respect to the whole xanthophyll pool and a correlated zeaxanthin development. A quite similar pattern is found both in leaves and in fruits, although in the latter Z production is emphasized since fruits very early in their development become defective for one of the dissipating pathways: photosynthesis (Cheng and Ma, 2004). In some tropical species a further contribution to qE is guaranteed by lutein epoxide

de-epoxidation (Lx) in lutein (L) promoted by VDE. Lutein has the same role of A and Z although its low affinity to ZE determines a slow lutein reversibility resulting in a background protection against photon excess (Matsubara et al., 2004). The inhibitory quenching (qI) could be considered as a passive mechanism since the inactive photosystems and photosystem monomers re-emit the absorbed energy as heat (Matsubara and Chow, 2004). The energy amount quenched by the inactive PSII is linearly related to the inactive PSII concentration (Anderson and Chow, 1997; He and Chow, 2003; Losciale et al., 2008). Some Authors reported the passive protection role of this mechanism (Chow et al., 2005). When PSII recovery is temporarily not permitted, a decrease of active PSII occurs, although even increasing the photon exposure, about 10-20% of the total PSII population remains active. Probably the damaged PSII protect the surviving PSII in further dissipating the incoming energy. In a mutual advantage the active PSII pay this protection creating the optimal pH (i.e. water splitting) necessary for activation of recovery enzymes (inactive PSII-mediated quenching; Chow, 2002). The transition quenching (qT) is due to transition state process and it does not seem to be very important for photoprotection in higher plants (Niyogi, 1999).

1.2.2.2. Photochemistry dissipation

Photochemical pathways involve photosynthesis as well and consist in activating and accelerating the electron transport mechanisms in order to balance the incoming photon pressure (Chow, 1994); these processes operate at different levels along the photosynthetic complex.

Cyclic transport on PSII

This mechanism has so far only been observed in vitro. Electrons are cyclically moved among P_{680}, pheophytin and cytochrome b6f (Cyt b6f) being taken from the linear electron transport (Whitmarsh et al., 1994).

Cyclic transport on PSI

The main function of this pathway is to generate additional H^+ in the thylakoid lumen used by the ATPase pump for ATP synthesis. The electrons exiting PSII reduce ferredoxin; as well as reducing $NADP^+$ ferredoxin can give back electrons to the quinol pool placed between PSII and cytochrome b6f, activating the cyclic transport. During the process $2H^+$ for each electron are transferred from stroma to thylakoid lumen (Fig. 4), thus increasing the proton-motive force (Joliot and Joliot, 2002). When $NADP^+$ are less available to be reduced (i.e. low regeneration rate comparing with photon pressure) the cyclic transport on PSI is boosted in order to avoid ROS formation and to decrease lumen pH for VDE activation (Heber and Walker, 1992).

Water-Water Cycle (W-WC)

This pathway is so called because water formation down to PSI corresponds to the water oxidation in the oxygen evolving complex. The W-WC is named Meheler-Peroxidase reaction as it is the sum of these two reactions as well (Fig. 5). Some researches estimated the water-water cycle is able to dissipate up to 30% of the total electron flux (Asada, 1999). As well as giving back electrons to the quinol pool (cyclic transport on PSI), ferredoxin can reduce oxygen forming the super-oxide ion (Meheler reaction). The dangerous reactive oxygen species should be converted as soon as possible to an inactive one as water. A super-oxide dismutase (SOD) placed in the stroma side of the thylakoid membrane promotes the H_2O_2 formation taking $2H^+$ from the stroma. Afterwards the trans-membrane ascorbate peroxidase (t-Apx) catalyzes the H_2O_2 reduction to water oxidizing the ascorbic acid (AsA) to mono de-hydro ascorbate (MDA). Finally AsA is regenerated using reducing power (ferredoxin and/or $NADPH(H^+)$). The water-water cycle is an alternative way for electrons and it is able to increase the trans-thylakoidal ΔpH necessary for the xanthophyll cycle (Asada, 1999).

Photorespiration

Photorespiration could be considered the dark side of Rubisco activity since assimilated CO_2 is lost, although this pathway is important for energy excess dissipation. Inhibition of photosynthesis and photo-oxidative damage increase was found when photorespiration was blocked with mutations or inhibitors (Artus et al., 1986). Considering the carboxylative activity of Rubisco, for each CO_2 2 phosphoglyceric acid (PGA) molecules are synthesized using 2NADPH(H^+). The PGA generation rate (V_{PGA}) is 2 fold the carboxylation rate (V_C).

$$V_{PGA} = 2V_C$$

Considering the oxygenase activity of Rubisco, for each O_2 1 PGA and 1 phosphoglycolate molecule is formed. From the latter a half PGA and half CO_2 molecule is generated. Hence the PGA synthesis rate is 1.5 fold the oxygenation rate (V_O).

$$V_{PGA} = 1V_O + 0.5V_O$$

Since for each PGA synthesis 1 molecule of NADPH(H^+) is used

$$V_{NADPH} = V_{PGA} = 2V_C + 1.5V_O$$

In the oxygenation reaction 0.5 molecules of ammonium are released and re-fixed for each O_2, using 0.5 molecules of NADPH(H^+).

$$V_{NADPH} = 2V_C + 1.5V_O + 0.5V_O = 2V_C + 2V_O$$

As two electrons are used to generate 1 NADPH(H^+), the electron transport rate for the total Rubisco activity (V_e) is

$V_e = 2(2V_C + 2V_O) = 4V_C + 4V_O)$

Photorespiration uses the reducing power re-generating $NADP^+$, which becomes available for receiving electrons again (Farquhar et al., 1980). The importance of this pathway seems to be increased when a mild stomatal conductance limitation reduces photosynthesis (Galmés et al., 2007).

1.2.3. Scavenging

Not all the electrons are intercepted by the several dissipative mechanisms, therefore ROS formation occurs; the role of scavenging pathways is to neutralize these toxic species (Asada, 1994). Ascorbic acid is considered the most important scavenger molecule for its abundance in chloroplasts and its participation in the principal photo-protective cycles (i.e. xanthophyll cycle and water-water cycle). Furthermore AsA is directly involved in tocopherols regeneration and in $^1O_2$, O_2^- and OH· scavenging (Smirnoff, 1996). As a consequence ascorbic acid regeneration is fundamental for photoprotection. In addition to direct MDA to AsA reduction operated by ferredoxin, plants developed a dedicated cycle for ascorbic acid re-generation: the glutathione- ascorbate cycle.

When O_2^- is formed, a stromatic super-oxide dismutase (Cu-Zn SOD) promotes H_2O_2 generation. A stromatic ascorbate peroxidase (S-Apx) then reduces the H_2O_2 to water, oxidizing the ascorbic acid to mono de-hydro ascorbate (MDA). MDA can be directly re-reduced to AsA receiving electrons from $NADPH(H^+)$; alternatively, it can be reduced to de-hydro ascorbate (DHA) by a stromatic mono dehydroascorbate reductase (MDA-r). Afterwards DHA reduction to AsA is promoted by a dehydroascorbate reductase (DHA-r) oxidizing glutathione. The glutathione-ascorbate cycle is finally closed with the glutathione regeneration catalyzed by a glutathione reductase (GSH-r), using $NADPH(H^+)$ as electron donor (Fig. 6). The glutathione-ascorbate cycle re forms the AsA, scavenges the super-oxide ion, increases the trans-thylakoid ΔpH using stromatic H^+ to form water and

it can be considered as an alternative way for electrons since it uses reducing power. Furthermore the glutathione-ascorbate cycle is a direct scavenger of $^1O_2$ and OH· and defends the thyol groups of stroma enzymes against oxidation (Noctor and Foyer, 1998).

Tocopherols are involved in $^1O_2$, O_2^- and OH· scavenging; since they are lipophilic, these molecules are able to protect membranes against peroxidation (Foyer et al., 1994). The last scavenger molecules are carotenoids. In LHCII, xanthophylls are ^{3}Chl and $^1O_2$ scavenger while β-carotene scavenges $^1O_2$ (Külbrandt et al., 1994). In the PSII core complex only β-carotene molecules were found while xanthophylls seem to be highly compatible to LHCII because of the high presence f Chlorophyll b (Telfer et al., 1994).

1.3. RECOVERY

In spite of the complex and multi-level photo-protective machine, photodamage occurs. The main target for inactivation is the D1 protein (Aro et al., 1993), which is placed between the oxygen evolving complex and the LHCII. D1 is thus located in a region very rich of ^{3}Chl and O_2: a perfect combination to generate ROS. This "planned" destruction is used to avoid an uncontrolled and widespread damage (Krieger-Liszkay, 2005), as plants developed an effective, efficient and conservative mechanism for D1 recovery (Bottomely et al., 1974; Eaglesham and Ellis, 1974; Anderson et al., 1997; Chow and Aro, 2005). In nature the recovery rate should be similar to the photodamage rate since it is quite difficult to detect a net loss of PSII activity. Hence the D1 protein turnover could be considered one of the major photo-protective strategies (Anderson et al., 1997). PSII photo-inactivation in vivo is not restricted to high light but also occurs at low irradiance (Anderson and Aro, 1994; Keren et al., 1995; Park et al., 1995; Tyystjärvi and Aro, 1996). by inhibition of D1 recovery it is possible to

appreciate the real PSII damage (Aro et al., 1994). In absence of repair the decrease of PSII activity is function of photon exposure (the product between irradiance and time of exposure), following the reciprocity law (Jones and Kok, 1966; Park et al., 1995; Lee et al., 1999). In other words photoinhibition is related to light dosage rather than light intensity (Chow et al., 2005). The function relating active PSII amount and photon exposure is a negative exponential curve where functional PSIIs decline with increasing photon exposure and the photoinhibition rate (curve slope) gradually decreases with photon exposure enhancement. The rate of photoinhibition is highest when all photosystems are active and available to be inactivated. The photon exposure enhancement reduces the functional PSII thus the active photosystems to be damaged become more and more limiting (Chow et al., 2005).

The recovery mechanism is very energy saving since only the damaged component is replaced, while the remaining active sub-units are re-assembled (Komenda and Barber, 1995). The recovery process can be summarized in the following key aspects:

- electron transport alteration caused by PSII damage;
- structural variation identification signalling the damage ;
- PSII monomerization and partial complex de-assembly in order to make the damaged sub-unit accessible;
- damaged D1 degradation and new synthesis of functional D1;
- sub-units and monomers re-assembly.

The altered molecules seem to have the role of messengers for psbA gene activation, involved in D1 new synthesis (Lindhal et al., 2000). The damaged D1 degradation is performed by the protease FtSH. They are bound to the thylakoid membrane and are assembled in a way forming an esameric trans-membrane canal. The damaged D1 protein transit across the esameric ring is ATP-dependent and the final degradation is promoted by the FtSH prosthetic group in the stroma consuming ATP as well (Fig. 7). Besides using energy for D1 re-generation, plants consume energy for the

rapid D1 degradation in order to avoid photo-oxidative risks (Nixon et al., 2005).

The dangerous consequences of photo-oxidation stimulated plants to evolve a complex and multi-pronged machine for photoprotection and recovery with a mutual support among the several processes involved. Plants pay a high price for this equipment. These pathways use CO_2 and reducing power decreasing the photosynthetic efficiency. Since some intercepted photons are not used for carboxylation, but also because an active CO_2 and reducing power loss occurs (Foyer, 1995).

1.4. PHOTODAMAGE AND PHOTOPROTECTION: HOW TO MEASURE THEM?

Photoinhibition and photo-protective mechanisms can be detected using several techniques as the assay and dosage of enzymes and molecules involved in the pathways, but the most useful method, particularly because it can be used in vivo as well, is the measure of chlorophyll fluorescence (Krause and Weis, 1991; Govindjee, 1995; Maxwell and Johnson, 2000). When chlorophyll is excited it can dissipate energy using three strategies: quenching heat, transferring electrons for the electron transport and re-emitting energy as fluorescence (660-685 nm). Inducing chlorophyll to emit the absorbed energy as fluorescence and being able to measure this re-emission, it is possible to quantify and discriminate the contribution of pathways in which the incoming photon pressure is engaged.

A fluorimeter is made up of a light source (control unit) attached to an optical fibre able to transmit the actinic light generated by the control unit to the leaf lamina, and to channel back the fluorescence re-emitted by the leaf to the control unit. Several measurements are needed for a full complement of data: usually the first measure is performed on dark adapted leaves or at predawn in the field. In this stage the photosynthetic system is completely

relaxed since each component is fully functional and the quinone A (Q_A) is completely oxidized and available to receive electrons. At this time a low intensity light pulse (0.1-0.5 $\mu molm^{-2}s^{-1}$) is supplied. These few photons are able to excite the LHCII chlorophylls hence the P_{680} with charge separation between P_{680} and pheophytin (P_{680}^{+}/Ph^{-}). The latter transfers electron to the fully oxidized Q_A, which can be reduced. The electron transport occurs in 10^{-12} seconds therefore more favourable than fluorescence (10^{-8}s) from a thermodynamic point of view. The measured fluorescence (F_o) represents the minimum chlorophyll fluorescence in dark adapted conditions, when PSIIs are completely "open". At this time a short (less than 1s) saturation pulse (10000 – 20000 $\mu mol\ m^{-2}s^{-1}$) is flashed, determining an energy congestion in the systems. The incoming photon pressure is very excessive compared to the capacity of the Q_A electron transport to the following electron acceptors. Therefore the over-reduced Q_A is unable to receive more electrons. The photochemical transport is saturated, thus heat and fluorescence remain the dissipative ways. The increased chlorophyll fluorescence (F_m) recorded is the maximum fluorescence of dark-adapted leaves and it represents the amount of energy re-emitted by chlorophylls when Q_A is completely reduced and the reaction centres are "closed". The difference between F_o and F_m ($F_v = F_m - F_o$) standardized for F_m (F_v/F_m) is the maximum quantum yield of PSII and it indicates the maximum amount of energy chlorophyll is able to trap and which can potentially be used for photosynthesis (Fig. 8). When the leaf is in an optimal state with fully relaxed and repaired photosystems, F_v/F_m is about 0.8-0.85. PSII damage or its not complete relaxation leads F_v/F_m to decrease. F_v/F_m reduction can derive from an F_m decrease or an F_o increase. The first case occurs when PSII is not functional because of D1 damage (Govindjee, 1995; Maxwell and Johnson, 2000). F_o increase can be interpreted as Q_A being unable to pass electrons to the following acceptor Q_B although the reason is not the light excess, since the photon pressure supplied is minimal. The F_o increase could also be determined by an uncoupling among some PSII components.

Some Authors interpret this event as a further photo-protective mechanism preventing the energy excess from arriving to the PSII core complex; on the other hand in several studies the PSII impairment is considered as an effective damage. The F_o increase was however recorded mainly in high temperature conditions (Yamane et al., 2000).

Once the maximum quantum yield is measured, actinic light at a determined intensity is supplied using the light source or the natural solar light. An initial fluorescence peak is recorded because the photosynthetic system is in the "photo-activation" state. Actinic light drives the electron transport and one electron leaves P_{680} to follow the Z scheme. Since the oxygen evolving cluster (OEC) is not yet attached to Photosystem II, P_{680} can not return to the fundamental state picking up an electron from water splitting; the excited molecule dissipates energy via fluorescence emission. As soon as the OEC is connected with PSII the electron transport is permitted and fluorescence decreases because the most thermodynamically favourable pathway is chosen. Fluorescence detected at this stage is called steady-state fluorescence (F_s) and represents the residual chlorophyll fluorescence re-emitted in light-adapted conditions. In presence of actinic light, F_s continues to decrease reaching a steady state, at this time the F_s value is recorded and a further saturating pulse is furnished obtaining a fluorescence peak $F_{m'}$: maximum fluorescence in light-adapted condition. Even in this case the saturating pulse causes Q_A over-reduction, therefore energy can be dissipated as heat and fluorescence. Generally $F_{m'}$ is lower than F_m since a fraction of energy is quenched as heat able to dissipate energy faster than fluorescence (10^{-12}s). The difference between F_m and $F_{m'}$ standardized for $F_{m'}$ ($NPQ = (F_m-F_{m'})/F_{m'}$) is called Non Photochemical Quenching (NPQ) and represents the amount of energy trapped by Chlorophyll and quenched by light-dependent thermal dissipation associated with inactivated PSII and promoted by the photo-protective Non Photochemical Quenching via the xanthophyll cycle. Finally the actinic light is turned off and only far red light (30 μmol $m^{-2}s^{-1}$ at 720-730 nm for about 4s) is supplied in order to

activate preferentially PSI, completely relaxing the Photosystem II. The fluorescence recorded in presence of far red ($F_{o'}$) is the minimum fluorescence with light-adapted leaves and its physiological meaning is the same of F_o even tough the two values could be unequal. The difference between $F_{m'}$ and $F_{o'}$ standardized for $F_{m'}$ ($(F_{m'}-F_{o'})/F_{m'}$) is the PSII maximal photochemical efficiency in light adaptation condition and represents the energy amount entering into the PSII core complex, which therefore could be used for photochemistry. Not all the energy arriving to PSII exits the photosystem, however. ΦPSII ($1-F_s/F_{m'}$) is the effective photochemical efficiency of PSII and represents the energy effectively going through PSII and used for photosynthesis, photorespiration and the alternative transports such as the water-water cycle, the cyclic transport around PSI and the glutathione-ascorbate cycle (Genty et al., 1989; Govindjee, 1995; Maxwell and Johnson, 2000; Baker and Rosenqvist, 2004). The difference between F_s and F_o, standardized for $F_{m'}$ ($(F_s-F_{o'})/F_{m'}$ represents the energy trapped in PSII but not exiting from it. This energy could be used to supply some alternative transports as the glutathione-ascorbate cycle, to hypothetically generate singlet oxygen (Demming-Adams et al., 1996) or could be re-emitted as basal heat and fluorescence (Fig. 8). Knowing ΦPSII is possible to calculate the electron transport rate (ETR) exiting from PSII (μmol $m^{-2}s^{-1}$)

$$ETR = \Phi PSII \times PPFD \times \alpha \times 0.5$$

where PPFD is the photosynthetic photon flux density, α is the leaf absorptance (0.84-0.85, Krall and Evans, 1992; Schultz, 1996) and 0.5 takes into account that one electron is moved by 2 photons (Genty, 1989).

The fluorescence technique permits to partition the NPQ in the energetic quenching and inhibitory quenching. After NPQ determination the leaf is dark adapted for 45-60 minutes. This time is necessary to inhibit the xanthophyll cycle since no H^+ are generated. After the dark adaptation F_v/F_m is measured. The difference between the maximal quantum efficiency

at predawn or before any photo-inhibitory event (F_v/F_{mM}) and F_v/F_m after 45-60 minutes in the dark is the energy lost as heat by the damaged PSII (Fig. 9) since the controlled thermal dissipation is inactive (Maxwell and Johnson, 2000; Müller et al., 2001; Baker and Rosenqvist, 2004).

1.4.1. Quenching Partitioning

The analysis of fluorescence parameters gives a qualitative information about plant energy management, although it is difficult to appreciate the relative weight in energy partitioning of each pathway; while ΦPSII or F_v/F_m are quantum yields, therefore indicate the energy fraction used by those processes, NPQ is not an efficiency, in fact it can attain values higher than 1. Several approaches were attempted in order to evaluate the relative importance of all mechanisms (Cailly et al., 1996; Demming-Adams et al., 1996; Kramer et al., 2004; Kornyeyev and Hendrickson, 2007). The most recent was suggested by Hendrickson and colleagues (2005) using the approach suggested by Cailly et al. (1996) and upgraded by Kornyeyev and Hendrickson (2007). The postulate on which this quenching partitioning analysis is based is one of the most accredited concept of photo-biology: the quantum yield of any process (Φ) involved in light utilization and dissipation is equal to the ratio of the rate constant for this process to the sum of all the rate constants (Kitajima and Butler, 1975; Genty et al., 1989; Roháček, 2002). The involved processes are fluorescence (rate constant k_f), constitutive thermal dissipation (k_D), photochemistry (k_{PSII}), regulated thermal dissipation (k_{NPQ}), and thermal dissipation associated to damaged PSII (k_{NF}).

Considering a pool of PSII as a whole in which sub-populations differing in the Q_A oxidation state co-exist

$$\Phi_f + \Phi_D + \Phi_{NF} + \Phi_{NPQ} + \Phi_{PSII} = 1 \qquad (1)$$

When a sample is light adapted F_s is measured

$$\Phi_f = \frac{k_f}{k_f + k_D + k_{NPQ} + k_{NF} + k_{PSII}} \quad (2)$$

The measured F_s therefore is

$$F_s = \Phi_{f(Fs)} = \frac{k_f}{k_f + k_D + k_{NPQ} + k_{NF} + k_{PSII}} \quad (3)$$

When F_s=$F_{m'}$ the photochemical system is completely saturated therefore $k_{PSII} = 0$ (i.e. Q_A is completely reduced).

$$F_{m'} = \Phi_{f(Fm')} = \frac{k_f}{k_f + k_D + k_{NPQ} + k_{NF}} \quad (4)$$

by equation (1) Φ_{PSII} can be derived

$$\Phi_{PSII} = 1 - (\Phi_f + \Phi_D + \Phi_{NF} + \Phi_{NPQ}) \quad (5)$$

then

$$\Phi_f + \Phi_D + \Phi_{NPQ} + \Phi_{NF} = \frac{k_f + k_D + k_{NPQ} + k_{NF}}{k_f + k_D + k_{NPQ} + k_{NF} + k_{PSII}} \quad (6)$$

$$\Phi_{PSII} = 1 - \frac{k_f + k_D + k_{NPQ} + k_{NF}}{k_f + k_D + k_{NPQ} + k_{NF} + k_{PSII}} \quad (7)$$

by equation (3)

$$k_f + k_D + k_{NPQ} + k_{NF} + k_{PSII} = \frac{k_f}{F_s} \quad (8)$$

and by equation (4)

$$k_f + k_D + k_{NPQ} + k_{NF} = \frac{k_f}{F_{m'}} \qquad (9)$$

substituting in equation (5)

$$\Phi_{PSII} = 1 - \frac{\frac{k_f}{F_{m'}}}{\frac{k_f}{F_s}} = 1 - \frac{F_s}{F_{m'}} \qquad (10)$$

According to excitons/radical pair equilibrium theory (Schartz et al., 1988) the quantum yield of the first charge separation (P_{680}^+ Ph^-) is very high (~ 0.96) while the subsequent electron transfer from pheophytin to the primary quinine acceptor is much slower. Therefore the increased life time of the radical pair (P_{680}^+ Ph^-) can determine a charge recombination yielding an excited singlet or possible triplet state. The excited species could return to a fundamental state dissipating energy as fluorescence and constitutive thermal energy (Chow, 2003).

Considering

$$\Phi_{f,D} = \Phi_f + \Phi_D \qquad (11)$$

$$\Phi_{f,D} = \frac{k_f + k_D}{k_f + k_D + k_{NPQ} + k_{NF} + k_{PSII}} \qquad (12)$$

At predawn or however in non-photoinhibitory conditions, when a saturating pulse is supplied $F_s = F_{mM}$. Where F_{mM} is the maximum chlorophyll fluorescence re-emitted by fully functional PSII. The saturating pulse blocks the photochemical way and $k_{PSII} = 0$, furthermore no photo-damage occurs ($k_{NF} = 0$) and the non photochemical quenching is inactive as VDE is inactive because of the high lumen pH ($k_{NPQ} = 0$).

$$F_{mM} = \Phi_{f(FmM)} = \frac{k_f}{k_f + k_D} \quad (13)$$

Re-arranging equation (13)

$$k_f + k_D = \frac{k_f}{F_{mM}} \quad (14)$$

using the equation (3) and (14) the equation (12) can be re-written as

$$\Phi_{f,D} = \frac{\frac{k_f}{F_{mM}}}{\frac{k_f}{F_s}} = \frac{F_s}{F_{mM}} \quad (15)$$

Considering the regulated thermal dissipation quantum yield

$$\Phi_{NPQ} = \frac{k_{NPQ}}{k_f + k_D + k_{NPQ} + k_{NF} + k_{PSII}} \quad (16)$$

by equation (1)

$$\Phi_{NPQ} = 1 - \Phi_{PSII} - (\Phi_{f,D} + \Phi_{NF}) \quad (17)$$

Using the rate constants the equation (17) can be re-written as

$$\Phi_{NPQ} = 1 - \Phi_{PSII} - \left(\frac{k_f + k_D + k_{NF}}{k_f + k_D + k_{NPQ} + k_{NF} + k_{PSII}} \right) \quad (18)$$

After a light treatment, the 45-60 minutes dark adaptation is able to inactivate the xanthophyll cycle. When a further saturating pulse is furnished a fluorescence peak is recorded. F_m is the maximal chlorophyll fluorescence of a sample dark-adapted but after a potential photoinhibitory

treatment (i.e. actinic light). The difference between F_v/F_{mM} and F_v/F_m represents the energy quenched as heat by the inactive PSII. The saturating pulse over-reduced the Q_A and k_{PSII} is 0; since dark adaptation inhibited the regulated thermal dissipation even k_{NPQ} is 0. in this stage $F_s = F_m$, therefore

$$\mathrm{F_m} = \Phi_{f(Fm)} = \frac{k_f}{k_f + k_D + k_{NF}} \tag{19}$$

Rearranging the equation (18)

$$k_f + k_D + k_{NF} = \frac{k_f}{\mathrm{F_m}} \tag{20}$$

Substituting the equation (3) and (19) in equation (18)

$$\Phi_{NPQ} = 1 - \Phi_{PSII} - \frac{\frac{k_f}{F_m}}{\frac{k_f}{F_s}} \tag{21}$$

$$\Phi_{NPQ} = 1 - \left(1 - \frac{F_s}{F_{m'}}\right) - \left(\frac{F_s}{F_m}\right) \tag{22}$$

By equation (1), (10), (15) and (22) is possible to calculate the quantum yield of energy lost by the non functional PSII (Φ_{NF})

$$\Phi_{NF} = 1 - \Phi_{PSII} - \Phi_{f,D} - \Phi_{NPQ} \tag{23}$$

$$\Phi_{NF} = 1 - \left(1 - \frac{F_s}{F_{m'}}\right) - \left(\frac{F_s}{F_{mM}}\right) - \left(\frac{F_s}{F_{m'}} - \frac{F_s}{F_m}\right) \tag{24}$$

$$\Phi_{NF} = \frac{F_s}{F_m} - \frac{F_s}{F_{mM}} \tag{25}$$

Chlorophyll fluorescence measurement gives a lot of information about photoinhibition, photoprotection and energy utilization in plants, although this technique is able to probe only the first layers of leaf lamina (Losciale et al., 2008). A new method for determining the inactive PSII, based on P_{700} redox kinetic is presented in the next sections.

FIGURES

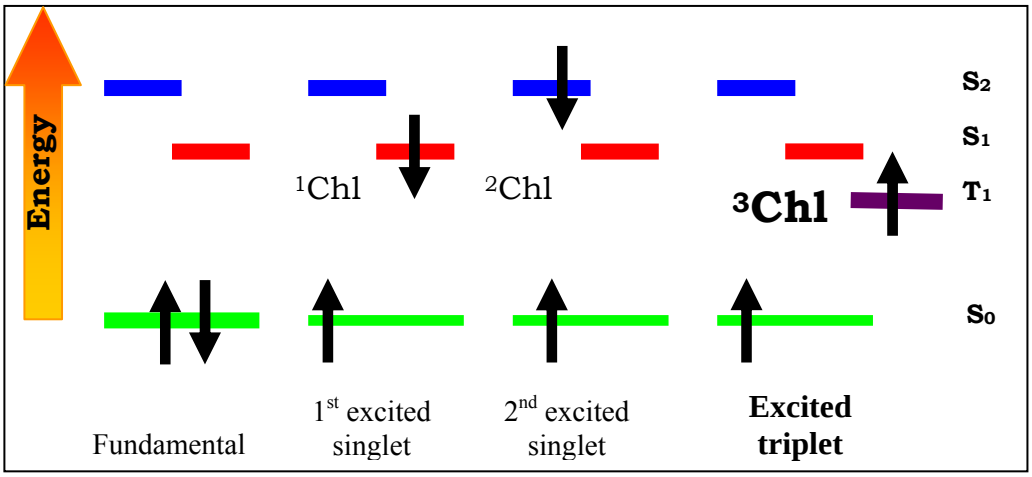

Fig. 1: energy promoted chlorophyll excited estates. Arrows in different positions represent electron position and spin on orbitals.

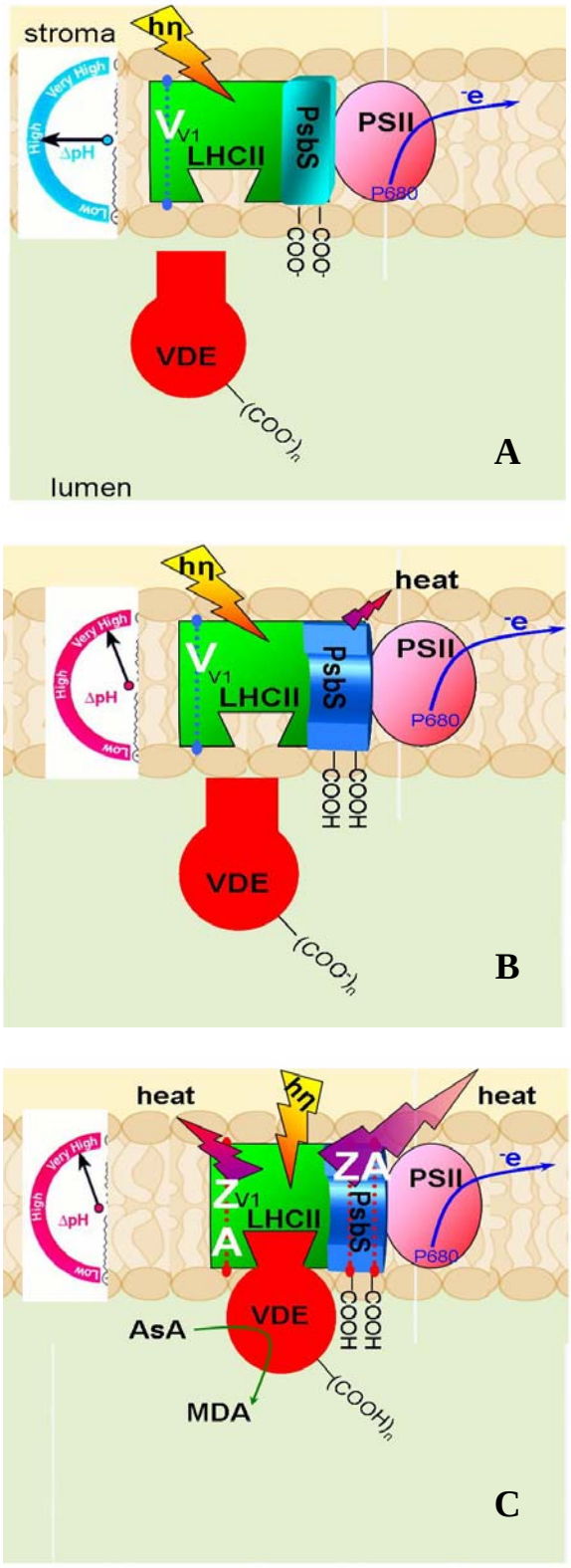

Fig. 2: representation of the principal complexes involved with xanthophyll cycle at normal trans-membrane ΔpH condition (A), at the first stage of NPQ according to Morosinotto, 2003 (B) and at the second stage of NPQ proposed by Ort, 2001 (C).

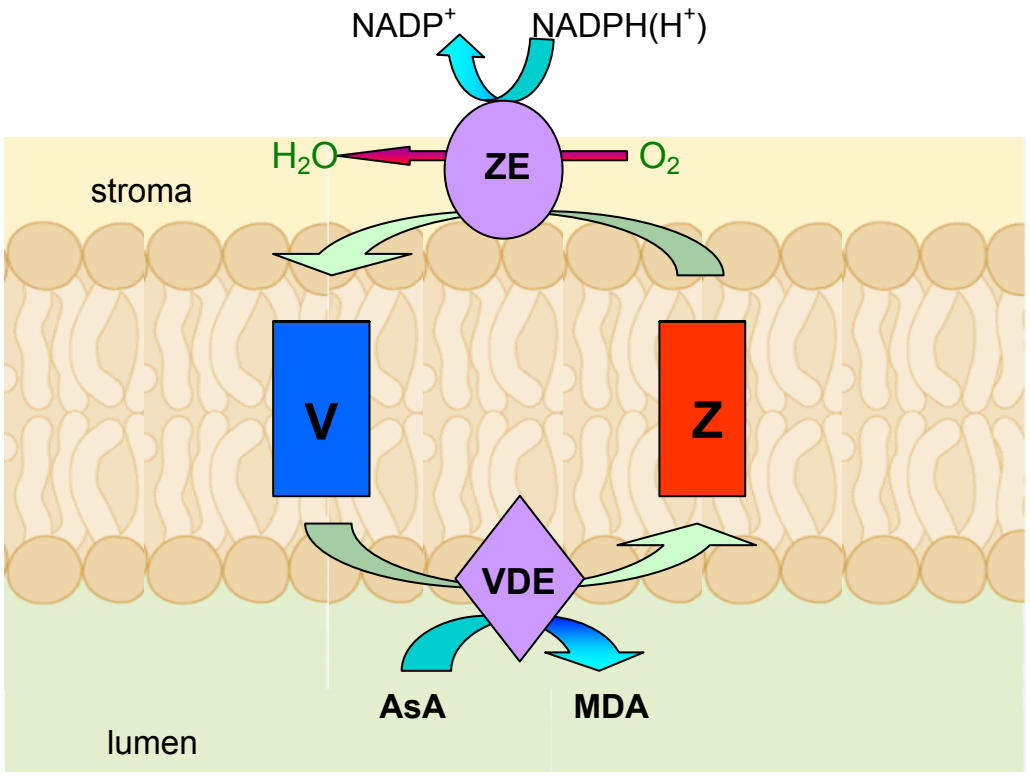

Fig. 3: violaxanthin de-epoxidation and regeneration promoted by violaxanthin de-epoxidase (VDE) and zeaxanthin epoxidase (ZE), respectively.

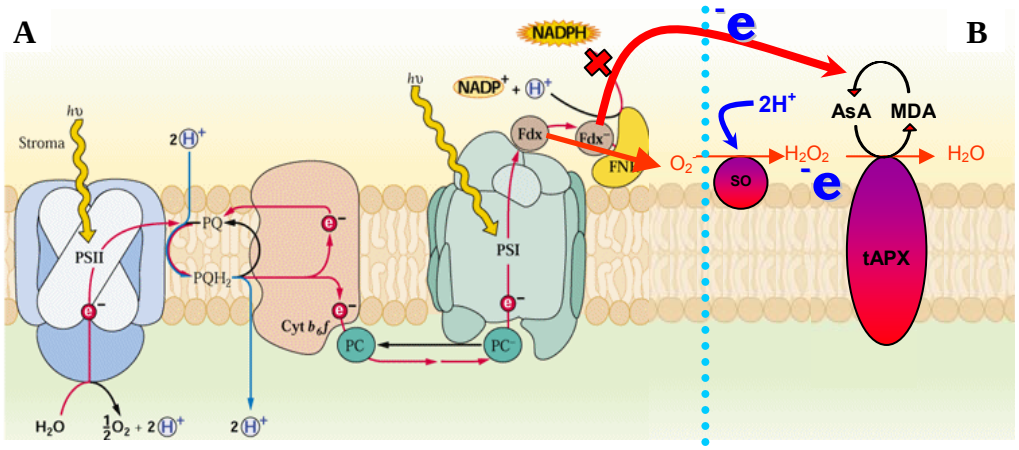

Fig. 4: water-water cycle representation divided by the cyan dashed line into Meheler reaction (A) and peroxidase reaction (B).

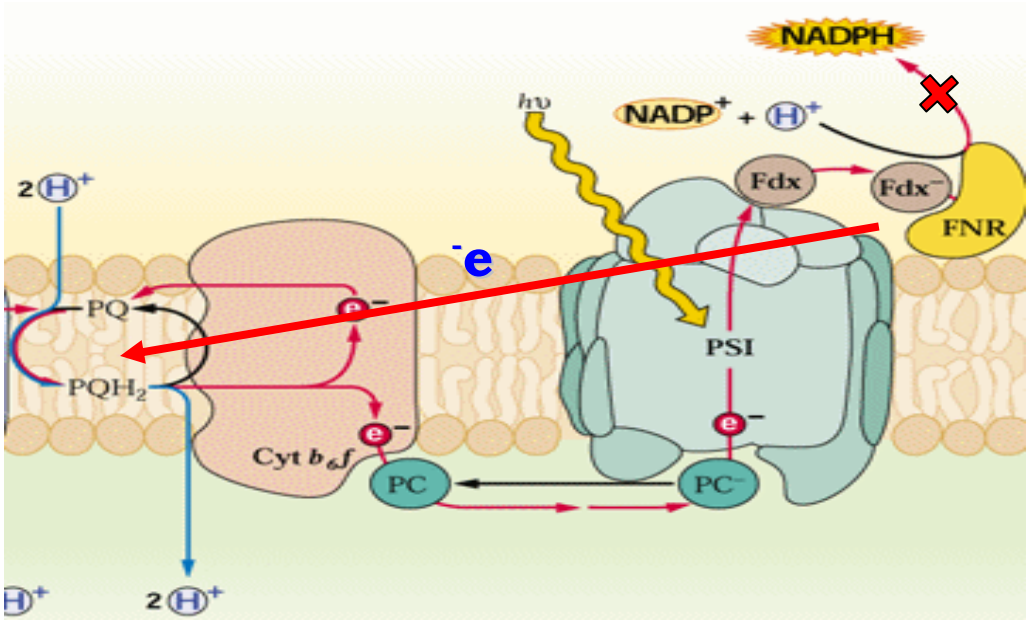

Fig. 5: cyclic transport around PSI representation.

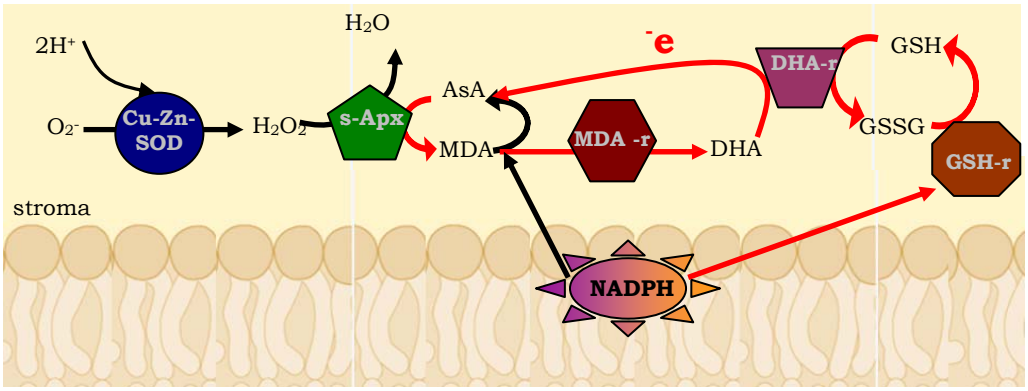

Fig. 6: glutathione-ascorbate cycle representation

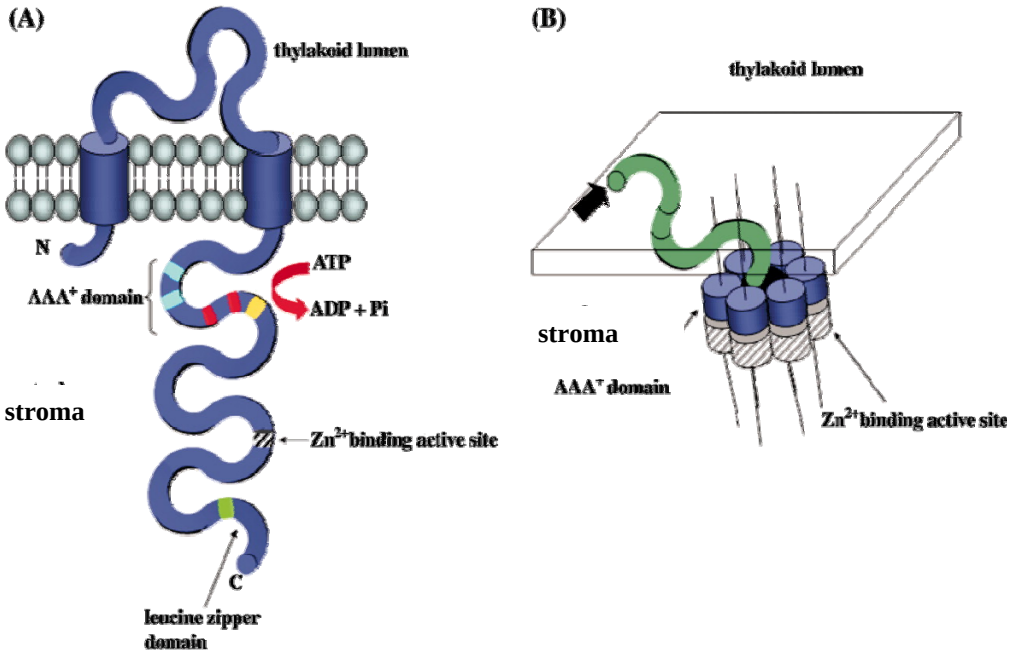

Fig. 7: FtsH protease monomeric (A) and esameric structure (B). The damaged protein transits across the trans-membrane ring to be degraded in stroma by the FtsH prosthetic group (Nixon et al., 2005).

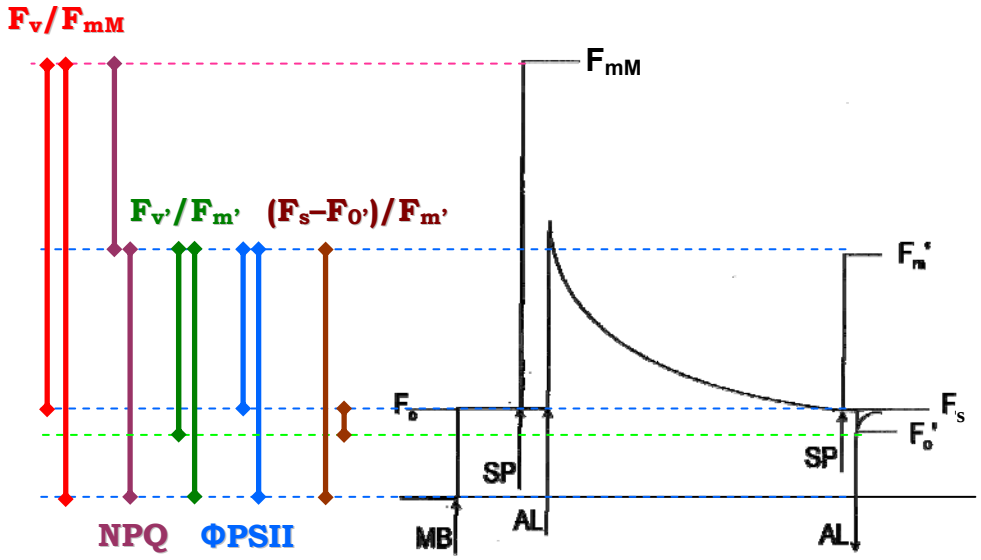

Fig. 8: principals calculated parameters obtained by modulated chlorophyll fluorescence measurement. MB = Measure beam, SP = Saturating pulse, AL = Actinic light. Adapted from Maxwell and Johnson (2000).

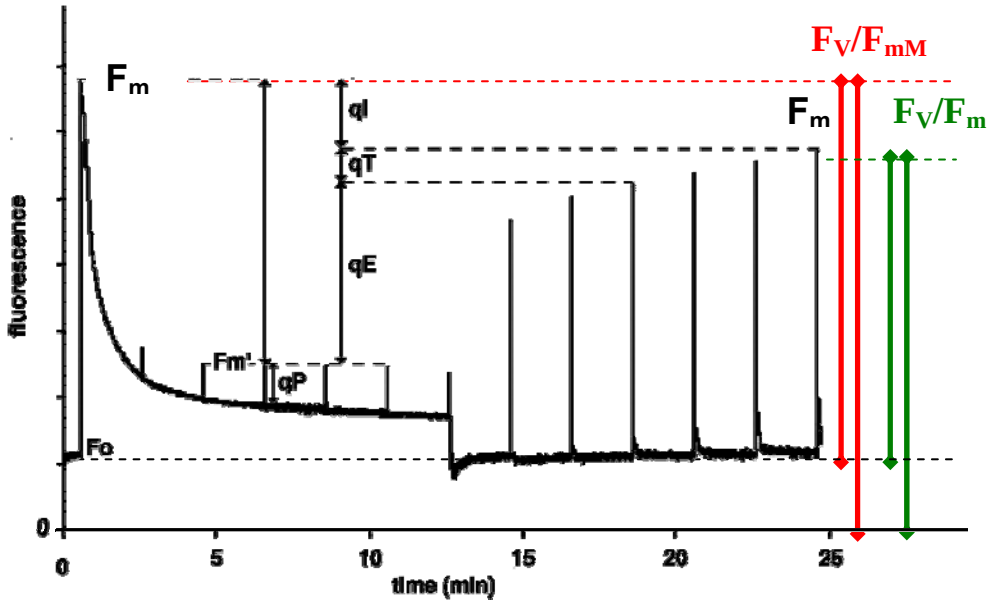

Fig. 9: xanthophyll cycle inactivation after leaf dark adaptation. The difference between the maximum quantum yield of not photoinhibited samples (F_V/F_{mM}) and the maximum quantum yield after a potential photoinhibitory treatment represents the energy amount dissipated by damaged PSII as heat. Adapted by Müller et al. (2001).

Chapter II

AIMS OF THE STUDY

The relation between the intercepted light and orchard productivity was considered linear, although this dependence seems to be more subordinate to planting system rather than light intensity. At whole plant level not always the increase of irradiance determines productivity improvement. One of the reasons can be the plant intrinsic un-efficiency in using energy. Generally in full light only the 5 – 10% of the total incoming energy is allocated to net photosynthesis. Therefore preserving or improving this efficiency becomes pivotal for scientist and fruit growers.

Even tough a conspicuous energy amount is reflected or transmitted, plants can not avoid to absorb photons in excess. The chlorophyll over-excitation promotes the reactive species production increasing the photoinhibition risks. The dangerous consequences of photoinhibition forced plants to evolve a complex and multilevel machine able to dissipate the energy excess quenching heat (Non Photochemical Quenching), moving electrons (water-water cycle , cyclic transport around PSI, glutathione-ascorbate cycle and photorespiration) and scavenging the generated reactive species. The price plants must pay for this equipment is the use of CO_2 and reducing power with a consequent decrease of the photosynthetic efficiency, both because some photons are not used for carboxylation and an effective CO_2 and reducing power loss occurs.

Net photosynthesis increases with light until the saturation point, additional PPFD doesn't improve carboxylation but it rises the efficiency of the alternative pathways in energy dissipation but also ROS production and photoinhibition risks.

The wide photo-protective apparatus, although is not able to cope with the excessive incoming energy, therefore photodamage occurs. Each event increasing the photon pressure and/or decreasing the efficiency of the described photo-protective mechanisms (i.e. thermal stress, water and nutritional deficiency) can emphasize the photoinhibition.

Likely in nature a small amount of not damaged photosystems is found because of the effective, efficient and energy consuming recovery system. Since the damaged PSII is quickly repaired with energy expense, it would be interesting to investigate how much PSII recovery costs to plant productivity.

This PhD. dissertation purposes to improve the knowledge about the several strategies accomplished for managing the incoming energy and the light excess implication on photo-damage in peach. The thesis is organized in three scientific units. In the first section a new rapid, non-intrusive, whole tissue and universal technique for functional PSII determination was implemented and validated on different kinds of plants as C3 and C4 species, woody and herbaceous plants, wild type and Chlorophyll b-less mutant and monocot and dicot plants. In the second unit, using a “singular” experimental orchard named “Asymmetric orchard”, the relation between light environment and photosynthetic performance, water use and photoinhibition was investigated in peach at whole plant level, furthermore the effect of photon pressure variation on energy management was considered on single leaf. In the third section the quenching analysis method suggested by Kornyeyev and Hendrickson (2007) was validate on peach. Afterwards it was applied in the field where the influence of moderate light and water reduction on peach photosynthetic performances, water requirements, energy management and photoinhibition was studied.

Chapter III

A RAPID, WHOLE-TISSUE DETERMINATION OF THE FUNCTIONAL FRACTION OF PHOTOSYSTEM II AFTER PHOTOINHIBITION OF LEAVES BASED ON FLASH-INDUCED P_{700} REDOX KINETICS

INTRODUCTION

Chlorophyll (Chl) fluorescence provides a convenient, non-intrusive probe into photosynthetic function in vivo and in vitro, and in the laboratory and in the field, made more powerful by technical advances (Papageorgious and Govindjee, 2004). Accordingly, a number of attempts have been made, with some success, to correlate Chl fluorescence parameters with gas-exchange measurements, with a view to predicting photosynthetic rate from Chl fluorescence measurements. For example, Weis and Berry (1987) reported a linear relation between ϕ_{O2}/q_P and q_N, where ϕ_{O2} is the ratio of the gross rate of oxygen evolution to the irradiance or quantum yield of oxygen evolution; q_P a photochemical quenching coefficient, and q_N a non-photochemical quenching coefficient. From such a linear relation, measurement of q_P, q_N and the irradiance would give the gross rate of photosynthesis. Many plant species conform to a single straight line; however, there are occasional exceptions to the single straight line (Öquist and Chow, 1992) So the linear relationship should ideally be determined for each plant species.

In another approach, Genty et al. (1989) reported an almost linear relation between the Chl fluorescence parameter $(1 - F_s/F_m')$ and ϕ_{CO2} in wild type barley, maize and Chl *b*-less barley, where ϕ_{CO2} is the ratio of the

rate of carbon assimilation to the irradiance or quantum yield of carbon assimilation, and F_s and F_m' are the steady-state and maximum Chl fluorescence yield during actinic illumination, respectively. Seaton and Walker (1990) examined a number of C3 and C4 species, obtaining a seemingly universal curvilinear relation between $(1 - F_s/F_m')$ and ϕ_{CO2}. They also showed that the major oscillations in the oxygen evolution observed in spinach could be predicted from concurrent measurements of $(1 - F_s/F_m')$, using a linear relation derived from data for several species not including spinach. Furthermore, Edwards and Baker (1993) demonstrated that Chl fluorescence parameters could be used to predict accurately and rapidly CO_2 assimilation rates in maize, a C4 plant. Despite these successes, however, some exceptions to a single curvilinear correlation were found, notably in the Chl *b*-less barley mutant (Öquist and Chow, 1992). Therefore, Chl fluorescence is not yet a perfect substitute for gas-exchange measurements during steady-state photosynthesis in continuous light.

Illumination with saturating single-turnover, repetitive flashes in the presence of far-red light has been used to quantify PS II reaction centres in leaf tissue (Chow et al., 1989; Chow et al., 1991). This is one of the most direct methods, relying on the reasonable assumption that each functional PS II will evolve one oxygen molecule after four flashes. The content of functional PS II obtained by this technique in a number of plant species is slightly smaller than the total content of PS II, assayed as 3-(3,4-Dichlorophenyl)-1,1-dimethylurea-binding sites, the ratio of functional PSII to total PSII being 0.88 on average (Chow et al., 1989). Herbicides-binding sites refer to the total number of PSII complex, a small fraction of which may not undergo a successful charge separation that leads to oxygen evolution. Such a miss factor may explain in the ratio of functional PSII to total PSII being 0.88 on average (Chow et al., 1991). Although the oxygen yield per flash can be measured from leaf segments without artifacts that may arise from the isolation of thylakoids, it is time-consuming to accumulate a measurable quantity of oxygen that is evolved only after many

flashes. Therefore, surrogate Chl fluorescence parameters have been used to substitute for the oxygen yield per flash as a measure of the fraction of functional PSII. Commonly, the ratio of variable to maximum fluorescence yield in the dark-adapted state, F_v/F_m, a measure of the maximum photochemical efficiency of PSII, is used to indicate loss of functional PSII reaction centres after, for example, photoinactivation. The rationale is that, as more and more non-functional PS II reaction centres are formed, a greater proportion of the absorbed light energy is dissipated as heat rather than being used for photochemistry; the overall photochemical efficiency of PSII is, therefore, decreased. Measurement of F_v/F_m is rapid, but is sometimes not linearly related to the content of PS II as assayed by the oxygen yield per flash (Park et al., 1996).

Another Chl fluorescence parameter, $1/F_o - 1/F_m$ (Havaux et al., 1991; Walters and Horton, 1993), where F_o is the minimum Chl fluorescence yield corresponding to open PS II reaction center traps in the dark-adapted state, has been found to be linearly correlated with the oxygen yield per flash (Lee et al., 1999; Lee et al., 2001; Kim et al., 2001) which is itself linearly correlated with the light-limited quantum yield of oxygen evolution under steady light (Chow et al., 2002). In the case of photoinhibited capsicum leaf tissue, the linear correlation between $1/F_o - 1/F_m$ and the oxygen per flash can be comfortably constrained to pass through the origin (Lee et al., 1999; Lee et al., 2001). In cucumber (Kim et al., 2001) or in some batches of capsicum grown under different conditions, however, the straight line does not pass through the origin. Thus, a precise measure of the content of functional PSII reaction centres from Chl fluorescence requires a predetermined calibration of the fluorescence parameter against the oxygen yield per flash for a particular plant species grown under specific conditions.

It appears that the main obstacle to establishing a universal relation between a change in a Chl fluorescence parameter and that of the oxygen yield per flash after a photoinhibition treatment is that the former is

representative of the chloroplasts near the measured leaf surface, while the oxygen measurement refers to the whole tissue; variation in the relation between the two measures may be because of a variation in leaf anatomy. In a search for a rapid, whole-tissue assay of functional PS II reaction centres remaining after photoinhibition treatment, we explored the flash-induced delivery of electrons from PS II to P_{700}^{+} (dimeric Chl cation in PSI reaction centre), the oxidized primary donor in PSI. Depending on the functionality of PSII, the number of electrons delivered by a flash from water to P_{700}^{+} will vary. Using a new type of modulation system, Schreiber et al. (1988) detected P_{700}^{+} formation by an absorbance change at 830 nm, a wavelength at which the radiation, not being absorbed by the bulk pigments in leaves, is able to penetrate the whole tissue. Using this signal, Asada et al. (1992) estimated the pool size of electrons that can be donated, from stromal components via the intersystem chain, to P_{700}^{+} in leaves. Further work by these workers showed that such an electron pool size in leaves is much larger in the C4 plant maize than in C3 plants (Asada et al., 1993). As the P_{700}^{+} signal at this wavelength is contaminated to some extent by absorbance changes of plastocyanin and ferredoxin (Harbinson and Hedley, 1989; Klughammer and Schreiber, 1991; Oja et al., 2003), a reference wavelength at 780 nm is used to obtain a purer P_{700}^{+} signal (Klughammer and Schreiber, 1998). In this study, we used the dual-wavelength system to monitor the concentration of P_{700}^{+} and examine whether the signals of P_{700}^{+}, representing the whole tissue, may be more robustly correlated with the oxygen yield per flash among different plant species representing C3 and C4 modes of photosynthesis, herbaceous and woody species, a wild-type and a Chl-b-less mutant, and monocot and dicot plants.

MATERIALS AND METHODS

Growth of plants

Capsicum annuum L. cv Newtown No. 3 plants were grown at 24/21 °C (day/night), with a 10-h photoperiod (300 μmol photons $m^{-2}s^{-1}$). The potting mixture was supplemented by a slow release fertilizer. Barley (wild-type and Chl-b-less mutant) plants were grown at 20/16 °C, 12-h photoperiod, and 300 μmol photons $m^{-2}s^{-1}$. *Arabidopsis thaliana* cv Columbia wild-type plants were initially grown in a high (0.5%) CO_2 environment (22/19 °C, 10-h photoperiod, 150 μmol photons $m^{-2}s^{-1}$) and were acclimated in normal air in a growth chamber (23/18 °C, 8-h photoperiod, 150 μmol photons $m^{-2}s^{-1}$) for 7–10 days before use. *Flaveria bidentis* L. plants were grown in a temperature-controlled glasshouse (30/20 °C) during summer/autumn with PAR regularly reaching 1600 μmol photons $m^{-2}s^{-1}$. Peach *(Prunus persica* (L.) Batsch var. laevis) nectarine cv Red Gold was grafted on seedling rootstock, and the well-watered and fertilized plants were grown in the open during summer.

Photoinhibition treatment

Leaf discs were floated ab-axial side up, in a position that facilitates gas exchange (Sun et al., 2006), on a 1 mM lincomycin solution for 2 h in darkness. They continued to float with the ab-axial side up on the lincomycin solution (23 °C) during illumination on the ad-axial side at 750–1300 μmol photons $m^{-2}s^{-1}$. The photoinhibition light was directed vertically upwards through a transparent water bath to reach a clear Petri dish in which the leaf discs were floated.

PSII functionality

The functional PSII content was quantified by flash induced oxygen evolution, using repetitive single turnover, saturating xenon flashes and assuming that each functional PSII evolves one O_2 molecule after four

flashes (Chow et al., 1989, Chow et al., 1991). A gas-phase oxygen electrode (Hansatech, King's Lynn, UK) was adapted to receive saturating, single-turnover flashes from a xenon lamp (type FX200, EG & G). The upper water jacket was disused; instead, the lid and the water were removed to allow close access of the flash lamp to the leaf disc in the chamber. A Calflex C heat-reflection filter was placed in front of the flash lamp to prevent UV (and heat) from reaching the leaf disc, while visible light was readily transmitted. The old model gas-phase oxygen electrode, with a thick Perspex layer above the leaf disc, also helped to absorb any UV that might have leaked through the heat-reflection filter. The flash lamp output was determined by a 0.72 μF capacitor, which was charged to 1500 V. With this small capacitance, the flash duration (full width at half peak height) was about 3 μs, close to being single turnover. Precaution was taken to minimize temperature drifts affecting the signal, which by necessity was highly expanded. Flashes were given at 10 Hz. The first train of flashes over a 6-min interval were given to fully activate the functional PSII complexes, followed by a 6-min dark period, then another 6-min flash illumination and one more dark period. The gross rate of oxygen evolution during the second train of flashes, taking the average dark drift into account, when compared with the flash frequency, gives the oxygen yield per flash. A piece of green cloth was substituted for the leaf disc to test for any heating artefact as a result of the flash, and the signal was corrected for the heating artefact when necessary. The O_2 yield $flash^{-1}m^{-2}$ of photoinhibited leaf segments was normalized to the value of the non-photoinhibited control to obtain the functional fraction of PSII.

Measurement of redox kinetics of P_{700}

After oxygen measurements, leaf segments of each species were used for measurement of redox changes of P_{700}, with a dual-wavelength (820/870 nm) unit (EDP700DW) attached to a pulse amplitude modulation fluorometer (Walz, Effeltrich, Germany) and used in the reflectance mode

(Chow and Hope, 2004a). To obtain redox changes as the result of a flash superimposed on continuous far-red light, a steady state was sought by illumination with far-red light (12 μmol photons $m^{-2}s^{-1}$, peak wavelength 723 nm, 20 nm full width at half peak height, 102-FR, Walz) for ≥2 min. Then a single-turnover xenon flash (XST 103 xenon flash) was applied to the ad-axial side of the leaf disc. When necessary, the transmitted energy of the flashes was lowered in steps by introducing neutral-density films. Timing of triggering the flash, the start of data acquisition (time constant = 95 μs) and the repetition rate of flash illumination were controlled by a pulse/delay generator (Model 555, Berkeley Nucleonics Corporation, San Rafael, CA). The analogue output (of duration 700 ms in all cases except for the C4 species, *F. bidentis*, for which the duration was 900 ms) from the fluorometer was digitized and stored in a computer using a home-written program. Flashes were given at 0.2 Hz, and 25 consecutive signals were averaged. The maximum signal immediately after the flash was taken as the total amount of photo-oxidizable P_{700} and used to normalize the trace.

A kinetic model of the redox kinetics of P_{700}^{+}

Consider a reservoir of P_{700}^{+}, at a fractional concentration y, the maximum value of y being 1.00. Under far-red illumination of leaf discs, P_{700}^{+} is generated by photo-oxidation at a rate $k_o(1 - y)$, where k_o is the rate coefficient of photo-oxidation. P_{700}^{+} is reduced by a steady basal electron flux B.

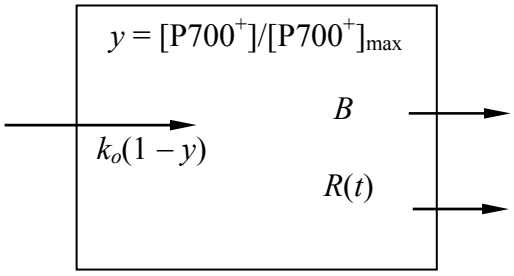

The photo-oxidation rate $k_o(1 - y)$ depends on such factors as the far-red irradiance and the effective antenna size of PS I. The basal rate B may have a number of contributing factors, e.g. (1) far-red light induced PS II activity (Chow and Hope, 2004a; Hughes et al., 2006); (2) far-red light induced cyclic electron flow around PS I; (3) reducing power originating in the stroma or the cytosol; and (4) any charge recombination in PS I during far-red illumination. This steady electron flux prevents complete oxidation of P_{700} by far-red light. When a flash is applied, a transient electron flux arrives (mainly from PS II) at P_{700}^+ with a time-dependent rate $R(t)$, while at the same time, far-red light restores y to the steady-state value y_{ss}. In the steady state, $R(t) = 0$, so $B = k_o(1 - y_{ss})$, with the oxidation state of P_{700} determined by B and k_o. At a given instant, the rate of increase of y is

$$dy/dt = k_o(1 - y) - B - R(t) \qquad (1)$$

$$\therefore \; R(t) = k_o(1 - y) - B - dy/dt \qquad (2)$$

The total transient electron input to PSI is

$\Sigma = \int_0^T R(t)dt$, where time T is long enough so that $y_T \to y_{ss}$.

Substituting $k_o(1 - y) - B - dy/dt$ from Equation (2) for $R(t)$,

$$\Sigma = (1 - y_{ss}) + k_o \int_0^T (y_{ss} - y)dt \qquad (3)$$

Integration of the algebraic difference between y_{ss} and y was performed over the time interval from 0 (flash trigger) to T. Evaluation of Σ, however, required an estimation of k_o. To estimate k_o, we fitted the kinetic trace from time 0 to T, using the explicit expression for $R(t)$. We

empirically describe the rate at which electrons arrive at P_{700}^{+} by the equation:

$$R(t) = R_{\max}(1 - e^{-k_d t})e^{-k_p t},$$

where R_{max} is the maximum rate of electron arrival that decayed with the rate coefficient k_p, which describes the speed with which the rate of electron delivery to PSI was diminished. To take account of a slight delay (approximately 2–4 ms) in the downward trend of the signal after the flash and to improve the curve fitting, we introduced the factor $[1 - \exp(-k_d t)]$ where the rate coefficient k_d is inversely related to the duration of the delay. Equation (1) then becomes

$$\frac{dy}{dt} + k_o y = R_{\max} e^{-(k_d + k_p)t} - R_{\max} e^{-k_p t} + (k_o - B) \qquad (4)$$

This linear first order differential equation is of the form

$$\frac{dy}{dt} + P(t)y = Q(t)$$

With the boundary conditions that (1) when $t = 0$, $y = 1.0$ and (2) as $t \to \infty$, $y_{ss} = B/k_o$, Equation (4) was solved to give

$$y = \frac{R_{\max}}{k_o - k_d - k_p} e^{-(k_d + k_p)t} - \frac{R_{\max}}{k_o - k_p} e^{-k_p t} + \left(\frac{R_{\max}}{k_o - k_p} - \frac{R_{\max}}{k_o - k_d - k_p} + 1 - y_{ss} \right) e^{-k_o t} + y_{ss} \qquad (5)$$

Equation (5) was used to fit each kinetic trace using the software Origin 7.0 (Origin Lab Corporation, Massachusetts, USA), allowing the parameters R_{max}, k_o, k_d and k_p to vary from their initial guess values and to

converge after the iterations. The resulting k_o value was used to evaluate Σ according to Equation (3).

Measurement of PS II photochemical efficiency by Chl fluorescence (F_v/F_m)

After oxygen measurements, leaf segments of each species were used (at about 30-45 min after cessation of photoinhibition treatment) for the determination of the minimal (F_o) and maximal (F_m) fluorescence yield using a phase amplitude modulation fluorometer (Walz, Effeltrich, Germany) fitted with blue excitation modulated light (0.1 μmol $m^{-2}s^{-1}$). The whole spectrum of Chl fluorescence was detected from 660nm to longer wavelengths so as to minimize the relative contribution of PSI. Chl fluorescence was measured on both the ad-axial and ab-axial side of each leaf segment. In the case of capsicum, F_v (= $F_m - F_o$) and F_m were measured with a Plant Efficiency Analyzer (Hansatech, King's Lynn, UK).

RESULTS

Ad-axial and ab-axial measurements of F_v/F_m

PSII functionality was monitored in leaf segments after photoinactivation in the presence of lincomycin, an inhibitor of repair that depends on chloroplast-encoded protein synthesis. The number of functional PSII complexes in leaf segments was quantified by the oxygen yield per flash, followed by measurement first of the flash-induced redox kinetics of P_{700} and then of F_v/F_m in the same leaf samples on both the ad-axial and ab-axial surfaces. Fig. 1A shows the correlation between the ad-axial F_v/F_m and the oxygen yield per flash for two herbaceous species, one monocot and its Chl-b-less mutant, and a woody species and a C4 species. In general, a somewhat linear relation was observed (r^2 = 0.83 in a linear regression), although there was considerable scatter, with greater deviation of nectarine and *F. bidentis* from linearity and from the general line. When

ab-axial F_v/F_m was correlated with the oxygen yield per flash, the relation was curvilinear, the initial loss of functional PSII reaction centres having minimal impact on ab-axial F_v/F_m (Fig. 1B). In this plot, it was *Arabidopsis* and *F. bidentis* that deviated most from the general curve. The average of ad-axial and ab-axial F_v/F_m seemed to be more linearly correlated with the oxygen yield per flash (Fig. 1C, $r^2 = 0.91$).

Redox kinetics of P_{700} induced by a flash in the presence of far-red light

In the presence of far-red light, the majority (almost 90%) of P_{700} was oxidized in the steady state (Fig. 2). When a xenon flash was superimposed, the remaining P_{700} was oxidized, giving a transient peak signal corresponding to the full content of photo-oxidizable P_{700}. Normalized to the transient peak value, the kinetic traces depict the fraction of P_{700} in its oxidized form at any instant. Thus, as electrons arrived at P_{700}^+ from PSII, a downward signal corresponded to chemical reduction of P_{700}^+. Concurrently, the continuous far-red light was oxidizing P_{700} back to the steady-state level. Fig. 2A shows that with increasing extent of photoinactivation of PSII, the dip in the signal became increasingly shallow, as fewer and fewer electrons per flash were delivered to PSI. A measure of the transient electrons arriving at P_{700}^+ per flash is given by the parameter Σ (see Equation 3 in Materials and methods). Evaluation of Σ requires an estimation of k_o. We estimated k_o. by fitting each trace with Equation (5), allowing four parameters to vary during fitting until they each converged to a constant value. Fig. 2B shows an example of a curve fitted to the data points. The k_o obtained from the fit allowed us to calculate Σ. It was important to ascertain that the Σ value was maximal at the full flash intensity. If the flash were not saturating, some PSII reaction centres would not be sampled in the measurement. Fig. 3 confirms that the flash was indeed saturating in terms of the value of Σ.

Correlation between Σ and the oxygen yield per flash

Fig. 4 depicts the linear correlation of Σ with the oxygen yield per flash for the various plant species. This correlation had much less scatter (r^2 = 0.96) compared with those using either ad-axial or ab-axial F_v/F_m or their average (Fig. 1). That is, the outlying data points of peach and the C4 species (Fig. 1A,B) and Arabidopsis (Fig. 1B,C) were in this measurement much closer to the single straight line for all plant species (Fig. 4). There was, however, a residual value (0.083) of Σ when the oxygen evolution per flash was zero.

DISCUSSION

Disadvantages of using Chl fluorescence to predict the functional fraction of PSII

The functional fraction of PSII or the absolute content is needed to evaluate such quantities as the rate coefficient of photoinactivation, the quantum yield of photoinactivation and the rate coefficient of repair (Chow et al., 2005). While Chl fluorescence (F_v/F_m) can be conveniently and non-intrusively used to indicate functionality of PSII, the exact relation of F_v/F_m to the oxygen yield per flash depends on plant species and experimental conditions. For example, when plotted against the relative functional PSII content (oxygen yield per flash) after photoinactivation treatment, F_v/F_m may be a (1) straight line that can be comfortably constrained to pass through the origin in the case of capsicum (H.-Y. Lee and W.S. Chow, The Australian National University, Canberra, unpublished material), (2) a straight line intercepting the x-axis above zero with a curved region at high values (Park et al., 1996) or (3) a curvilinear line that intercepts the x-axis above zero in the case of peach and a C4 species (Fig. 1A). Thus, each species has to have a calibration done to establish the exact relationship beforehand. Bearing in mind that the relationship between F_v/F_m and the

oxygen yield per flash may vary according to growth conditions even for a given species, a precise application of Chl fluorescence to determine the fraction of functional PSII is hampered by the absence of a "universal" relationship between the two parameters for all plant species. If one is to use F_v/F_m as a measure of the relative content of functional PSII during progressive photoinactivation, then one should at least use the average value for the ad-axial and ab-axial surfaces.

Another Chl fluorescence parameter, $1/F_o$ - $1/F_m$ (Havaux et al., 1991; Walters and Horton, 1993), has been found to be linear with the oxygen yield per flash in all cases tested so far. The straight line, however, has variable slope; it passes through the origin or close to it in the case of capsicum (Lee et al., 1999) but typically intercepts the y-axis above zero (e.g. cucumber, Kim et al., 2001; Arabidopsis, E.-H. Kim and W.S. Chow, The Australian National University, Canberra, unpublished material).

A likely factor that hampers the existence of a single relationship between a Chl fluorescence parameter and the oxygen yield per flash among various plant species is the fact that Chl fluorescence is detected from chloroplasts near the leaf surface being measured. Excitation light, whether red or blue, is quickly attenuated with depth in the leaf tissue, and any Chl fluorescence from the deeper tissue is readily reabsorbed by Chl, so that only the superficial layers of chloroplasts are sampled. On the other hand, the oxygen yield per saturating flash is representative of the whole tissue. When PSII complexes near the ad-axial surface are photoinactivated preferentially, then one would expect a correlation of ad-axial F_v/F_m with the oxygen per flash to curve downwards, as hinted in Fig. 1A; conversely, a correlation of ab-axial F_v/F_m with the oxygen per flash should curve upwards, as observed (Fig. 1B). Despite such shortcomings, Chl fluorescence provides a rapid and convenient measure of photosynthetic performance and non-photochemical dissipation in plant materials. Only when a universal relationship between a measured parameter and whole tissue performance is required does one need to find an alternative to Chl

fluorescence. When that need arises, the chosen conveniently measured parameter must, like the functional PSII content, involve measurement of the whole tissue.

Advantages in using P_{700} redox kinetics for monitoring PSII functionality

Measurement of P_{700} in a leaf segment involves the whole tissue. The measuring beam at 820 nm (with reference wavelength 870 nm) is readily transmitted through the tissue, being weakly absorbed. The actinic flash, provided it is saturating, as is the case in Fig. 3, is able to excite all PSII complexes in the tissue. As the whole tissue is sampled, it is much more likely that the P_{700} kinetic signal matches the oxygen signal, which is also induced by saturating flashes. Indeed, a plot of the transient electrons per flash against the oxygen yield per flash gave a straight line with relatively little scatter (compare Fig. 4 with Fig. 1). Even the Chl-b-less barely mutant, with only half the Chl content per unit area compared with the wild-type, followed the same straight line as the other plants (Fig. 4).

Measurement of the oxygen yield per flash has a significant scatter because of the small amount of oxygen evolved, especially from severely photoinhibited leaf segments. The measurement is also slow, each taking at least 30 min, including time for equilibration towards a stable baseline and for complete activation of the functional PSII complexes with flashes (Chow et al., 1991). In contrast, measurement of P_{700} redox kinetics requires only 1–2 min. While this is longer than required for measurement of F_v/F_m, the technique is akin to a Chl fluorescence measurement in that it is non-intrusive and can be applied on a leaf attached to a plant. Furthermore, portability of the equipment for data acquisition in the field and automatic evaluation of Σ are a real possibility in future.

Deficiencies in the method based on P_{700} redox kinetics

From Fig. 4, we see that the single regression line does not pass through the origin, but intercepts the y-axis at 0.083, although the intercept

is less than that of the plot of the average F_v/F_m (0.13, Fig. 1C). That is, about 8% of the flash-induced transient electrons appeared to arrive at P_{700}^+ even when there were no functional PSII reaction centres. The small amount of residue transient electrons could have travelled along a cyclic path involving PSI, while the majority originated in PSII. Alternatively, contamination of the P_{700}^+ signal by other components such as plastocyanin and ferredoxin could have been responsible for the apparent residual electrons. In any case, if the quantity Σ is used to evaluate the fraction of functional PSII, the small contribution of the residual 8% from flash-induced electron flow should be taken into account.

On close examination, the magnitude of Σ (approximately 0.7 units of P_{700}^+ in control samples) is less than the total content of P_{700}. This is an underestimation of the input of flash-induced electrons from PSII because the ratio of PSII to PSI reaction centres is considerably greater than 1.0 (Chow et al., 1988, Fan et al., 2007). For example, the PSII/PSI ratio is 2.1 in wild-type barley and 3.1 in Chl-b-less barley when grown in full glasshouse light (Chow et al., 1988) and 1.5 in wild-type Arabidopsis grown in a chamber (E.-H. Kim et al., unpublished material). Therefore, one expects more electrons per flash to be transferred from PSII to P_{700}^+ eventually than the magnitude of Σ indicates. Consistent with this expectation, even assuming a PSII/PSI stoichiometry of 2.0 and reasonable values for the kinetic coefficients and equilibrium coefficients for Cyt *f*/plastocyanine and P_{700}/plastocyanine reactions, we showed that not all of the electrons delivered into the high-potential components are expected to appear in P_{700}^+ immediately; an appreciable fraction resides on Cyt *f* and plastocyanine (Chow and Hope, 2004b). In fact, our modelling revealed that only 0.7–0.8 of P_{700}^+ was transiently reduced, despite a generation of 1 plastoquinol per flash and per P_{700}.

Because of the sharing of electrons among the high-potential components, determination of k_o in leaf tissue is difficult. Ideally, k_o should be measured from the time course of photo-oxidation of P_{700} when

plastocyanin is completely inhibited in the leaf tissue and electrons are rapidly withdrawn from the acceptor side of PSI. In practice, however, inhibition of plastocyanin is difficult to achieve in vivo. In Fig. 2B, the fitting of Equation (5) to the data points only gave an apparent k_o. This is because when a far-red photon oxidized P_{700}, another shared electron could quickly fill the electron hole. In that case, the k_o value obtained by curve fitting was only the net rate coefficient, not the gross rate coefficient of photooxidation by far-red light. The gross rate coefficient of photo-oxidation was probably about two-fold greater. A more rigorous determination of the true value of Σ will have to await a better method to determine k_o. The validity of the correlations reported here, however, is not affected by this factor.

Finally, it should be mentioned that the current study has been confined to leaves treated during a time interval in which photosynthetic acclimation to the light environment is negligible. In case of, e.g. cyanobacteria with rapid acclimation to light (MacKenzie et al., 2004), measurements of P_{700} can be much more complex. Furthermore, the present method of assaying electrons from PSII arriving at P_{700} is usable only if a treatment affects only PSII function but not PSI function.

CONCLUSIONS

We have found a single, robust linear relation between (1) Σ the integrated transient electron flow to P_{700}^{+} after a flash and (2) the fraction of functional PSII reaction centres, as assayed by the relative amount of O_2 per flash evolved from leaves of herbaceous and woody species, wild-type and Chl-b-less barley, monocot and dicot plants, and C3 and C4 species subjected to varying extents of photoinactivation of PSII. This correlation is far superior to that between (1) F_v/F_m measured on either leaf surface and (2) the fraction of functional PSII reaction centres, owing to the fact that Σ is a whole-tissue measure, as is the O_2 yield per flash. Measurement of Σ is non-intrusive, rapid and applicable to leaves attached to the plant; it may even be applicable in the field.

FIGURES

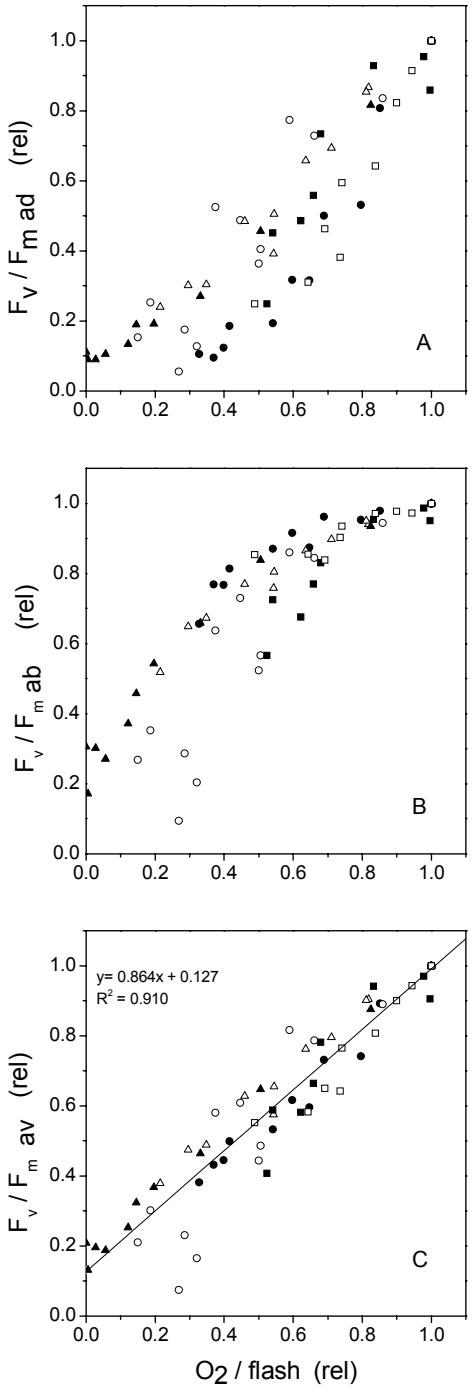

Fig. 1. Photochemical efficiency F_v/F_m, plotted against the functional fraction of PSII (relative O_2/flash), after various extents of photoinactivation. F_v/F_m was measured on the ad-axial surface (A), the ab-axial surface (B) and expressed as the average of the two values (C). The plant materials were nectarine (•), *Arabidopsis* (o), wild type barley (Δ), Chl *b*-less barley (■), capsicum (▲), and F.*bidentis* (□).

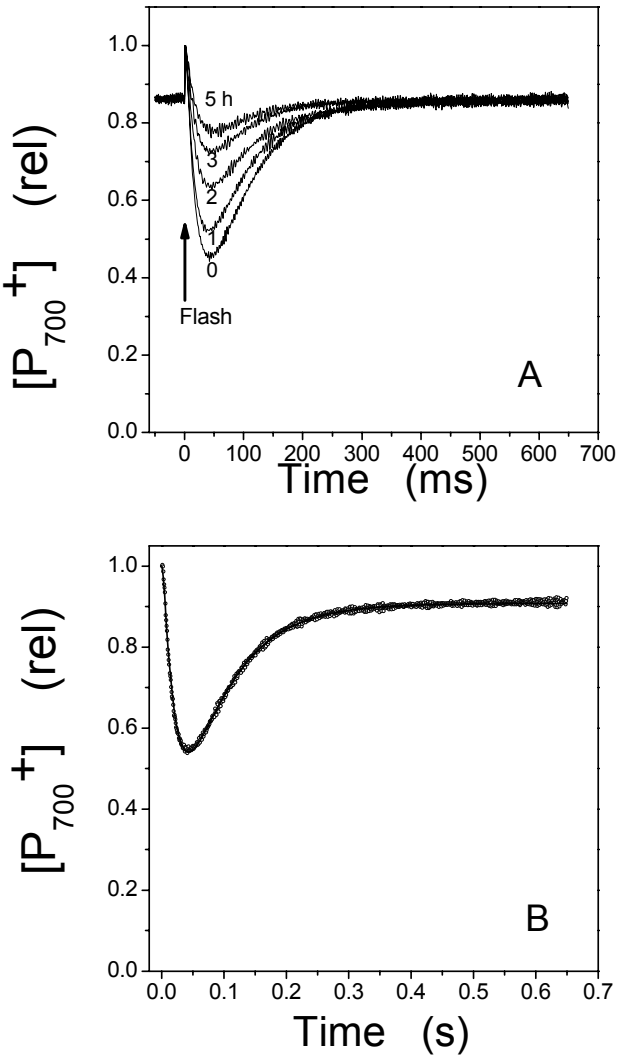

Fig. 2. Transient changes in the redox state of P_{700} upon adding a single-turnover flash to steady far-red light given to nectarine leaf segments. Leaf segments had been photoinhibited for various durations (0-5 h) prior to the measurement (A). In (B), the curve was fitted to the data points for a nectarine control sample using Equation (5).

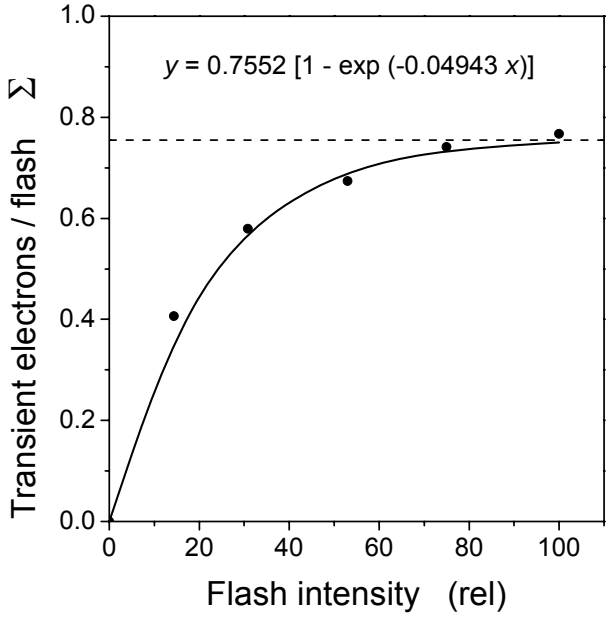

Fig. 3. The integrated flash-induced transient electron flow to P_{700} (Σ) as a function of relative intensity of flashes given to a nectarine leaf segment. The flash intensity was varied by plastic neutral-density filters.

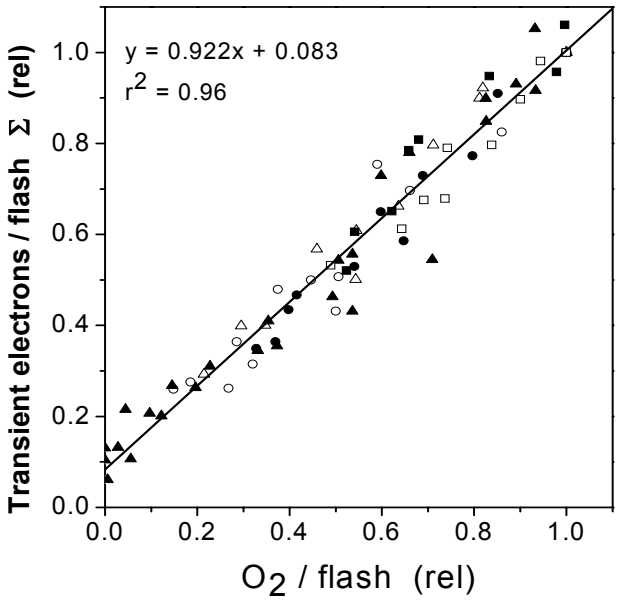

Fig. 4. Linear correlation of integrated flash-induced transient electron flow to P_{700} (Σ) with the functional fraction of PS II (relative O_2/flash) for all plant materials examined. Variations in both parameters were achieved by varied durations of photoinhibition. The plant materials were nectarine (●), *Arabidopsis* (o), wild type barley (Δ), Chl *b*-less barley (■), capsicum (▲), and F.*bidentis* (□).

Chapter IV

MODULATING THE LIGHT ENVIRONMENT WITH THE "ASYMMETRIC ORCHARD": EFFECTS ON GAS EXCHANGE PERFORMANCES, PHOTOPROTECTION AND PHOTOINHIBITION

INTRODUCTION

The energetic basis of orchard productivity lies in the interaction between the tree and sunlight. The amount of dry matter produced by a tree is linearly related to the amount of light it intercepts (Monteith, 1977; Lakso, 1994). This concept drew the evolution of the new intensive plantation systems (Corelli Grappadelli and Lakso, 2007). The goal is to cover as soon as possible the ground with a photosynthetic surface in order to increase light interception, maintaining good light distribution, for improving productivity (Palmer, 1980). Orchard light interception is related to 2 main factors: light intensity and planting density. Theoretically, the same orchard light interception could be obtained decreasing the number of plants and increasing the irradiance, with an expected change in orchard yield. Several Authors found a direct relation between planting density and fruit yield (t ha^{-1}) as a consequence of an increased Leaf Area Index (LAI) and orchard light interception (Caruso, 2000; Nuzzo et al., 2002; Guerriero et al., 1980; Loreti et al., 1989; Hutton et al., 1987; Chalmers and van Den Ende, 1989; Corelli Grappadelli et al., 2000). Not always though, a direct relation between light intensity and productivity was recorded. No difference for orchard yield was recorded on peach cv Ross trained as

Cordon and Kearney Agricultural Center Perpendicular V (KAC-V) at 1196 trees per hectare; nevertheless, the Cordon training system intercepted more light than the KAC-V (Grossman and DeJong, 1998).At the single tree level, for the Open vase (299 pt ha^{-1}), Cordon and KAC-V training systems a similar crop efficiency (expressed as fruit dry weight on trunk diameter) was recorded even if the Open vase intercepted less light than the KAC-V and the Cordon, respectively (Grossman and DeJong, 1998).

Photosynthetic Photon Flux Density (PPFD) gives energy for the electron transport generating ATP and reducing power (NAPDPH(H^+)) used in the Calvin-Benson cycle for carboxylation. Leaf net photosynthesis increases with PPFD until no improvement is found for increasing light irradiance (Bohing and Burnside, 1956). The light intensity above which the response becomes flat is called the saturation point. This can be different for plant species, plant nutritional and water status, light environment during leaf growth and leaf age. In grape (*Vitis vinifera* L.) a saturation point of ~ 800-1000 μmol $m^{-2}s^{-1}$ was recorded (Escalona et al., 1999; Iacono and Sommer, 1999); in apple (*Malus* x *domestica* Borkh) leaf net photosynthesis increased linearly until 400-1000 μmol $m^{-2}s^{-1}$. This high variation was dependent by leaf Nitrogen content (Cheng et al., 2001). In kiwifruit (*Actinidia deliciosa* - (A.Chev.) C.F.Liang.& A.R.Ferguson) no net photosynthesis increase was recorded above 700 μmol $m^{-2}s^{-1}$ in shade grown leaves (250 μmol $m^{-2}s^{-1}$) and above 1000 μmol $m^{-2}s^{-1}$ in highlight adapted ones (Greer, 2001; Greer and Halligan, 2001). In peach (*Prunus persica* L.) the saturation point was reached at about 700-900 μmol $m^{-2}s^{-1}$ (Kappel and Flore, 1983; Gaudillere and Moing, 1992). In several parts of the world, under clear sky the PPFD reaches commonly 2000 μmol $m^{-2}s^{-1}$ or above (Nobel, 1983), therefore for photosynthesis at leaf level, about half of the available light may be in excess (Corelli Grappadelli and Lakso, 2007). Furthermore, ameliorating effects were found for the photosynthetic performance in apple and in grapefruit (*Citrus paradisi* L.) reducing the

excessive light interception with light reflective kaolin particles sprayed on the leaves (Glenn et al., 2001; Jifon and Syvertsen, 2003).

At the whole tree level however, the saturation point is not always easily detectable. Genetically dwarf peach cv Valley Red didn't reach a steady state when photosynthesis was measured on entire trees (Corelli Grappadelli, 1996). On the other hand in grape fruit, plants covered with 30% and 60% shading net assimilated more dry matter than non shaded ones (Raveh et al., 2003). Whole plant gas exchange measurements carried out on apple trees sprayed with kaolin showed that reducing light and canopy temperature, net photosynthesis increased as a response to the reduced environmental stress (Glenn et al., 2003).

Energy absorbed by plant is managed through several pathways involving thermal processes, fluorescence and photochemistry, all of which are competitive mechanisms. The main purposes of these pathways are the photosynthetic carboxylation and the dissipation of energy excess for limiting Reactive oxygen species (ROS) formation and photo-oxidative risks (Niyogi, 1999). Light dependent thermal dissipation could be divided into photo-protective quenching and PSII photoinactivated re-emission (Björkman and Demming-Adams, 1994). The former is realized by the xanthophyll cycle and is able to dissipate up to 75 % of the total absorbed energy (Demming-Adams et al., 1996). The key enzyme of this mechanism, violaxanthin de-epoxidase (VDE), is in the thylakoid lumen and its activity is strictly trans-thylakoidal ΔpH dependent (Ort, 2001). In particular the maximum VDE activity is reached when lumen pH is lower than 6.5 (Bratt et al., 1995). Photo-inactivated PSII quenching is an un-controlled process, caused by thermal re-emission of photodamaged PSII complexes (Walters and Horton, 1993; Müller et al., 2001; Lee et al., 2001; Matsubara and Chow, 2004). Recent research suggests that this dissipation pathway could be considered as a slow, reversible, protective mechanism since damaged complexes could work as light screen, protecting the surviving PSII from photon pressure. On the other hand, the remaining functional PSII are

necessary to create the pH environment for new protein synthesis in chloroplasts, aimed to repair (Sun et al., 2006). Photodamaged PSII thermal dissipation contributes in small amount because the complexes are quickly repaired (Aro et al.,1994; Matoo and Endelman, 1987; Matoo et al., 1984). The remaining absorbed energy is utilized to move electrons through several photochemistry processes, including photosynthesis. Electrons exiting the PSII core complex can be used to create reducing power for photosynthesis and photorespiration, otherwise can be dissipated via alternative transports such as the water-water cycle, cyclic transport around PSI and glutathione-ascorbate cycle (Niyogi, 1999). Moreover, these alternative energy users would pump supplementary H^+ into the lumen to generate the proton gradient across the thylakoid membrane supporting VDE activity (Heber and Walker, 1992; Asada, 1999; Noctor and Foyer, 1998). Despite this wide photo-protective pool, plants are not able to avoid photodamage. In fact during the day almost the whole PSII complex pool can be destroyed and quickly repaired (Chow and Aro, 2005).

Managing the energy captured by the tree arouses great interest among scientists. Through fluorescence measurements using the energy partitioning proposed by Cailly et al. (1996), modified by Hendrickson et al. (2004), it is possible to determine and compare the fraction of absorbed energy used in photosynthesis, quenched by thermal and photochemical protective processes and dissipated by damaged PSII. Moreover, with simultaneous fluorescence and gas exchange measurements a further partitions of photochemistry transports were proposed by several Authors, permitting to consider separately each process involved (Cheng et al., 2001; von Caemmerer, 2000; Galmés et al., 2007).

The goal of this study was to investigate, at whole plant level, the relation existing between light environment and photosynthetic performance, water use and PSII damage on peach. In addition, the effect of variation in photon pressure at the leaf level on energy management is considered.

MATERIALS AND METHODS

Plant material

Trials were carried out in 2006 at the University of Bologna Experiment Farm in Cadriano, Bologna, on 3-year-old trees of the peach nectarine *(Prunus persica* (L.) Batsch var. laevis) cv Alice col., grafted on GF305 rootstock, spaced 5 m between rows, while the spacing is variable along the row, depending on the treatment. This cultivar as a pillar growth habit naturally lending at forming spindle-type canopies. The orchard is called "asymmetric" because the rows vary in orientation and inclination, forming 3 different types of asymmetric light interception during the day. In addition to vertical, N-S oriented, trees forming the control, rows are either NW-SE (E) or NE-SW (W) oriented. The former are inclined 30° to the East from vertical, thus facing West, and the latter are 30° inclined to the West from vertical, thus facing Est. Each treatment is replicated three times in the orchard (Fig. 1-2),each rep containing 40-50 plants. In the N-S oriented rows trees were spaced 1.2 m. In the treatments W and E, trees were spaced 1 m along the row. The goal of this "unusual" tree arrangement was to increase the natural light variation during the day obtaining three different light environments at the same time of the day without modifying the remaining pedo-climatic conditions.

Whole plant measurements

Two plants with similar vigour, crop load and phytosanitary state, were chosen for each treatment .

During fruit cell extension (ST-III), when shoot growth is minimum, the daily whole plant intercepted radiation was measured in a clear day using a custom-built light scanner (Giuliani et al., 2000). The scanner is made up of a line of 48 PPFD sensors (NPN Silicon phototransistor P800, TRW Optron, TRW Inc., Carrolton, Texas, USA) spaced 0.05 m. Incoming PPFD was measured on unobstructed ground; after that the quantum sensor was

placed below the canopy. The light reaching the ground under the tree was measured moving the scanner parallel to the row, in order to cover the whole shadow cast by the tree, recording data every 0.2 m. The irradiance measured by each sensor was considered as representative of the PPFD falling on $0.01m^2$ (0.05m x 0.2m). The difference between the incoming full light and the light reaching the ground under the trees equals the total light flux intercepted by the plant ($\mu mol\ s^{-1}$).

Leaf area per tree was estimated by a calibration equation obtained plotting area against dry weight of an increasing number of leaves for each tree. At the end of the season all the leaves of each plant were collected and their dry weight was measured.

In ST-III and in post-harvest (PHV), whole-canopy gas exchanges were monitored using a custom-built open system, modelled after that described by Corelli Grappadelli and Magnanini (1993, 1997), with some modifications. Six polyethylene chambers were built, each enclosing one tree for 6 and 8 days in ST-III and PHV, respectively. Air was forced through each assimilation chamber by a fan and the flow of air was measured by a custom-built flow gauge, calibrated using the standard gas approach reported by Corelli Grappadelli and Magnanini (1993). Each flow gauge was connected to a CR10X datalogger (Campbell Scientific Ltd. Leicestershire, UK), continuously monitoring the flow rate. A sample of gas from the inlet and outlet manifold was drawn trough PVC tubes to an infrared gas analyzer (CIRAS SC, PP Systems, Hitchins, UK), for CO_2 (ppm) and H_2O (mbar) determination (Fig. 3). The CR10X datalogger also controlled the operation of a bench of solenoid valves which switched the inlet and outlet flows from each chamber to the IRGA. A complete set of readings for each plant included: measurement of water vapour pressure and CO_2 concentration at the inlet and outlet of the chamber and the amount of air flowing through that chamber. Each plant was monitored every 15 minutes. Whole-canopy net carbon and water exchange rate was calculated by multiplying the CO_2 and H_2O differential between the inlet and the

outlet of each chamber by the molar flow through the chamber (obtained from the flow measured, corrected for inlet air temperature). Dividing the gas exchange parameters for the total leaf area, the specific Net CO_2 Uptake (NCU μmol $m^{-2}s^{-1}$) and the specific transpiration (Tr_{WP} l m^{-2} h^{-1}) was calculated and hourly averages were computed for each chamber. The cumulative CO_2 and water loss was calculated integrating the hourly CO_2 uptake and transpiration. Incident light energy density flux (Wm^{-2}) was measured using a pyranometer attached to a weather station (AdCon telemetry GMBH, Austria) placed near the orchard. Since gas exchange parameters are strictly related to the environmental conditions (particularly to solar radiation) clear days with a similar radiative profile were chosen for the present analysis. In order to increase the number of replicates net carbon and water exchange values obtained from the two plants for each treatment were averaged.

Fully expanded leaves were used to calculate the quantum yield of photoinhibition (Qy). Leaf disks were floated in a lincomycin solution following the same protocol used by Losciale et al. (2008). The light treatment was imposed for 0, 30, 60, 90, 120 minutes at 800 and 1250 μmol m^{-2} s^{-1}. The PSII activity was detected by fluorescence measurements (F_v/F_m) on both leaf sides after 45 minutes of dark adaptation (Losciale et al., 2008) with a leaf fluorimeter attached to an open circuit infrared gas exchange system (Li-COR 6400, LI-COR inc., Lincoln Nebraska U.S.A.). PSII activity decay depends on photon exposure, the product between irradiance and time of exposure (mol m^{-2}) according to the reciprocity law (Nagy et al., 1995). Increasing photon exposure PSII activity decreases following a single exponential decay because the active PSII destroyed become limiting (Chow et al., 2005). Since in nature a quite complete recovery occurs continuously the maximum slope of the exponential function (Qy) represents the PSII amount destroyed by one mol of photons (μmol mol^{-1}). Multiplying Qy by the photon exposure intercepted by the whole plant it is possible to estimate the damaged PSII amount (μmol m^{-2})

in a known range of time (Hendrickson et al., 2004). Daily PSII damage was estimated using the quantum yield of photoinhibition, the intercepted light density (μmol s^{-1}) and leaf area measured on each plant.

Single leaf measurements

On the same trees, during fruit cell division (ST-I), stone hardening (ST-II), cell extension (ST-III) and post harvest (PHV) 6 attached, well exposed leaves were selected on the East and West side of each tree. The complex interaction among canopy side, row inclination and orientation should determine 6 different light environments. at all times during the day. Photosynthetic photon flux density (μmol m^{-2} s^{-1}), leaf and air temperature (ºC), gas exchange and fluorescence parameters were measured on the leaves 4 times in the day using an open circuit infrared gas exchange system fitted with a leaf fluorimeter and a PPFD sensor (Li-COR 6400, LI-COR inc., Lincoln Nebraska U.S.A.). Illumination was supplied by an artificial LED light source. Light intensity was previously set to the natural irradiance positioning the light sensor parallel to the leaf lamina before measurements. The maximum quantum yield of the total amount of Photosystem II (F_v/F_m) was measured predawn, after complete Photosystems relaxation and recovery during the night (Hikosaka et al., 2004).

Analysis of the partitioning of excitation energy

Quenching analysis was carried out using the model suggested by Hendrickson et al. (2004), combined with photosynthesis modelization proposed by von Caemmerer, (2000). Considering 1 the total amount of energy absorbed by photosystems:

$\Phi_{f,D} = F_s/F_m$ is the combined quantum efficiency of fluorescence and constitutive thermal dissipation. Variations in light do not alter this parameter (Hendrickson et al., 2004);

Φ_{NPQ} = $(F_s/F_{m'})$ – (F_s/F_m) is the quantum efficiency of light dependent thermal dissipation associated with inactivated PSII and promoted by the photo-protective non photochemical quenching via the xanthophyll cycle;

Φ_{PSII} = 1-$(F_s/F_{m'})$ is the quantum efficiency of photochemical transports used for photosynthesis, photorespiration, mitochondrial respiration and alternative transports (water-water cycle, cyclic transport around PSI and ascorbate-glutathione cycle);

To allow comparisons among all the energetic components, data were expressed as electron transport rates J (μmol m^{-2} s^{-1}) multiplying each quantum efficiency (Φ) for the total amount of electrons movable by the absorbed energy:

J_{TOT} = 0.5 x 0.85 x PPFD where the coefficient 0.5 takes in account that 1 electron is moved by 2 photons (Melis et al., 1987) and 0.85 is an average leaf absorptance (Schultz, 1996).

Through gas exchange measurements J_{PSII} could be partitioned into several components:

$J_{CO2} = P_n*4$ is the electron transport rate for net carboxylation, where P_n is the net carbon assimilation (μmol m^{-2} s^{-1}) multiplied by 4 electrons used to carboxylate 1 molecule of CO_2;

$J_{NC} = J_{PSII} - J_{CO2}$ represents the residual absorbed energy used for non net carboxylative processes such as photorespiration, alternative transports and dark respiration.

According to von Caemmerer, 2000:

$$J_A = \frac{(P_n + R_d)(4C + 8\Gamma_*)}{(C - \Gamma_*)}$$

is the electron transport rate to photosynthesis and photorespiration, where R_d (μmol m^{-2} s^{-1}) is the dark respiration, C is the chloroplast CO_2

concentration (μbar) and Γ* is the compensation point in absence of mitochondrial respiration (μmol m^{-2} s^{-1}). Therefore

J_{AT} = J_{PSII} - J_A represents the energy dissipated by alternative transports;

$J_R = J_A - J_{CO2}$ represents the energy used for mitochondrial respiration and photorespiration.

To evaluate a sorted behaviour of the data a multivariate principal component analysis (PCA) was performed in order to identify the main sorting parameters, using as variables: photosynthetic photon flux density (PPFD), stomatal conductance (g_s, mol m^{-2} s^{-1}) transpiration (Tr mmol m^{-2} s^{-1}), water use efficiency (WUE μmol $mmol^{-1}$), air temperature (T_{air}), leaf temperature (T_{lf}), Vapour pressure deficit (VPD, kPa), $J_{f,D}$, J_{NPQ}, J_{NC}, J_{CO2}, J_R and J_{AT}.

RESULTS

Whole tree

Light interception measurements were performed on July 7, a clear day, at 10.00, 11.00, 12.00. 13.30, 15.45, and 17.00 hours. W trees increased their light interception during the morning reaching the maximum value at 11.00 hours (426 μmol m^{-2} s^{-1}). In the following hours W trees light interception decreased and the lowest value was recorded at 17.00 hours (222 μmol m^{-2} s^{-1}). E trees showed the minimum value at 10.00 hours (237 μmol m^{-2} s^{-1}) and light interception gradually improved achieving the maximum at 17.00 hours (469 μmol m^{-2} s^{-1}) Control plants reached their maximum of intercepted energy at 10.00 hours (288 μmol m^{-2} s^{-1}) and decreased to the minimum value recorded at 12.00 hours (200 μmol m^{-2} s^{-1}). Afterwards light interception increased reaching 262 μmol m^{-2} s^{-1} at 17.00 hours (Fig. 4). W trees intercepted more light than E and C respectively, till

about 14.30 hours. Then E canopies started to intercept more light than the other samples and this difference was maintained until 17.00 hours. Excluding measurements performed at 10.00 and 17.00 hours, control plants showed the lowest light interception throughout the day (Fig. 4). Whole plant gas exchanges were measured from the 8th until the 13th of July in ST-III and from the 14th until the 21st of July after harvest. During fruit cell extension 4 days (10th -13th July) were chosen while 7 clear days (14th - 20th July) were selected in post harvest period. In ST-III the net assimilation daily patterns showed an increase for all treatments until 11.00 hours and no differences were recorded among the samples (Fig. 5A). The maximum net assimilation was recorded at 9.00 hours for C plants (~ 7.7 μmol m^{-2} s^{-1}) and at 10.00 hours for North-West inclined canopies (~ 7.9 μmol m^{-2} s^{-1}). The E treatment showed a further NCU increase reaching the maximum value at 12.00 hours (~ 7.95 μmol m^{-2} s^{-1}) remaining in a steady state until 14.00 hours; in the rest of the day E net photosynthesis gradually decreased. W and C net carboxylation diminished after 11.00 hours and no difference was detected between the two treatments (Fig. 5A). C showed lower values than E at 12.00 hours and at 13.00 hours. Excluding values recorded at 15.00 hours W net photosynthesis was lower than E from 13.00 till 17.00 hours. At 18.00 hours NCU became similar among three samples (Fig. 5A.). The transpiration (Tr_{WP}) increased until 11.00 hours without any difference among samples. W canopies reached the maximum value at 11.00 hours (0.108 l m^{-2} h^{-1}) with a subsequent decrease during the afternoon, while C and E continued to increase their transpiration reaching the maximum at 14.00 hours with values of 0.105 and 0.131 l m^{-2} h^{-1} for C and E plants, respectively; afterwards, Tr_{WP} decreased. Despite the fact that the maximum values were reached at two different times of the day, C and W transpiratory losses remained quite similar even in the afternoon and were lower than E until 14.00 hours. Afterwards, a difference was recorded between E and W and at 19.00 hours canopy transpiration was similar among treatments (Fig. 5B). Water use efficiency declined during the day

starting form the maximum value recorded at 6.00 hours (~ 0.046 mol l^{-1}) and reaching a steady state at 12.00 hours (~ 0.018 mol l^{-1}); no differences were re recorded among treatments (Fig. 5C). Cumulative CO_2 assimilation was similar and increased constantly until 14.00 hours (Fig. 6A). At 15.00 hours the assimilation rate started to change among the samples and at 18.00 hours E trees assimilated more CO_2 than C and W samples. Even though no differences were recorded, E daily uptake was 6 and 10% higher than C and W, respectively (Fig. 6A). The same pattern was followed by cumulative water loss and at 14.00 hours E plants lost more water than the remaining treatments (Fig. 6B). This difference was maintained until 18.00 hours when E canopies showed a daily water loss 10.5% and 14% higher than C and W plants, respectively (Fig. 6B). In post harvest, net photosynthesis increased during the morning until 8.00 hours maintaining quite similar values till 10.00 hours (Fig. 7A). No differences were recorded among treatments. C plants reached the maximum NCU at 8.00 hours (~7.62 μmol m^{-2} s^{-1}), while W samples showed the maximum specific assimilation at 9.00 hours (~ 7.88 μmol m^{-2} s^{-1}). After 10.00 hours net photosynthesis decreased in C and W canopies reaching the minimum values at 18.00 hours. At 15.00 and at 16.00 hours W net uptake was lower than C values (Fig. 7A). After 10.00 hours E NCU continued to increase reaching the maximum at 13.00 hours (~ 8.35 μmol $m^{-2}s^{-1}$), afterwards it decreased reaching the minimum at 18.00 hours (Fig. 7A). Excluding values recorded at 18.00 hours in the afternoon E tree showed higher NCU than the other two treatments (Fig. 7A). Whole canopy transpiration increased during the morning and W reached the maximum value at 10.00-11.00 hours (~ 0.105 l m^{-2} h^{-1}); afterwards a rapid decrease was observed over the following hours (Fig. 7B). C transpiration achieved the maximum value at 10.00 hours (~ 0.94 l m^{-2} h^{-1}) maintained a steady state until 15.00 hours, and decreased in the following hours (Fig. 7B). E transpiration continued to raise reaching the maximum at 14.00 hours (~ 0.128 l m^{-2} h^{-1}) and decreasing afterwards (Fig. 7B). No differences were recorded among

treatments during the morning. In the afternoon C transpiration was higher than W from 15.00 till 17.00 hours while E trees showed higher Tr_{WP} during the afternoon. At 18.00 hours no differences were recorded (Fig. 7B). Also in post harvest the water use efficiency was similar among treatments (Fig 7C.). The maximum value was recorded in the early morning (~ 0.05 μmol l^{-1}) and decreased reaching a minimum, steady WUE at 12.00 hours (~ 0.02 μmol l^{-1}). The CO_2 accumulation rate was constant in all trees until 13.00 hours and no differences were recorded among samples (Fig. 8A). At 14.00 hours E trees uptake rate started to raise and at 16.00 hours the cumulative CO_2 assimilation became higher than in the W trees. At 18.00 hours the daily CO_2 assimilation was 10.8 and 11.3% greater than C and W respectively (Fig. 8A). The daily water loss followed the same pattern and at 14.00 hours the transpiration rate started to be different among samples (Fig. 8B). At. 16.00 hours E canopies showed a higher cumulative water loss than W and this difference was maintained until 18.00 hours. E daily water loss was 15.6 and 16% higher than C and W plants (Fig. 8B).

At each measurement W trees showed a higher cumulative PSII damage than the other samples while in the morning the inactive PSII centers were similar between C and E (Fig. 9). In the afternoon the increase in damaged PSII in E was more rapid than C plants and at 17.00 hours E had more inactive PSII than C. At 17.00 hours the amount of damaged PSII was about 8 and 29% higher in W than E and C, respectively (Fig. 9).

Single leaf results

Measurements were performed the 16th of May, 12th -13th of June, 4th -5th of July and 10th of August in Step I, II, III and post-harvest, respectively. The incident radiation changed along the day in the 3 canopies from ~ 150 till ~ 2100 μmol $m^{-2}s^{-1}$.

The Multivariate Principal Component Analysis (PCA) showed that the two calculated engine-values (Factor I and Factor II) explained the collected

data sorting by more than 80%. This percentage fell under 70% only in ST-III (Fig. 10). In the 4 stages a significant, positive relation was recorded among $J_{f,D}$, J_{NPQ}, J_{NC} and PPFD, and these four parameters were strictly correlated to Factor I (factor loading, $r > 0.9$) while correlation among these parameters and the second engine-value was not statistically significative (Fig. 10). Excluding Stage III, Stomatal conductance (g_s) was highly correlated to Factor II ($r > 0.8$). During fruit cell expansion (ST-III) g_s didn't show any correlation with both engine-values (Fig. 10C) and the calculated factor loadings were 0.4 and 0.2 for engine-value I and II, respectively. Air temperature, leaf temperature and the vapour pressure deficit were more correlated to the second engine-value than to Factor I. T_{air}, T_{lf} and VPD were linearly related, while a negative correlation with stomatal conductance was found (Fig. 10). In all stages the correlation between J_{CO2} and Factor I was higher than with the second engine value. Although significative factor loadings ($r > 0.9$) were recorded in ST-II and PHV, in the remaining two stages it never exceeded 0.8 (Fig. 10B,D). The J_{CO2}/Factor II correlation was never significant, however J_{CO2}, J_R and especially J_{AT} showed the highest correlation with Factor II among all electron transport rates (Fig. 10).

The energy used in the several dissipating processes was expressed as electron transport rate and plotted against irradiance in each stage. $J_{f,D}$ increased linearly with PPFD (Fig. 11A-14A), while in all the stages J_{NPQ} increased following an expo-linear pattern ($r^2 > 0.99$), with increasing response until 800-1000 μmol $m^{-2}s^{-1}$, when the maximum slope was attained and the energy dissipated as heat started to increase linearly with light intensity (Fig. 11B-14B). The electron transport rate exiting PSII (J_{PSII}) followed an exponential pattern in all the stages ($r^2 > 0.96$). The maximum slope was reached at the lowest irradiances and the electron transport rate used in photochemistry reached a steady state around 1000-1200 μmol m^{-2} s^{-1} (Fig. 11C-14C). Also non net carboxylative transports (J_{NC}) increased exponentially with PPFD ($r^2 > 0.9$), reaching saturation at

~1000-1200 μmol m^{-2} s^{-1} and the maximum slope was recorded at low light intensities (Fig. 11C-14C). J_{CO2} was directly related to PPFD. Fitting an hyperbolic function to the data revealed a relevant scatter in ST-I (Fig. 11C). A similar pattern was followed in the remaining stages, although in ST-II the relation had much less scatter (r^2 = 0.95; Fig. 12C). Generally the electron transport rate effectively funnelled to net photosynthesis (J_{CO2}) increased linearly to a saturation point at about 1000-1200 μmol m^{-2} s^{-1} (Fig. 11C-14C). Partitioning J_{NC} allowed to calculate the energy allocated to respiration/photorespiration (J_R) and to the alternative transports (J_{AT}). J_R was also directly related to PPFD. In ST-I and II a linear relation was recorded and a curvilinear one in ST-III (Fig. 11D-13D). A curvilinear pattern was also found post harvest, although a considerable scatter was recorded (Fig. 14D). In all the stages examined, the relation between the electron transport for the alternative transports (J_A) and PPFD was not clear, although the highest values were always recorded at middle-high irradiances (Fig. 11D-13D).

DISCUSSION

Canopy inclination and row orientation were able to impose 3 different light environments in the field. W trees intercepted more light than E and C during the morning until 14.30 hours. Subsequently, E canopies received more direct light (in particular their West side) and their light interception became higher than C and W (Fig. 4).

Daily patterns for gas exchange parameters were similar in ST-III and post harvest. In spite of the light interception differences recorded in the morning, NCU and transpiration did not differ among treatments. Light seemed not to be limiting for net photosynthesis and the optimal water and temperature status occurring normally in the morning is not limiting for stomatal conductance in all treatments (Jifon and Syvertsen, 2003; Glenn et

al., 1999). At midday, W light interception was still the highest and NCU and Tr_{WP} started to decrease suggesting a stomatal limitation rather than a light influence (Fig. 5A,B; 7A,B). In the afternoon W light interception decreased while the opposite trend was followed by E and C plants. The same gradient among treatments was however maintained till 14.30 hours (Fig. 4). E canopies showed a further NCU increase till 14.00 hours while net assimilation continued to decrease in C and W trees. The NCU decrease in W might be related to stomatal closure. The evapo-transpiration demand increased in the afternoon and plants contrasted water loss with stomatal closure, which was followed by photosynthetic reduction (Fig. 5A,B; 7A,B). Probably the high photon pressure intercepted by W trees led to canopy temperature increases and to the increase in the strictly related vapour pressure deficit. Stomatal closure can reduce water loss and net photosynthesis (Burrows and Milthorpe, 1976; Farquhar and Sharkey, 1982; Shulze, 1986). Compared to W plants, the E canopy inclination reduced morning light interception and probably canopy temperature. VPD increased until 14.00 hours but not so critically to reduce the stomatal conductance and NCU. The increased evapo-transpiration demand led an increase in transpiration and the light environment, not limiting, maintained NCU at maximum values (Fig. 5A,B; 7A,B). A similar behaviour was observed in apple by Glenn et al. (2003), who applied highly reflective white particle film to tree canopies and reduced leaf temperature, stomatal limitation and increased whole plant net assimilation . In the afternoon C transpiration increased until 14.00 while NCU continued to decrease (Fig. 5A,B; 7A,B), probably due to stomatal closure caused by the increasing evapo-transpiration demand. After 15.00 hours E stomatal conductance probably decreased reducing water loss and NCU as well, regardless of the photon pressure increase (Fig. 5A,B; 7A,B). Even though E plants showed the best photosynthetic performances, WUE was similar among treatments because E was also the highest water user (Fig. 5C, 7C). The daily cumulative CO_2 uptake and water loss showed E plants assimilated 6 and

10% more than C and W in ST-III and 10.8 and 11.3% more in post harvest (Fig. 6A, 8A). This higher photosynthesis must be put in the perspective of higher water consumption, which was 10.5 and 14% more than C and W in ST III, and 15.6 and 16% in post harvest (Fig. 6B, 8B).

Lincomycin was able to inhibit PSII recovery permitting to observe the real damage occurring during the day. W canopies, which intercepted the most light, showed the lowest daily CO_2 assimilation (Fig. 9) and the highest PSII damage: about 50% of the total PSII population commonly found in higher plants (Chow and Aro, 2005). E plants had the highest photosynthetic performance and damage was 8 % less than W. The lowest photon exposure was recorded in C plants with PSII damage 29% lower than E and similar daily CO_2 uptake (Fig. 9).

The interaction among row orientation, inclination and canopy side increased light variability during the day, permitting to have a natural PPFD range of 150-2100 μmol $m^{-2}s^{-1}$at any time of the day. The multivariate principal component analysis showed that all electron transport rates (J) were correlated with Factor I and directly related to PPFD since their purpose should be to dissipate the incoming energy (Fig. 10). Stomatal conductance (g_s), air (T_{air}) and leaf (T_{lf}) temperature and vapour pressure deficit (VPD) were correlated with Factor II and g_s showed a negative correlation with T_{air}, T_{lf} and VPD. The latter is directly proportional to saturating vapour pressure and therefore to temperature. On the other hand, leaves coped with water loss reducing stomatal conductance (Gindaba and Wand, 2007). J_{CO2} and J_{AT} showed the weakest correlation to Factor I among all calculated electron transport rates (Fig. 10), but a fairly significant correlation with the second engine value (Fig. 10), suggesting a relation between these two energy users and Factor II, particularly with stomatal conductance and temperature (Farquhar, 1980).

$J_{f,D}$ was linearly proportional to light intensity (Fig. 11A-14A): the energy fraction ($\Phi_{f,D}$) dissipated in this way remained constant regardless of irradiance. As found by Hendrickson et al., (2004) this constant thermal and

fluorescence dissipation is un-affected by light intensity and is explained as a consequence of un-synchronized electron transport rate between P_{680}, Pheophytin and the primary quinone acceptor, increasing the life time of the radical pair P_{680}^{+} Ph^{-} (Chow, 2003). J_{NPQ} followed an expo-linear pattern reaching the maximum rate al 800-1000 μmol $m^{-2}s^{-1}$, while at middle-low irradiance it seemed to be limited (Fig. 11B-14B). Non net carboxylative transports (J_{NC}) increased quite linearly with PPFD until 1000-1200 μmol m^{-2} s^{-1}, following, probably, an enzymatic first-order relation (Fig. 11C-14C). The key enzymes involved in all the cycles were fully activated, therefore as more electrons were moved by light more electrons were dissipated via photochemistry. Above 1000-1200 μmol m^{-2} s^{-1} J_{NC} reached its maximum value maintaining a steady state probably because the electron carriers regeneration was limiting (Foyer, 1995). Even though non net carboxylative transports are generally more dangerous than NPQ, because with electron movement ROS formation risks increase, plants used these mechanisms first since NPQ appeared limited at middle-low irradiances. The xanthophyll cycle is strictly trans-thylakoidal ΔpH-dependent: the optimum lumen pH for violaxanthin de-epoxidase activity is under 6.5 (Bratt et al., 1995). Probably at middle-low irradiance thylakoid lumen was not so acid to completely activate VDE. The leaves thus tried to dissipate the energy excess using alternative ways (Fig. 11-14 B,C). It is noteworthy that the water-water cycle, cyclic transport on PSI and glutathione-ascorbate cycle all are able to increase the trans-thylakoidal ΔpH working as added engines to create the optimal pH environment for VDE (Heber and Walker, 1992; Asada, 1999; Noctor and Foyer 1998). Above 800-1000 μmol $m^{-2}s^{-1}$ lumen pH was probably optimal for VDE activation and J_{NPQ} started to increase linearly. So, also this response can be explained in terms of the amount of incoming energy.

Net photosynthesis, expressed as J_{CO2}, followed the usual saturating pattern when plotted against PPFD. After a linear increase J_{CO2} reached the saturating point at 1000-1200 μmol m^{-2} s^{-1} (Fig. 11C-14C). Further increases

in light intensity proved in excess and must be quenched by the remaining energy users, first of all non photochemical quenching. A considerable scatter was nonetheless recorded (Fig. 11C, 13C, 14C), probably because, as showed in PCA analysis, net photosynthesis was related to several parameters such as temperature and stomatal conductance as well as PPFD (Farquhar, 1980). In ST-II however, when the correlation between J_{CO2} and the first engine value was higher than 0.9 (Fig. 10B), a significant relation J_{CO2}/PPFD was recorded (Fig. 12C). J_R increased proportionally with PPFD showing linear (ST-I, III) or, sometime, curvilinear patterns (ST-II, PHV), however in all investigated cases it didn't reach a saturating point (Fig. 11D-14D). Photorespiration consumed CO_2 but might be a necessary loss to deal with light excess or other environmental stresses (Osmond, 1981; Galmés et al., 2007). In all the stages considered, J_{AT} didn't follow a clear pattern when plotted against PPFD (Fig. 11D-14D); probably this estimated electron transport rate was strictly linked to several parameters such as leaf temperature, chloroplast conductance, net photosynthesis, compensation point and dark respiration (see PCA analysis), easily influenced by the environment (von Caemmerer, 2000). As an example, in table 1 the effect of stomatal conductance and temperature on quenching partitioning is reported, maintaining PPFD constant. In leaves with relatively low conductance (0.17 mol m^{-2} s^{-1}) and high temperature, J_{CO2} decreased and light excess was funnelled to alternative transports (J_{AT}) without changing the other energy components (tab.1). Flexas et al. (2000) found a similar behaviour in grape where net photosynthesis decreased with stomatal conductance reduction but NPQ remained stable and alternative transports improved until stomatal conductance fell to 0.1 mol $m^{-2}s^{-1}$ (Flexas et al., 2000).

CONCLUSIONS

"Asymmetric" training system was a good way to study light energy, photosynthetic performance and water use relations in the field.

At whole plant and single leaf level net carboxylation increased with PPFD reaching a saturating point. Light excess rather than improve photosynthesis might emphasize water and thermal stresses leading to stomatal limitation. Intercepting less light, C plants showed the lowest photoinhibition but equalled W for CO_2 uptake and water use. E trees assimilated the highest CO_2 amount losing more water than C and W and their PSII damage was intermediate. The worst combination was found in W samples with the highest photodamage and CO_2 assimilation and water loss similar to the control plants. Too much light didn't promote net carboxylation but PSII damage. Since in nature the damaged Photosystems are quickly repaired with energy expense (Chow and Aro, 2005; Nixon et al., 2005), it would be important to investigate how much PSII recovery costs in terms of fruit and/or whole plant productivity.

Focusing on single leaf, incoming energy management seemed to be modulated by light photosynthesis. Net photosynthesis and the other photochemistry pathways increased linearly with PPFD while NPQ seemed to be pH limited. These alternative pathways were the principal quenching mechanisms in low light environment and might be used for creating the optimal trans-thylakoidal ΔpH for violaxanthin de-epoxidase as well. At over saturating light, when the xanthophyll cycle was fully activated, NPQ became the main dissipation pathway, further supported probably by photorespiration. Alternative transports and light irradiance relation was unclear, however these energy users seemed to be involved in dissipation at sub-optimal conductance range.

TABLES AND FIGURES

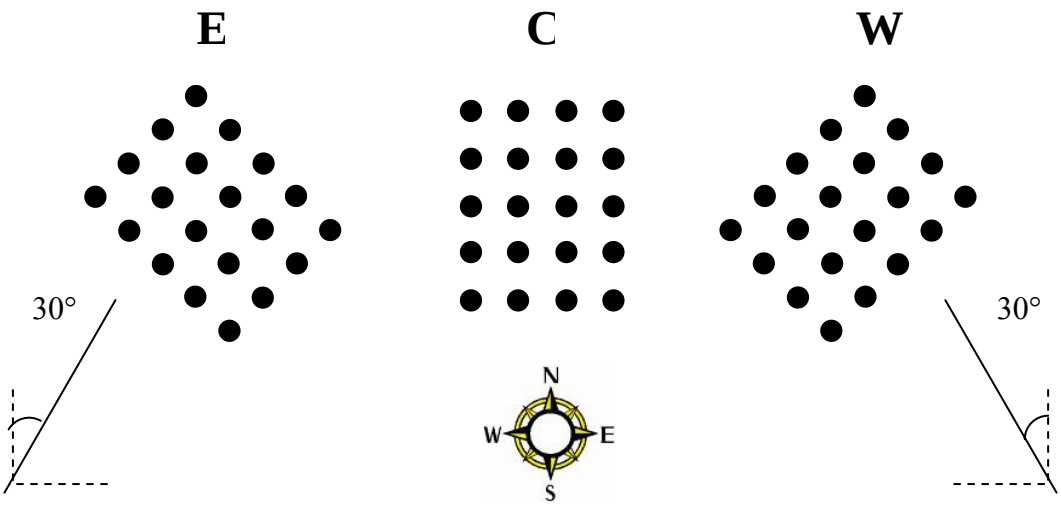

Fig. 1. Asymmetric orchard graphic representation.

Fig. 2. Asymmetric orchard during whole plant gas exchange measurements.

Fig. 3. The figure depicts the whole canopy gas exchange system. In the gray box is placed the IRGA unity and the datalogger, each plant is involved in a polyethylene chamber. Air is forced through each assimilation chamber by a fan and the flow of air was measured by a custom-built flow gauge.

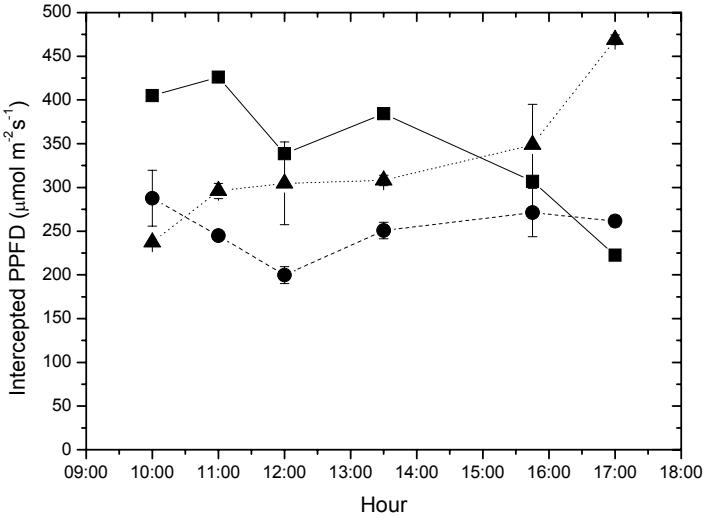

Fig. 4. Daily light interception pattern measured on W (-■-), E (·▲·) and C (-●-) plants: Each point represents the average of 2 measurements ± s.e.

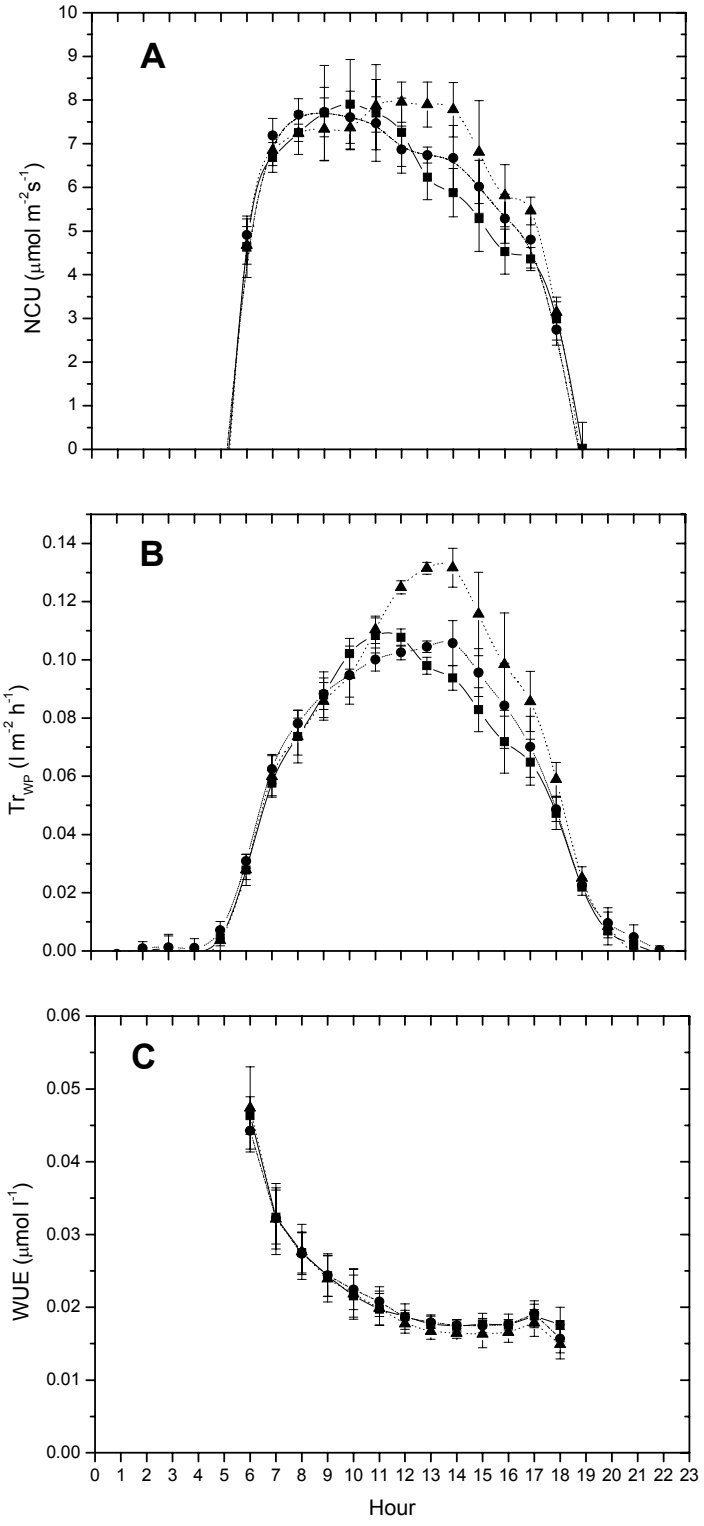

Fig. 5. Daily gas exchange pattern recorded in ST-III on W (-■-), E (·▲·) and C (-●-) plants. Each point represents the average of 8 measurements ± s.e.

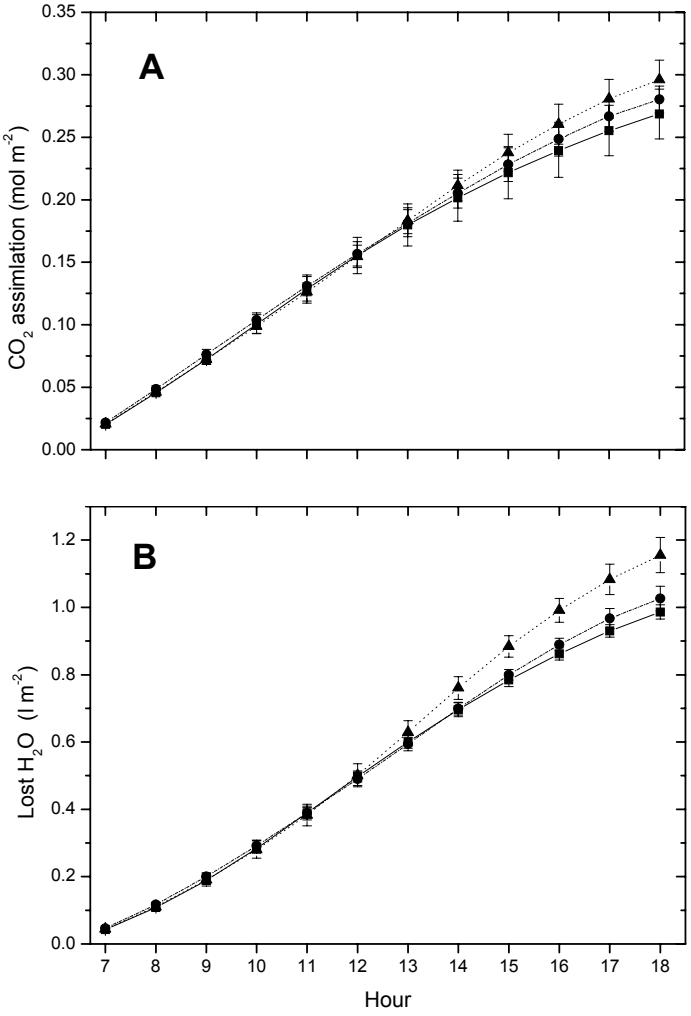

Fig. 6. Cumulative CO_2 assimilation (A) and water loss (B) during the day in ST-III calculated for W (-■-), E (·▲·) and C (-●-) plants. Each point represents the average of 14 measurements ± s.e.

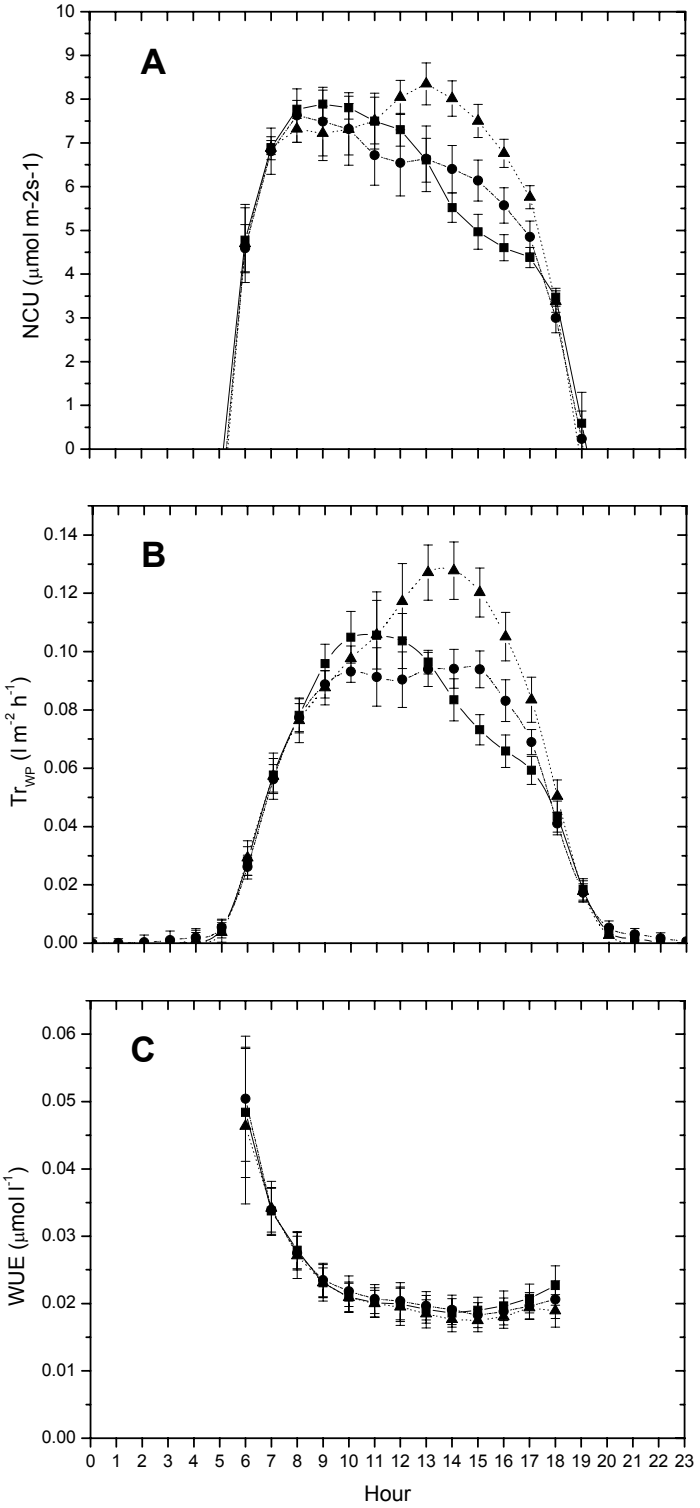

Fig. 7. Daily gas exchange pattern recorded in PHV on W (-■-), E (·▲·) and C (-●-) plants. Each point represents the average of 14 measurements ± s.e.

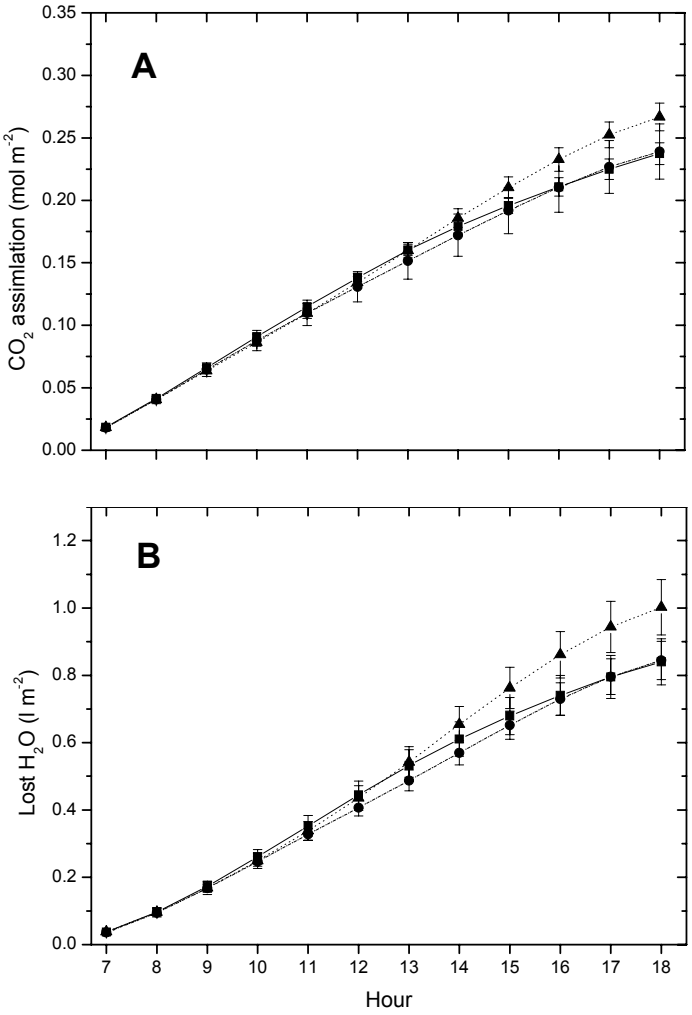

Fig. 8. Cumulative CO_2 assimilation (A) and water loss (B) during the day in PHV calculated for W (-■-), E (·▲·) and C (-●-) plants. Each point represents the average of 14 measurements ± s.e.

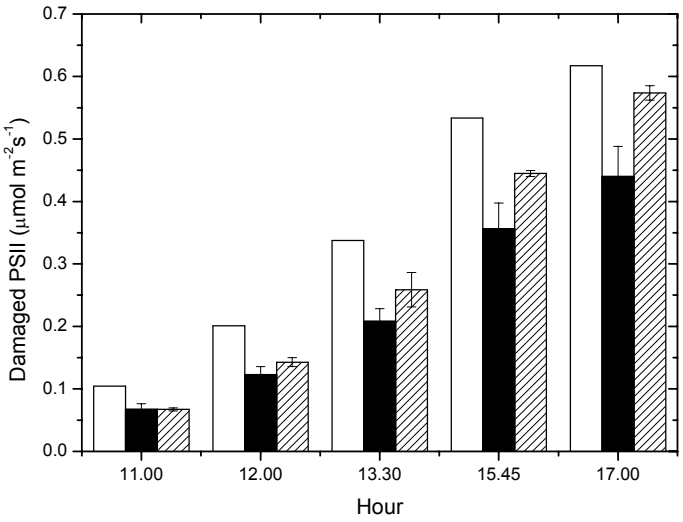

Fig. 9. Daily PSII damage estimated on W (White bars), E (dashed bars) and C (black bars) plants. Each point represents the average of 2 measurements ± s.e.

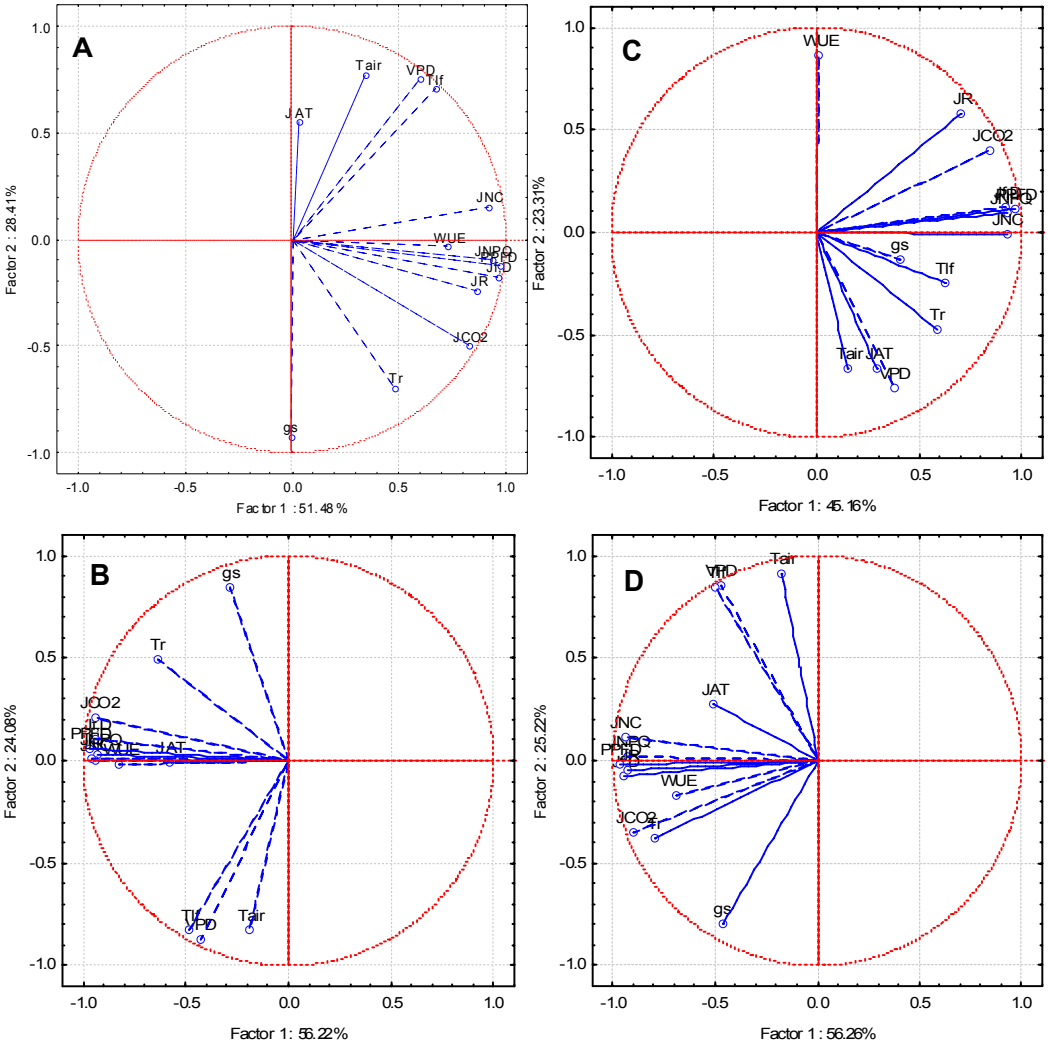

Fig. 10. Multivariate Principal Component Analysis performed for ST-I (A), ST-II (B), ST-III (C) and PHV (D). Each of 13 values is represented by a vector, and its direction and length indicates how each variable contributes to the two principal factors.

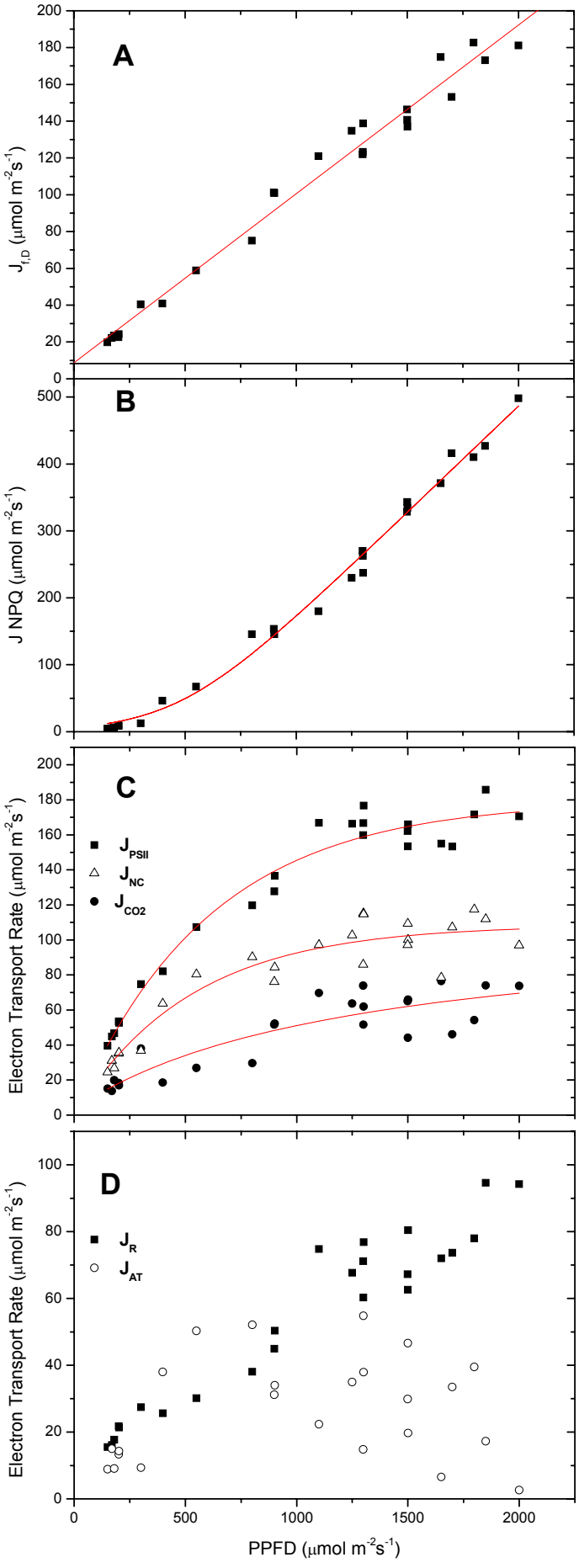

Fig. 11. Light response of: (A), fluorescence and constitutive thermal dissipation, $J_{f,D}$ ($y = ax + b$, r^2= 0.98); (B) light dependent thermal dissipation of inactive PSIIs and promoted by xanthophyll cycle J_{NPQ} ($y= (a/b)*log(1+exp(b*(x-c))$, r^2= 0.99); (C) photochemical electron transports exiting from PSII J_{PSII} ($y= a*(1-exp(-k*x))$, r^2= 0.97), Non net carboxylative transports J_{NC} ($y= a*(1-exp(-k*x))$, r^2= 0.90), effective electron transport for net photosynthesis J_{CO2} ($y=y_0+ ax/(b+x)$, r^2= 0.79); (D) electron transport rate for dark respiration and photorespiration, J_R and alternatives transports, J_{AT} in ST-I. Each point represents the average of 6 leaf measurements.

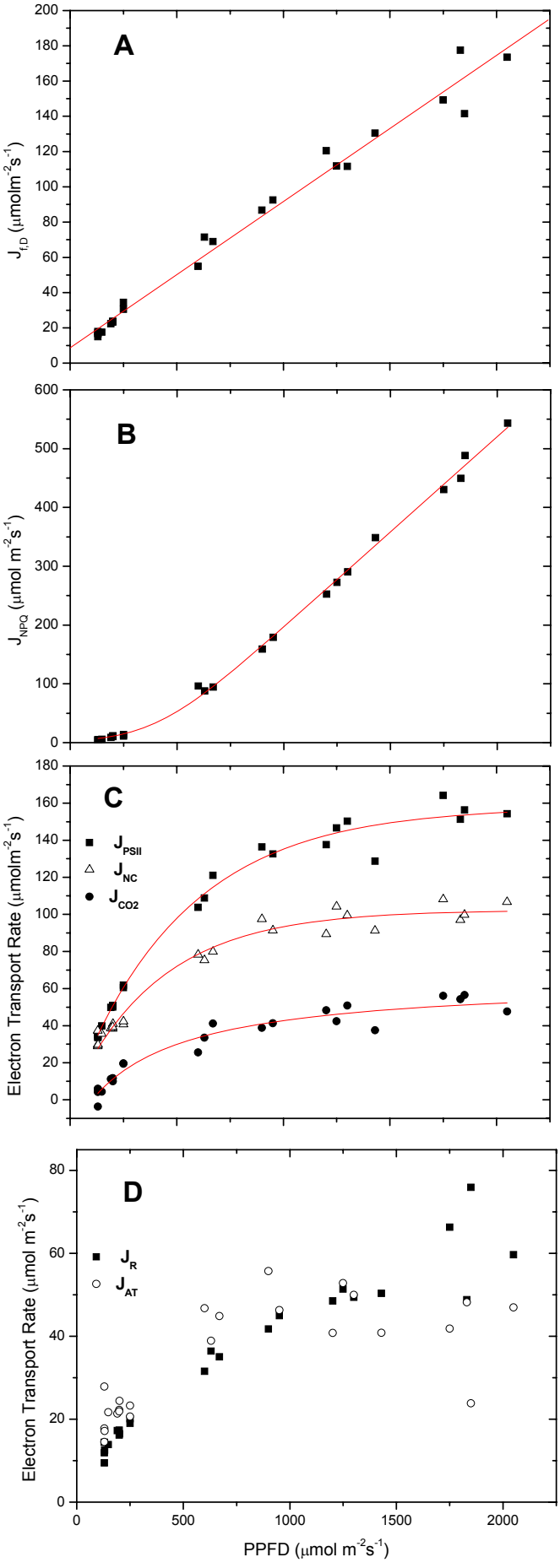

Fig. 12. Light response of: (A), fluorescence and constitutive thermal dissipation, $J_{f,D}$ ($y = ax + b$, r^2= 0.98); (B) light dependent thermal dissipation of inactive PSIIs and promoted by xanthophyll cycle J_{NPQ} ($y= (a/b)*log(1+exp(b*(x-c))$, r^2= 0.99); (C) photochemical electron transports exiting from PSII J_{PSII} ($y= a*(1-exp(-k*x))$, r^2= 0.99), Non net carboxylative transports J_{NC} ($y= a*(1-exp(-k*x))$, r^2= 0.97), effective electron transport for net photosynthesis J_{CO2} ($y=y_0+ ax/(b+x)$, r^2= 0.95); (D) electron transport rate for dark respiration and photorespiration, J_R and alternatives transports, J_{AT} in ST-II. Each point represents the average of 6 leaf measurements.

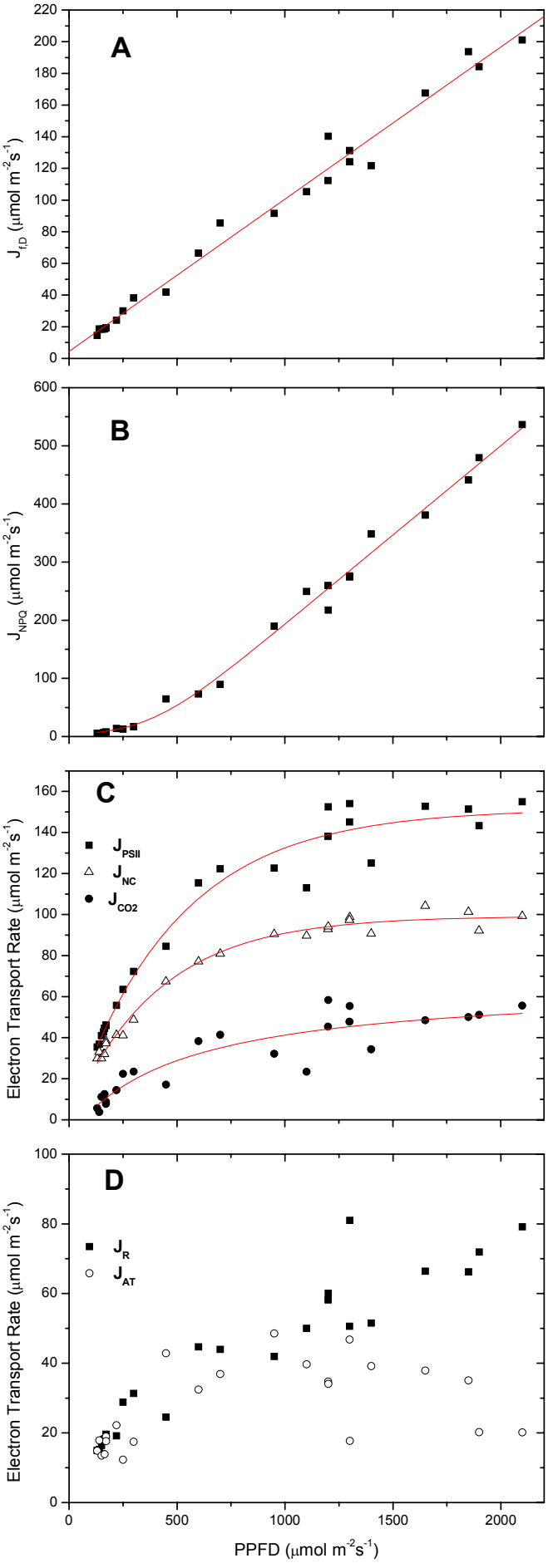

Fig. 13. Light response of: (A), fluorescence and constitutive thermal dissipation, $J_{f,D}$ ($y = ax + b$, r^2= 0.98); (B) light dependent thermal dissipation of inactive PSIIs and promoted by xanthophyll cycle J_{NPQ} ($y= (a/b)*log(1+exp(b*(x-c))$, r^2= 0.99); (C) photochemical electron transports exiting from PSII J_{PSII} ($y= a*(1-exp(-k*x))$, r^2= 0.97), Non net carboxylative transports J_{NC} ($y= a*(1-exp(-k*x))$, r^2= 0.99), effective electron transport for net photosynthesis J_{CO2} ($y=y_0+ ax/(b+x)$, r^2= 0.85); (D) electron transport rate for dark respiration and photorespiration, J_R and alternatives transports, J_{AT} in ST-III. Each point represents the average of 6 leaf measurements.

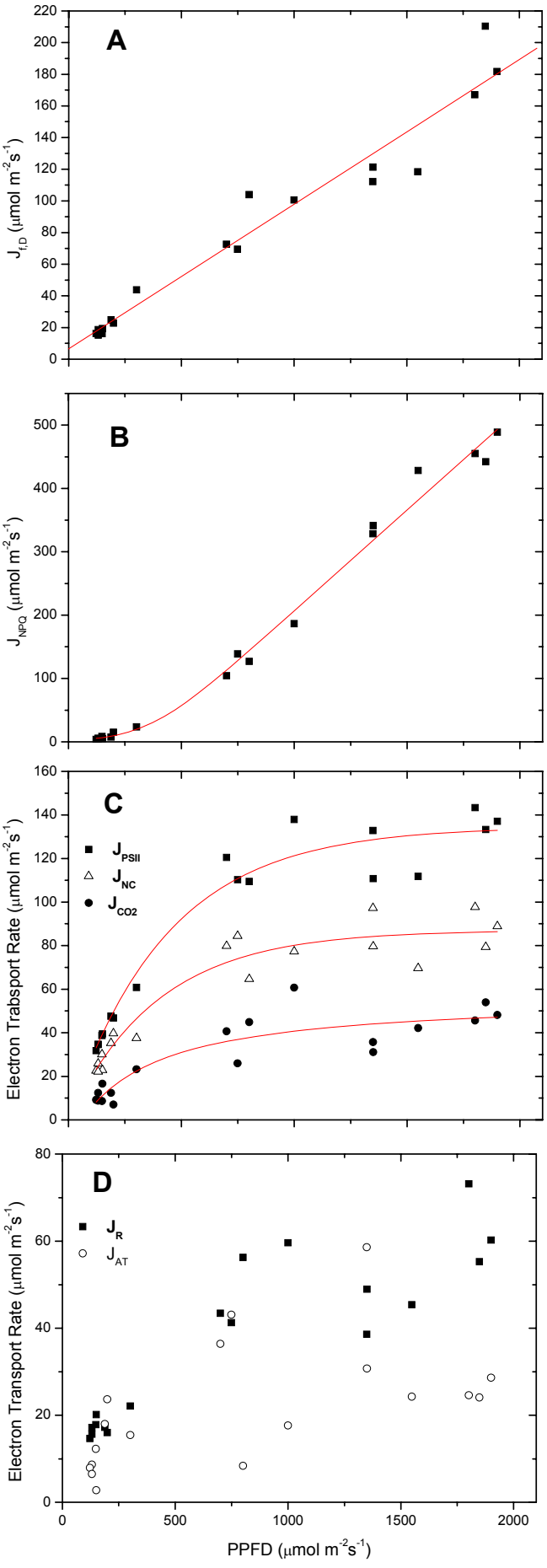

Fig. 14. Light response of: (A), fluorescence and constitutive thermal dissipation, $J_{f,D}$ ($y = ax + b$, r^2= 0.95); (B) light dependent thermal dissipation of inactive PSIIs and promoted by xanthophyll cycle J_{NPQ} ($y= (a/b)*log(1+exp(b*(x-c))$, r^2= 0.99); (C) photochemical electron transports exiting from PSII J_{PSII} ($y= a*(1-exp(-k*x))$, r^2= 0.96), Non net carboxylative transports J_{NC} ($y= a*(1-exp(-k*x))$, r^2= 0.92), effective electron transport for net photosynthesis J_{CO2} ($y=y_0+ ax/(b+x)$, r^2= 0.81); (D) electron transport rate for dark respiration and photorespiration, J_R and alternatives transports, J_{AT} in PHV. Each point represents the average of 6 leaf measurements.

PPFD (µmol m^{-2} s^{-1})	**T_{AIR}** (°C)	**T_{lf}**	**g_s** (mol m^{-2} s^{-1})	**$J_{f,D}$**	**J_{NPQ}**	**J_{CO2}** (µmol m^{-2} s^{-1})	**J_{NC}**	**J_R**	**J_{AT}**
1300	26.9	26.7	0.26	121.97	270.26	73.87	85.98	71.14	14.84
1300	31.2	31.0	0.17	123.30	262.31	51.60	115.15	60.31	54.83
n.s.	**	**	**	**n.s.**	**n.s.**	**	**	**n.s.**	**

Tab. 1. Estimated quenching partitioning in samples with the same irradiance (PPFD) and different air (T_{air}) and leaf (T_{lf}) temperature and stomatal conductance (g_s). Each value is the average of 6 measurement. Values in column triggered with (**) are statistically different at P = 0.01

Chapter V

EFFECTS OF MODERATE LIGHT AND WATER REDUCTION ON THE ABSORBED ENERGY MANAGEMENT, PHOTOPROTECTION AND PHOTODAMAGE

INTRODUCTION

Plants are un-efficient organisms since in full light they use only 5-10% of the total absorbed energy for net carboxylation (Long et al., 1994), while the remaining amount is dissipated via alternative mechanisms. Small changes in carboxylation efficiency and phtosyntate allocation could modify the primary net and commercial plant productivity (Flore and Lakso, 1988). Net photosynthesis increases with light intensity to a saturation point. The excess light absorbed is funneled to alternative pathways, increasing the light use efficiency of this protective mechanisms (Asada, 1999). Moreover, the light intercepted increases leaf temperature and is one of the drivers of water loss via transpiration (Massonnet et al., 2007).

The energy absorbed by the leaf is utilized or dissipated through several mechanisms involving thermal processes, fluorescence and photochemistry, all of which are competitive mechanisms. The main purposes of these pathways are the photosynthetic carboxylation and the dissipation of excess energy to limit the formation of active oxygen species (AOS) and photooxydative risks (Niyogi, 1999). Light-dependent thermal dissipation can be divided into photo protective quenching and PSII-

photoinactivated re-emission (Björkman and Demming-Adams, 1994). The former is accomplished by the xanthophyll cycle and can dissipate up to 75% of the total absorbed energy (Demming-Adams et al., 1996). The key enzyme of this mechanism, violaxanthin de-Epoxidase (VDE), is restricted to the thylakoid lumen and its activity is strictly trans-thylakoid-ΔpH-dependent (Ort, 2001). The maximum VDE activity is reached when the lumen pH is lower than 6.5 (Bratt et al., 1995). PSII photoinactivation quenching is an uncontrolled process, caused by thermal re-emission of photodamaged PSII complexes (Walters and Horton, 1993; Müller et al., 2001; Lee et al., 2001; Matsubara and Chow, 2004). Recent research suggests that this dissipation pathway could be considered as a slow, reversible, protective mechanism, since damaged PSII complexes would act as protective shields from photon pressure for the surviving PSII complexes. On the other hand, the remaining functional PSII centers, splitting water, create the optimal pH level for activation of enzymes promoting the new protein synthesis in chloroplasts, used for repair (Sun et al., 2006). Photodamaged PSII thermal dissipation contributes in small amount because the complexes are quickly repaired (Aro et al., 2005; Matoo and Endelman 1987, Matoo et al., 1984).

The remaining absorbed energy is engaged to mobilize the electrons through several photochemistry processes, including photosynthesis. Electrons exiting from the PSII core complex can be used to create reducing power for photosynthesis and photorespiration; otherwise, they can be dissipated via alternative transports such as the water-water cycle, cyclic transport around PSI and glutathione-ascorbate cycle (Niyogi, 1999). Moreover, these alternative energy users pump supplementary H^+ in the lumen, thus contributing to generate the proton gradient across the thylakoid membrane that supports VDE activity (Heber and Walker, 1992; Asada, 1999; Noctor and Foyer,1998). Despite this broad array of photoprotective mechanisms, plants are not able to avoid photodamage

(Havaux et al., 1986). In fact during the day the PSII complex pool can be almost entirely destroyed and quickly repaired (Chow and Aro, 2005).

The management of the energy entering the plant arouses great interest among scientists. With fluorescence measurements, using the energy partitioning proposed by Cailly et al. (1996), modified by Hendrickson et al. (2005) and upgraded by Kornyeyev and Hendrickson (2007), it is possible to measure the fraction of absorbed energy engaged for photosynthesis, of that quenched by thermal and photochemical protective processes and that dissipated by damaged PSII. Moreover, with concurrent fluorescence and gas exchange measurements a further partitioning of photochemistry transports have been proposed by several Authors, allowing to consider separately each process involved (Cheng et al., 2001; von Caemmerer, 2000; Galmés et al., 2007).

This study was carried out to validate the quenching analysis method in peach, and to apply this method to investigate the influence of moderate light and water reduction on peach photosynthetic performances, water requirements and energy management, pointing out the effect of light reduction on PSII damage.

MATERIALS AND METHODS

The trials reported were carried out at the Research School of Biological Science, of the Australian National University, Canberra (Australia), and at the Dipartimento di Colture Arboree, University of Bologna (Italy).

Plant material

The maiden trees (1-yr-old) used in Australia belonged to the nectarine *(Prunus persica* (L.) Batsch var. laevis) cultivar Red Gold and were grafted on seedling rootstocks, grown in pots receiving abundant

water and fertilizer. In Italy, 4-yr-old trees of the nectarine "Alice-col" (a columnar-habit cultivar) were used, grafted on "GF-305" seedling, spaced 5 x 1.2 m and trained as spindle. At 80 days after full bloom (pit hardening), two contiguous lots of 40 plants (8 rows with 5 plants each) were chosen. One of them was shaded with a neutral-density, black shading net (40% reduction). In each lot, 4 contiguous rows received half the irrigation supplied to the other trees (16 ld^{-1}), obtaining 4 sub-plots: High light well-watered (HLW), High light water stressed (HLS), Low light well-watered (LLW) and Low light water stressed (LLS). Details of the experiments are given according to the site.

Experimental

In Australia, during summer (January 2007), well expanded attached leaves were labelled and covered in order to avoid any photo damage,. Leaf discs were floated with their ab-axial side up, in order to facilitate gas exchange (Sun et al., 2006), on a 1mM lincomycin solution (an inhibitor of the D1 protein repair; Aro et al., 1994) for two hours in darkness. They continued to float with the ab-axial side up on the lincomycin solution (23 °C) during illumination on the ad-axial side at 500, 1000 and 2000 $\mu molm^{-2}s^{-1}$ for 30, 60, 90 and 120 minutes. The photoinhibiting light was directed vertically upwards, through a transparent water bath, to a clear Petri dish in which the leaf discs were floated. Before the photoinhibitory treatment, 9 leaf disks (3 for each light intensity) were used as non-photoinhibited controls. On these discs, the functional PSII content ($\mu mol\ m^{-2}$) was then quantified by flash-induced oxygen evolution, assuming that each functional PSII evolve one O_2 molecule after four flashes (Chow et al., 1989; Chow et al., 1991). On each leaf segment the relative functional PSII (normalized to the value of the non-photoinhibited control) was quantified by the measurement of the redox kinetic of P_{700} according to Losciale et al. (2008), with a dual wavelength (820/870) unit (ED-P700DW) attached to a phase amplitude modulation fluorometer (Walz, Effeltrich, Germany).

Assuming that in the non-photoinhibited state the relative functional PSII amount is 1, multiplying the relative functional PSII content by the real functional PSII amount (obtained by oxygen evolution measurements) the functional PSII amount can be calculated for each photoinhibition treatment. After the photoinhibition treatment, fluorescence measurements were performed using a phase amplitude modulation fluorometer (Walz, Effeltrich, Germany) fitted with blue excitation modulated light. Leaf disks were maintained at the same intensity as the photoinhibiting light and after stabilization the steady state fluorescence yield in light (F_s) was measured. A saturating pulse was triggered to measure the maximal fluorescence yield in light ($F_{m'}$). After about 45 minutes of dark adaptation the minimal (F_o) and maximal (F_m) fluorescence yield were measured. Dark adaptation inhibits quite completely the xanthophylls de-epoxidation and the non photochemical quenching (NPQ). F_v/F_m represents the non-damaged PSII quantum efficiency, therefore the difference between F_v/F_{mM} (quantum yield efficiency of control disks, where F_{mM} is the maximal florescence measured on control disks) and F_v/F_m for each photoinhibition treatment indicates the quantum yield lost as heat by inactive PSII (Maxwell and Johnson, 2000). Quenching analysis was conducted according to the method proposed by Kornyeyev and Hendrickson (2007).

In Italy, during July 2007 (slightly before harvest), after 1 month adaptation to the new environment conditions, stem water potential (Ψ, MPa) was monitored predawn and at 10.00, 13.30 and 16.30 using a Scholander chamber (Soilmosture Equipement Corp., Santa Barbara California, U.S.A) measuring the water potential of 5 leaves placed in internal parts of the canopy which had been covered with aluminium foil for 1h according to Naor et al., 1995, to allow equilibration with the stem.

HLW and LLW fully expanded leaves were used to calculate the Quantum yield of photoinhibition (Qy). Leaf disks were floated in a lincomycin solution following the same protocol used in Australia. Light at 800 and 1250 μmol m^{-2} s^{-1} was supplied for 0, 30, 60, 90, 120 minutes. PSII

activity was detected by fluorescence measurements (F_v/F_m) on both leaf sides after 45 minutes of dark adaptation (Losciale et al., 2008) with a leaf chamber fluorometer attached to an open circuit infrared gas exchange system (Li-COR 6400, LI-COR inc., Lincoln Nebraska U.S.A.). In absence of recovery the PSII activity decay depends on photon exposure, the product between irradiance and time of exposure (mol m^{-2}) according to the reciprocity law (Nagy et al., 2005). Increasing photon exposure, active PSII decrease following an exponential decay because the functional PSII to be destroyed become limiting (Chow et al., 2005). Since in nature an almost complete recovery occurs continuously, the maximum slope of the exponential function (Qy) represents the PSII amount destroyed by one mol of photons (μmol mol^{-1}). Multiplying Qy for the Photon exposure intercepted by the leaves it is possible to estimate the damaged PSII amount (μmol m^{-2}) in a fixed time interval (Hendrickson et al., 2004). Floating discs continuously in lincomycin may cause re-hydration of the samples, therefore the protocol described before was unusable to calculate Qy in water stressed leaves. To overcome this problem, attached leaves of both treatments were immersed in 1mM lincomycin solution all night long, and the samples were collected in the dark. The recovery depressor solution was removed 1h before measurements (Time 0) and ad-axial and ab-axial fluorescence measurements were performed during the day, computing the photon exposure, based on the light intensity at each measurement.

Two plants similar for vigour and crop load were chosen for each sub-plot. 4 attached, well exposed leaves facing either east or west were selected. Photosynthetic photon flux density (PPFD, μmol m^{-2} s^{-1}), leaf and air temperature (T_{air} ,ºC), gas exchange and fluorescence parameters were measured on the leaves using an open circuit infrared gas exchange system with a leaf chamber fluorometer attachment and a PPFD sensor (Li-COR 6400, LI-COR inc., Lincoln, Nebraska, U.S.A.). Illumination was supplied by a LED light source. Light intensity was set to the natural irradiance recorded on the leaf lamina immediately before measurement. The

maximum quantum yield of the total amount of Photosystem II (F_v/F_{mM}) was measured at predawn to allow complete relaxation and recovery of the photosystems during the night (Hikosaka et al., 2004). Measurements were performed in the morning, middle of the day and afternoon. Each time, F_v/F_m was measured after 45 minutes of dark adaptation using a reflecting cover in order to avoid any increase in leaf temperature.

Analysis of the partitioning of excitation energy

Quenching analysis was carried out using the model proposed by Hendrickson et al. (2005) and upgraded by Kornyeyev and Hendrickson (2007), combined with the photosynthesis model proposed by von Caemmerer (2000).

Considering 1 the total amount of energy absorbed by photosystems:

$\Phi_{f,D} = F_s/F_m$ is the combined quantum efficiency of fluorescence and constitutive thermal dissipation. Variations in light do not alter this efficiency (Hendrickson et al., 2004);

$\Phi_{NF} = (F_s/F_m) - (F_s/F_{mM})$ is the quantum efficiency of thermal dissipation associated with inactivated PSII ;

$\Phi_{NPQ} = (F_s/F_{m'}) - (F_s/F_m)$ is the quantum efficiency of thermal dissipation promoted by the photo-protective Non Photochemical Quenching via the xanthophyll cycle;

$\Phi_{PSII} = 1-(F_s/F_{m'})$ is the quantum efficiency of photochemical transports used for photosynthesis, photorespiration, mitochondrial respiration and alternative transports (water-water cycle, cyclic transport around PSI and glutathione-ascorbate cycle);

For uniformity, all the energetic components were expressed as Electron Transport Rate J (µmol m^{-2} s^{-1}), multiplying each quantum efficiency (Φ) for the total amount of electrons that can be moved by the absorbed energy:

$J_{TOT} = 0.5 \times 0.85 \times PPFD$

where 0.5 accounts for the fact that 1 electron is moved by 2 photons (Melis et al., 1987) and 0.85 is an average leaf absorptance (Schultz, 1996).

The gas exchange measurements allowed partitioning of J_{PSII} into several components:

$J_{CO2} = P_n*4$

is the electron transport rate for net carboxylation, where P_n is the net carbon assimilation (µmol m^{-2} s^{-1}) multiplied by 4 electrons used to carboxylate 1 CO_2 molecule;

$J_{NC} = J_{PSII} - J_{CO2}$

represents the residual absorbed energy used for non net-carboxylative processes such as photorespiration, alternative transports and dark respiration.

According to von Caemmerer (2000):

$$J_A = \frac{(P_n + R_d)(4C + 8\Gamma_*)}{(C - \Gamma_*)}$$

is the electron transport rate to photosynthesis and photorespiration, where R_d (µmol m^{-2} s^{-1}) is the dark respiration, C is the chloroplast CO_2 concentration (µbar) and Γ* is the compensation point in absence of mitochondrial respiration (µmol m^{-2} s^{-1}). Therefore

$J_{AT} = J_{PSII} - J_A$ represents the energy dissipated by alternative transports;

$J_R = J_A - J_{CO2}$ represents the energy used for mitochondrial respiration and photorespiration.

To assess differences between the four treatments in the field, a 2-way ANOVA statistical analysis with Alpha = 0.05 was performed at each time of the day for east and west side of canopy considering as factors the light treatments and the water supply. Means separation was by SN test.

RESULTS

Australian study

In the absence of repair the loss of functional PS II centres showed a single dependence on photon exposure, even though peach leaf discs were illuminated at 3 different intensities. The function representing this relation was negative exponential (r^2= 0.96) and the maximum slope of the curve (0.07 mol $m^{-2}s^{-1}$) is the quantum yield of photoinhibition (Fig. 1). In the presence of lincomycin the quantum yield of basal heat and fluorescence was not influenced by exposure time and light intensity and used ~ 20% of the total absorbed energy (Fig. 2A). The total light dependent thermal dissipation (sum of $\Phi_{NF} + \Phi_{NPQ}$) increased with increasing time of exposure and light intensity contributing to energy dissipation from ~ 35% at low intensities for 30 minutes to ~ 90% at 2100 μmol $m^{-2}s^{-1}$ for 120 minutes (Fig. 2B). After 30 minutes at 500 μmol $m^{-2}s^{-1}$ the contribution of thermal dissipation associated with PSII damage (Φ_{NF}) was about 5%, increasing with time of exposure and light intensity up to ~ 70% at the highest irradiance and duration (Fig. 3A). The non photochemical quenching Photo protective contribution (Φ_{NPQ}) was maximal after 30 minutes, slowly decreasing with increasing time of exposure. Significant differences among light intensities were recorded only after 30 minutes, when Φ_{NPQ} quenched ~ 50% of total energy at highest light intensity and about 30-35% at the other irradiances (Fig. 3B). The quantum yield of photochemistry (Φ_{PSII}) decreased with light intensity increase at 500 μmol $m^{-2}s^{-1}$ it was relatively unaffected by time of exposure, while at 1000 and 2100 μmol $m^{-2}s^{-1}$ it decreased with increasing time of exposure, becoming 0% after 120 minutes at maximal irradiance (Fig. 2C). While all Φ_{NF} values fitted the same curve when plotted against photon exposure, neither Φ_{NPQ} nor Φ_{PSII} followed a similar behaviour, showing different values for different light intensities at the same photon exposure (Fig. 4).

The relation between the total energy dissipated by active PSII centers (1-Φ_{NF}) and active PSII center concentration was linear (r^2=0.95) and according to the equation found, when 1-Φ_{NF} was 0 a residual PSII activity still occurred. At the lowest active PSII concentrations tested the relationship starts to show a curvilinear pattern (Fig. 5).

Italian results

Trials were carried out in June 2007 close to harvest period. Since the 2 way ANOVA analysis showed a significant interaction between light and water treatments a multiple comparison among means of all combination between light and water dosage was performed. Stem water potential (Ψ) at predawn was similar for all treatments. During the morning, Ψ generally decreased, with HLS values statistically more negative than the other 3 treatments. At 13.30, water potential was similar among treatments but in the afternoon HLS plants had again lower water potentials than the others treatments (Fig. 6).

Gas exchange and Quenching analysis

East side

Single leaf measurements were performed at 10.00, 13.30 and 16.30. In the morning plants in full light intercepted about 1800 μmol $m^{-2}s^{-1}$ while under the shading net the photon pressure (PPFD) was 1050 μmol $m^{-2}s^{-1}$ with a reduction of about 40%. Net photosynthesis (P_n) was similar among treatments although in HLW plants stomatal conductance (g_s) was higher than in the other treatments. Transpiration followed the same pattern determining lower water use efficiency (WUE) for HLW than the other treatments. Air temperature (T_{air}) was over 30°C for all samples and under the shading net it was generally lower than in full light (Tab.1).

The quenching analysis showed that, regardless of water treatment, plants in high light dissipated more energy than those shaded via basal heat and

fluorescence ($J_{f,D}$), heat by damaged PSII (J_{NF}) and Non Photochemical Quenching (J_{NPQ}). The latter used about 55% and 40% of the total absorbed energy respectively for full light and shaded leaves. The electron transport rate exiting Photosystem II (J_{PSII}) was similar among the 4 treatments; partitioning J_{PSII} allowed to estimate the electron transport rate for net photosynthesis and that dissipated through the non net-carboxylative transports (J_{NC}). Both energy components were not different among treatments and non net-carboxylative transports dissipated 11, 13, 19.5 and 19.2% of the total absorbed energy in HLS, HLW, LLS and LLW samples, respectively. J_{NC} was further partitioned into the electron transport rate for dark respiration and photorespiration (J_R) and alternative transports (J_{AT}). J_R was higher in shade than in full light without differences between water treatments. On the other hand, J_{AT} was statistically higher in high light samples than under the net (Tab.2). At 13.30 the incident irradiance decreased to 1600 μmol $m^{-2}s^{-1}$ in full light and to about 850 μmol $m^{-2}s^{-1}$ under the shading net, with a reduction of ~ 47%. In all treatments net photosynthesis and stomatal conductance were considerably lower than in the morning, with g_s always below 0.17 mol $m^{-2}s^{-1}$. P_n was similar among treatments while shaded plants had lower stomatal conductance than the ones in full light regardless of water treatment. In full light the water use efficiency decreased while the shaded trees maintained values similar to the morning, giving higher WUE than in full light, without differences between water treatments. Air temperature was generally higher in full light than under the net (Tab.1). Almost all the energy component values decreased compared to the morning data. The high light plants had higher $J_{f,D}$ and J_{NPQ} values than the shaded trees, while J_{NF} was highest for HLW, followed by the shaded treatments and HLS, which were similar to each other. Even though at 13.30 the photon pressure was lower than at 10.00, J_{NPQ} values remained similar and the energy amount quenched via NPQ increased to 70% and 50% respectively, for high light and shaded plants. The electron transport rate exiting PSII was similar for all treatments. This trend was

maintained by J_{CO2} and J_{NC}. The latter used 11% and 19% of the total absorbed energy respectively in high light and in shaded plants. J_R and J_{AT} were not statistically different for all treatments and compared to the morning the alternative transports generally increased (Tab.2). In the afternoon the minimum values of the day were recorded for all parameters. The incident radiation was 200 μmol $m^{-2}s^{-1}$ in full light and 100 μmol $m^{-2}s^{-1}$ under the net. No differences among treatments were recorded for net photosynthesis, water use efficiency and stomatal conductance, which was never higher than 0.1 mol $m^{-2}s^{-1}$. The temperature decreased to about 28°C and LLS had the lowest values (Tab.1). At this time, $J_{f,D}$, J_{NF}, J_{NPQ}, J_{PSII} and J_{NC} were higher in high light than in shade. No difference was recorded between water treatments. The energy dissipated through non photochemical quenching decreased to about 24% in high light and 14% under the net while J_{NC} dissipated 35%, 40%, 45% and 41% of the total absorbed energy respectively in HLS, HLW, LLS and LLW. Values of J_R, J_{AT} and J_{CO2} were no different among treatments although in high light samples J_{AT} and J_{CO2} were higher than in shaded plants (Tab.2).

West side

In the morning PPFD was 150 μmol $m^{-2}s^{-1}$ in highlight and 100 μmol $m^{-2}s^{-1}$ under the net. No differences were recorded for all gas exchange parameters, and at these low light levels stomatal conductance was not higher than 0.11 mol $m^{-2}s^{-1}$ (Tab 3). J_{NF} was generally very low without any difference among samples. $J_{f,D}$, J_{NPQ} and J_{PSII} values were higher in high light than in shade and no differences were recorded between water treatments. Non photochemical quenching used about 12-14% of the total absorbed energy, J_{CO2} was similar among treatments while J_{NC} was higher in high light than in LLS and LLW samples, dissipating 33, 27, 30 and 29% respectively in HLS, HLW, LLS, LLW plants. Also for J_R no difference was detected while J_{AT} showed negative values (Tab.4).

At mid-day all parameters increased in each treatment. The incident radiation was 1450 μmol $m^{-2}s^{-1}$ in full light and 900 μmol $m^{-2}s^{-1}$ under the net, a reduction of ~ 38%. Temperature was generally higher in full light than under the shading net. Net photosynthesis and stomatal conductance were similar among treatments, excluding LLS which had the lowest values (P_n 7.17 μmol $m^{-2}s^{-1}$ and g_s 0.11 mol $m^{-2}s^{-1}$). Water use efficiency was similar among all samples (Tab.3). Quenching analysis showed that $J_{f,D}$, J_{NF} and J_{NPQ} values were statistically higher in full light than in shade without any difference between water treatments. Compared to the morning the energy dissipated via NPQ increased to 54, 56, 50 and 42% in HLS, HLW, LLS and LLW, respectively. The electron transport rate exiting PSII was similar in the different light and water conditions, while LLS J_{CO2} values were lower than the other 3 treatments. Non net-carboxylative transports (J_{NC}) were similar among samples with a dissipation of about 13.5% in HLS, 15% in HLW 22% in LLS and 19% in LLW plants. Under the shading net full watered plants had higher J_R than LLS samples, while in full light HLS plants had negatives values (-9.36 μmol $m^{-2}s^{-1}$) for J_{AT} (Tab.4). In the afternoon, PPFD was 1650 μmol $m^{-2}s^{-1}$ in high light and 800 μmol $m^{-2}s^{-1}$ under the net, a reduction of about 50%. Under the net air temperature was lower than in full light. Net photosynthesis was similar while HLW stomatal conductance was higher than in the other 3 samples (0.23 mol $m^{-2}s^{-1}$). Under shade WUE was higher than in full light and no difference was recorded between water treatments (Tab.3). J_{NF} and J_{NPQ} increased in the afternoon, with higher values in full light than in shade, regardless of water treatment. The energy dissipated trough the xanthophyll cycle was 63% for HLS, 61% for HLW, 54% and 48% respectively for LLS and LLW. The HLW plants had a higher J_{PSII} value than LLS, with HLS and LLW at intermediate level. The electron transport rates derived by J_{PSII} partitioning were similar for each treatment. J_{NC} dissipated about 11% and 20% of the total absorbed energy respectively in high light and shade samples (Tab.4).

PSII decay

Both light and water treatments gave values of PSII activity following the same single exponential PSII decay curve when plotted against photon exposure (data not shown). The calculated quantum yield was 0.07 μmol m^{-2}, the same as that obtained for Red Gold in Australia (data not shown). On both the East and West sides at each time of the day more PSII complexes were destroyed in high light than under the shading net, reaching a difference of about 100% between the two light treatments (Fig. 7).

DISCUSSION

This work shows that the reciprocity law (Chow et al., 2005) holds in peach: in the presence of lincomycin a single exponential decay function in response to photon exposure was found (Fig. 1). Light intensity and time of exposure did not affect $\Phi_{f,D}$ (Fig. 2A). This constant thermal and fluorescence dissipation was explained as a consequence of un-synchronized electron transport rate between P_{680}, Pheophytin and the primary quinone acceptor increasing the living time of the radical pair P_{680}^{+} Ph^{-} (Chow, 2003). Φ_{NF} increased with time and light exposure since in absence of repair, the damaged PSII accumulated (Fig. 3A). In this study, the Φ_{NF} increase with time of exposure was not followed by a similar Φ_{NPQ} decrease. As a consequence, contrary to Kornyeyev and Hendrickson (2007) in capsicum, $\Phi_{NF} + \Phi_{NPQ}$ was not constant and Φ_{PSII} decreased with exposure (Fig. 2B). Probably peach is not as high-light adapted as capsicum., The slow decrease of quantum yield of non photochemical quenching (Φ_{NPQ}) after 60 minutes, regardless of light intensity, could be caused by the interaction of lumen pH limitation and energy limitation (Fig. 3B). For example, after 90 minutes Φ_{NF} was about 24, 39 and 61% respectively at 500, 1000 and 2000 μmol $m^{-2}s^{-1}$ while Φ_{NPQ} was similar

among light treatments. Leaf disks under high light were probably not lumen-pH limited but about 60% of total energy was subtracted by damaged PSII. On the contrary, samples in low light had not so much inactive PSII but low light intensity did not sustain lumen proton increase for the xanthophyll cycle. The strong relation between Φ_{NF} and photon exposure when recovery was inhibited, supports the dependence of this quantum efficiency on damaged PSII (Fig. 4A). In fact, the linear relation between energy used by active Photosystems ($1-\Phi_{NF}$), measured using fluorescence, and active PSII concentration based on P_{700} redox kinetics point to Φ_{NF} as a good photoinhibition estimator, although the general underestimation and the initial curvilinear pattern recorded at the lowest values indicate the need to calibrate this parameter. Similar results were found by Losciale et al. (2008) comparing F_v/F_m measured on the ad-axial side with oxygen evolution for 6 plant species. In peach, averaging measurements from the ad-axial and ab-axial leaf surfaces yielded a linear relationship and the underestimation was corrected. The difference between the two methods might depend on the fact that fluorescence is only able to detect the first layers of leaf cells (Losciale et al., 2008). Φ_{NPQ} and Φ_{PSII} seem to be dependent on light intensity as the reciprocity law was not respected (Fig. 4A,B).

In the field, the initial water status of the trees was similar for all treatments, however in the morning and afternoon the water treatment seemed to affect trees which were under high light (Fig. 6). The water stress imposed however, didn't limit net photosynthesis since no difference was recorded under high light at every time of the day for both sides of canopy (Tables 1, 3).

Shading reduced light intensity by 40%-50% without any net photosynthesis reduction. Ameliorating effects of light reduction were recorded in citrus under 60% shading net (Raveh et al., 2003) and in apple sprayed with reflective white particle film (Glenn et al., 2001). With diminishing incident light, air temperature seemed to decrease. Similar

results were observed in citrus treated with a reflecting kaolin foliar coating (Jifon and Syvertsen, 2003). In the morning on the East side of the canopy a 40% light reduction did not decrease P_n ,probably because the irradiance was however saturating and stomatal conductance was not limiting. Trees in HLW had the highest g_s, because they were not water limited and used transpiration to adjust leaf temperature, losing more water (Tab.1). The excess energy was dissipated as basal heat and fluorescence, damaged PSII and by non photochemical quenching. $J_{f,D}$ was linearly proportional to light intensity and the energy percentage dissipated this way was constant (Hendrickson et al., 2004) for all light and water treatments (Tab.2). The small energy amount dissipated by damaged PSII indicates that the recovery system was able to repair almost all damage, even though in plants exposed to full light the difference between recovery and damage rates was greater than in low light (Tab.2). The main energy dissipator was the xanthophyll cycle using about 55% of the total absorbed energy in high light against 40% in shaded plants. Non net-carboxylative transports reached the maximum values at 1050 μmol $m^{-2}s^{-1}$, therefore their relative importance is higher at middle-low irradiance than at over saturating PPFD, showing an efficiency of ~ 19% in shaded samples and ~ 12% in full light (Tab.2). Even though non net-carboxylative transports are generally more dangerous than NPQ, since they involve electron movement, leaves used these mechanisms first. The xanthophyll cycle is strictly trans-thylakoidal ΔpH dependent and the optimum lumen pH for violaxanthin de-epoxidase (VDE) activity is under 6.5 (Bratt et al., 1995). Probably at middle-low irradiance thylakoid lumen was not acid enough to completely activate VDE. In this “initial” state, leaves dissipate energy excess using mainly alternative ways, including the water-water cycle, the cyclic transport on PSI and the glutathione-ascorbate cycle. These pathways are able to increase the trans-thylakoidal ΔpH working as added engines to create the optimal pH environment for VDE (Heber and Walker, 1992; Asada, 1999; Noctor and Foyer, 1998). When conductance was not limiting, leaves in

low light used more energy for photorespiration than in full light. The opposite happened for alternative transports (Tab.2). These data appear in contrast with literature reporting an increase of photorespiration proportional to light irradiance (Heber et al., 1996). J_R and J_{AT} derived from the total energy used for carboxylation and oxygenation operated by Rubisco (J_A). This estimated electron transport is strictly linked to several parameters, such as leaf temperature, chloroplast conductance, net photosynthesis, compensation point and dark respiration (von Cammaerer, 2000), all easily influenced by environment conditions. In the middle of the day PPFD decreased and under the shading net it was lower than 1000 μmol $m^{-2}s^{-1}$. Even so, net photosynthesis was similar to high light samples, probably because the decreased conductance, recorded in all treatments, was the main limiting factor for photosynthetic performance. Still, plants in high light lost more water than the shaded ones, becoming less efficient in water use (Tab.1). Quenching analysis gave almost the same results as the morning confirming that the maximum rate for J_{NC} was reached at around 800-1000 μmol $m^{-2}s^{-1}$, when the xanthophyll cycle was still pH limited. The strong stomatal conductance decrease led P_n to fall; as a consequence more energy was allocated to NPQ that, in spite of the reduction in irradiance, maintained values similar to the morning (Tab.2). A similar behaviour was recorded in grape (*Vitis vinifera* L.) when stomatal conductance fell to 0.1 mol $m^{-2}s^{-1}$ (Flexas et al., 2002). An unexpected result was recorded for J_{NF} in HLS plants which, even though they were under high light pressure, had the lowest values (Tab.2). In the afternoon the incident radiation was very low and far from saturation. Low light and afternoon water limitation drove stomatal conductance to decrease (Jarvis, 1976) below 0.1 mol $m^{-2}s^{-1}$. Even in the afternoon the intercepted radiation difference didn't determine P_n variation among treatments (Tab.1). The energy surplus intercepted in full light but not used for increasing net carboxylation was dissipated using all the alternative ways. In this case the main dissipation component was J_{NC} using about 35 and 45% of the total absorbed energy in high light and

shaded samples, respectively, while NPQ used only 14 and 24%. At low irradiance the xanthophyll cycle was probably so strongly pH limited that its efficiency became lower than J_{NC} (Tab.2). Excluding stomatal conductance and water use efficiency, the water stress didn't seem to have an apparent effect on energy partitioning and photosynthetic performances (Tab.1,2).

In the morning the West side of the canopies received the lowest irradiance and the pattern of all parameters was similar to East side samples in the afternoon. Despite the best water conditions normally occurring in the morning, stomatal conductance was the lowest of the day for all treatments (Tab.3). As observed by Jarvis, conductance should depend not only on temperature and water status but also on irradiance (Jarvis, 1976). The clearly unreal negative values of J_{AT} (Tab.4) seem to confirm the difficulty of separating photorespiration rate from alternative transports. At 13.45, with general irradiance and temperature increasing, P_n and stomatal conductance increased except for LLS samples where low g_s (0.11 mol $m^{-2}s^{-1}$) led to a low P_n (Tab.3). The general pattern of quenching partitioning followed what previously discussed for East side samples at 13.30. In LLS leaves, stomatally limited, an increase of J_{NPQ} was observed (Tab.4). Even though the absorbed energy in LLS and LLW was the same, the former dissipated 50% of the absorbed radiation instead of 42% of LLW (Tab.4), confirming the role of NPQ when stomatal conductance reaches critical values (Flexas et al., 2002). In the afternoon a 50% light reduction due to shade didn't change the photosynthetic performances, although HLW samples showed a higher conductance than the other treatments and even in this case leaves exposed to 1650 μmol $m^{-2}s^{-1}$ were less water efficient than shaded ones (Tab.3). Quenching analysis pointed out that the $J_{f,D}$ efficiency is independent from the light environment since the percentage of used energy was constant; in high light the difference between rate of damage and rate of recovery is higher than under the net causing an increase of J_{NF}, although the very low values of J_{NF} indicate the small amount of residual

damage; the main dissipator was the xanthophyll cycle, pH limited at mid-low irradiance (Tab.4).

Lincomycin treatment was able to inhibit the PSII recovery permitting to observe the real damage occurring during the day. In peach the estimated total PSII concentration was about 1.2 μmol m^{-2} (Fig. 1) and the quite high destruction observed in high light at the end of the day was possible because new functional PSII molecules were continuously injected in the system. Despite the same photosynthetic performance, plants exposed to full light sustain more damage than shaded ones, and they consequently invest more energy for repair.

CONCLUSIONS

Energy partitioning is quite a comprehensive method to analyse a plant energy management under field conditions. Although it requires calibration, and taking into account that fluorescence is able to detect the first leaf cell layers, this method could give a good estimation of photodamaged PSII. Improvements should be done in order to separate the different pathways involved in leaf photochemistry.

In peach a moderate PPFD reduction didn't cause net carboxylation decrease. Light and temperature reduction appeared to cause a stomatal conductance decrease, improving water use efficiency. By reducing light intensity, water could be saved without compromising net photosynthesis. The quenching analysis permitted to partition absorbed energy in the several utilization, photoprotection and photo-oxidation pathways, although some unclear results were recorded for J_R and J_{AT}. When recovery was permitted only few destroyed PSII remained, however, reducing light interception by 40-50%, the net loss of PSII decreased. In over saturating light the main dissipation pathway was the non photochemical quenching, that at middle-low irradiance seemed to be pH limited. Thus other

transports, such as photorespiration and alternative transports, were used to support photoprotection and to contribute to create the optimal trans-thylakoidal ΔpH for violaxanthin de-epoxidase. These alternative pathways became the main quenching mechanisms in very low light environment. Another aspect pointed out by this study was the role of NPQ as alternative pathway when conductance becomes severely limiting. The energy management in sub-optimal conductance ranges remains to be investigated.

Light in excess of the photosynthetic optima did not promote net carboxylation but increased water loss and PSII damage. Since in nature damaged PSII is quickly repaired with energy expense, it would be interesting to investigate how much PSII recovery costs to plant productivity.

TABLES AND FIGURES

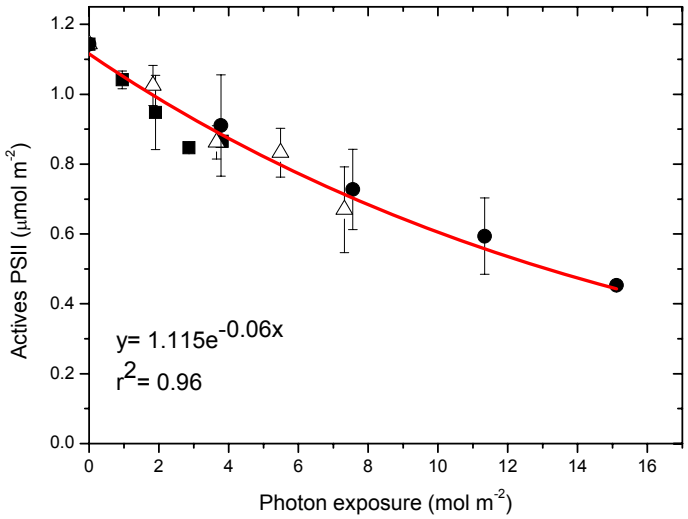

Fig. 1. Functional PSII decay with photon exposure increase in peach leaves segments subjected to 500 µmolm^{-2} s^{-1} (■),1000 µmolm^{-2} s^{-1} (Δ) and 2100 µmolm^{-2} s^{-1} (●) for 30, 60 and 120 minutes, in presence of lincomycin. Each point represents the average of 3 measurements ± s.e.

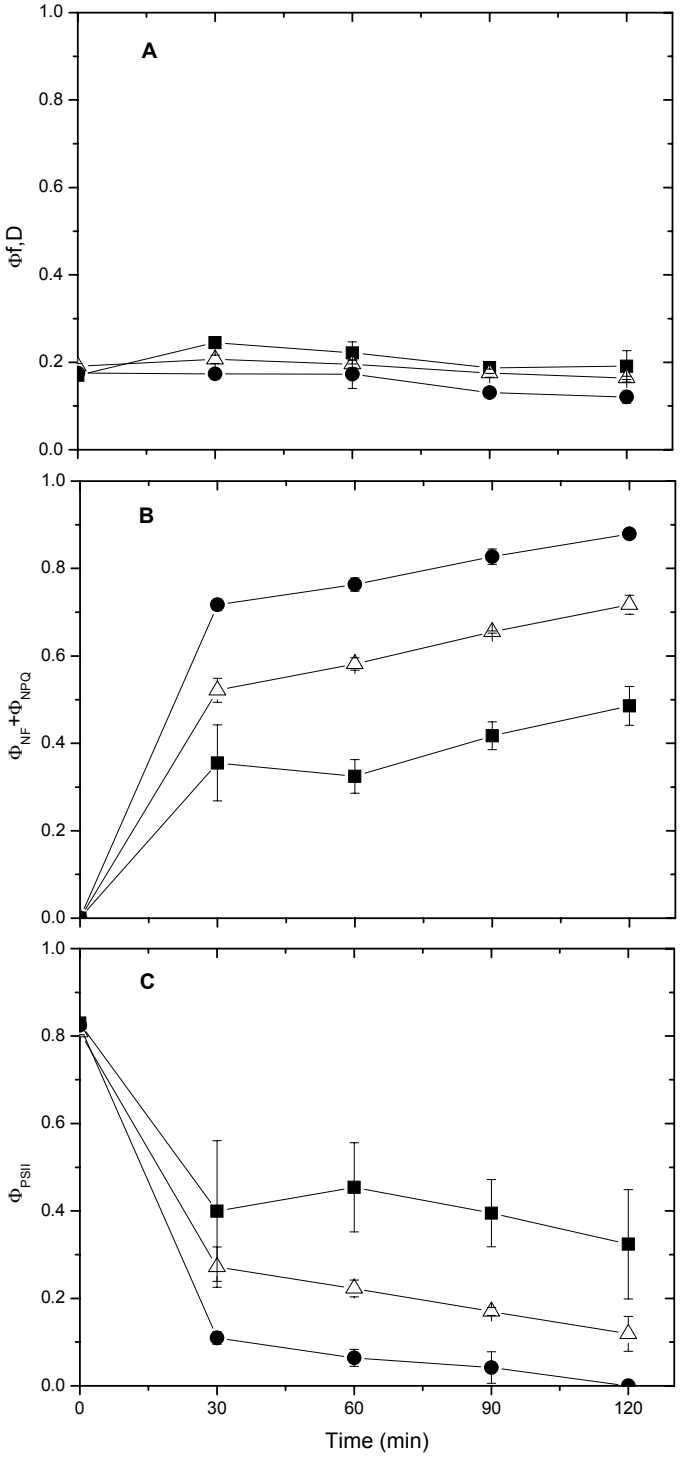

Fig. 2. Estimated absorbed energy fraction consumed via basal thermal and fluorescence dissipation (A), controlled and un-controlled Non Photochemical quenching (B) and photochemistry (C) in function of time of exposure with light treatment of 500 $\mu molm^{-2}\ s^{-1}$ (■),1000 $\mu molm^{-2}\ s^{-1}$ (Δ) and 2100 $\mu molm^{-2}\ s^{-1}$ (●) for 30, 60 and 120 minutes, in presence of lincomycin. Each point represents the average of 3 measurements ± s.e.

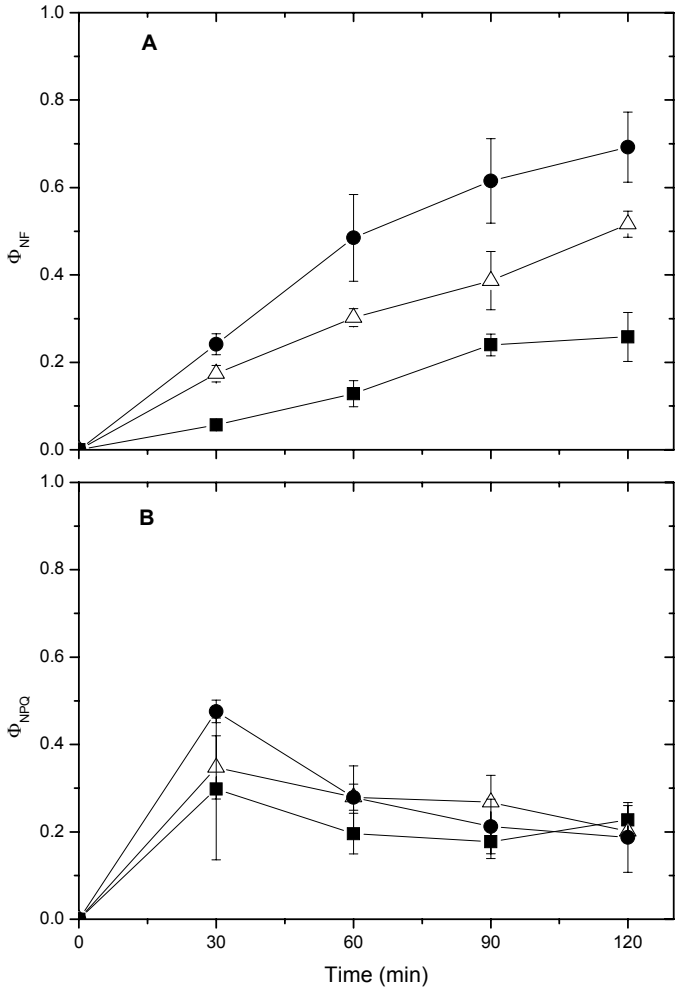

Fig. 3. Estimated absorbed energy fraction consumed via basal thermal dissipation associated with PSII damage (A) and thermal dissipation associated to pH dependent xanthophyll cycle (B) in function of time of exposure with light treatment of 500 $\mu molm^{-2}\ s^{-1}$ (■),1000 $\mu molm^{-2}\ s^{-1}$ (Δ) and 2100 $\mu molm^{-2}\ s^{-1}$ (●) for 30, 60 and 120 minutes, in presence of lincomycin. Each point represents the average of 3 measurements ± s.e.

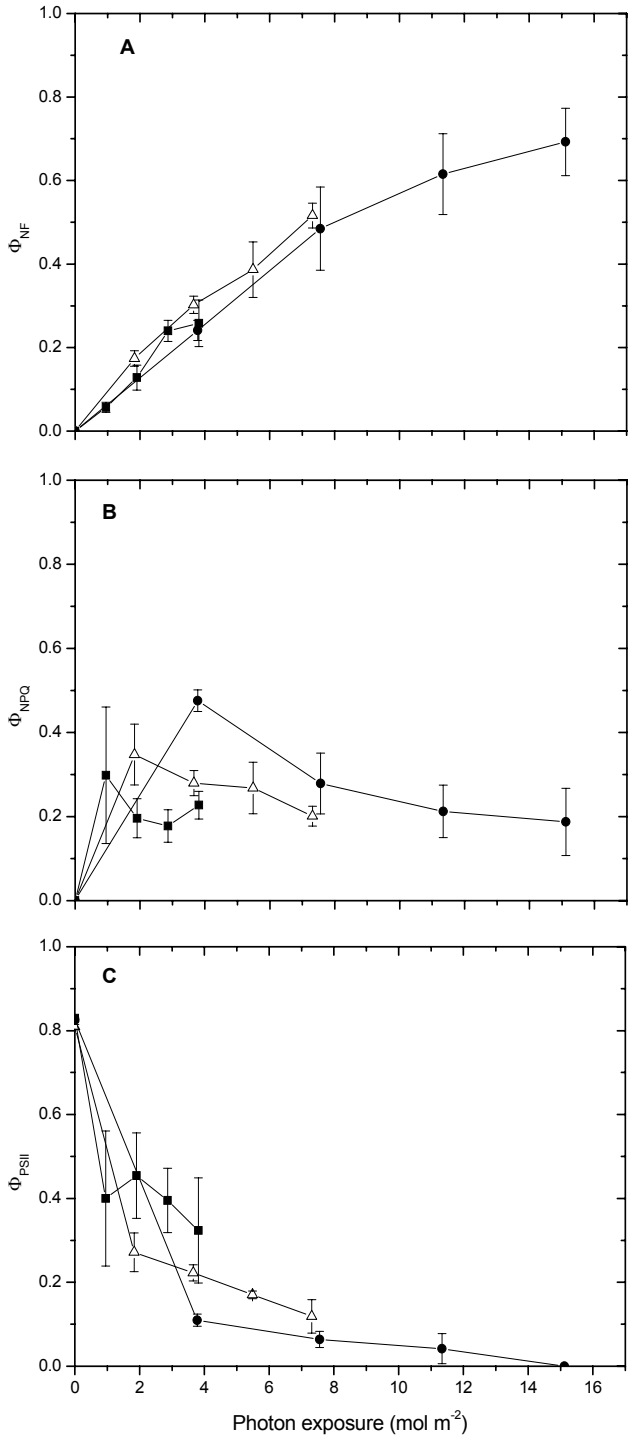

Fig. 4. Estimated absorbed energy fraction consumed via basal thermal dissipation associated with PSII damage (A), thermal dissipation associated to pH dependent xanthophyll cycle (B) and photochemistry (C) in function of photon exposure in peach leaves segments subjected to 500 μmolm^{-2} s^{-1} (■),1000 μmolm^{-2} s^{-1} (Δ) and 2100 μmolm^{-2} s^{-1} (●) for 30, 60 and 120 minutes, in presence of lincomycin. Each point represents the average of 3 measurements ± s.e.

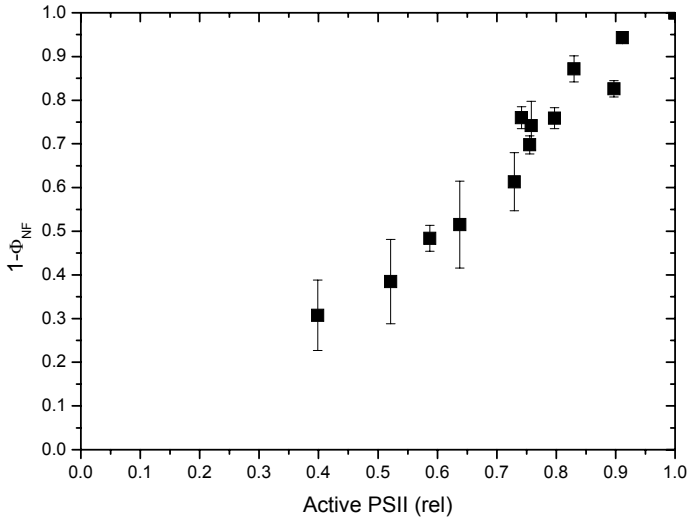

Fig. 5. Total energy dissipated by active PSII centers (1- ΦNF) plotted against the fraction of active PSII centers after various extents of photoinactivation. Each point represents the average of 3 measurements ± s.e.

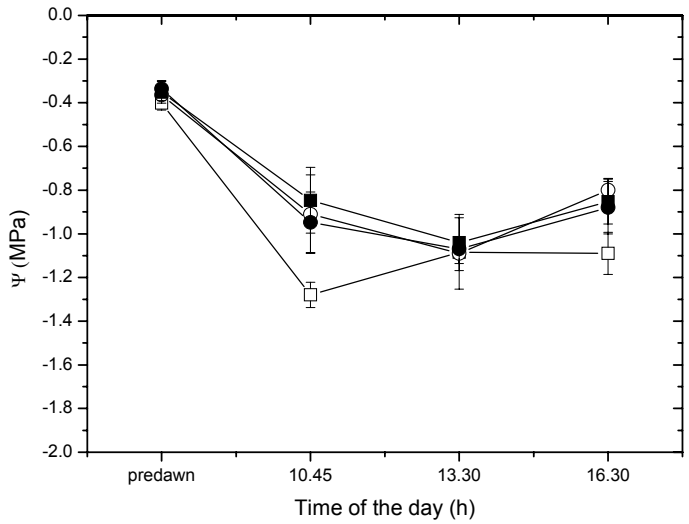

Fig. 6. Stem water potential pattern measured at predawn, morning, middle time of the day and afternoon in peach in highlight 100% watered (□), highlight 50% watered (○), shaded 100% watered (■) and shaded 50% watered (●). Each point represents the average of 3 measurements ± s.e.

Time	Trt	PPFD ($\mu molm^{-2}s^{-1}$)	P_n ($\mu molm^{-2}s^{-1}$)	g_s ($mol\ m^{-2}s^{-1}$)	WUE (µmol/mmol)	T_{air} (°C)
10.00	HLS	1800.33 a	17.67 a	0.25 b	3.44 a	30.5 b
	HLW	1801.33 a	18.43 a	0.33 a	2.77 b	31.1 a
	LLS	1050.33 b	19.77 a	0.27 b	3.12 ab	30.6 b
	LLW	1049.50 b	18.38 a	0.25 b	3.07 ab	30.5 b
13.30	HLS	1599.67 a	7.48 a	0.14 ab	2.13 b	31.3 a
	HLW	1599.00 a	10.20 a	0.17 a	2.69 ab	30.8 b
	LLS	849.67 b	8.22 a	0.10 b	3.27 a	29.3 c
	LLW	850.00 b	9.23 a	0.11 b	3.44 a	29.2 c
16.30	HLS	201.50 a	4.10 a	0.10 a	1.48 a	28.0 a
	HLW	201.67 a	3.14 a	0.07 a	1.74 a	28.2 a
	LLS	100.00 b	1.84 a	0.07 a	1.46 a	27.6 b
	LLW	100.00 b	2.43 a	0.08 a	1.48 a	28.2 a

Tab.1. Incident irradiance (PPFD), net photosynthesis (P_n), stomatal conductance (g_s), water use efficiency (WUE) and air temperature (T_{air}) measured on plants in highlight full watered (HLS), highlight 50% watered (HLW), moderate low light full watered (LLW) and moderate low light 50% watered (LLW) in 3 different time of the day on east side of canopy. For each time of the day values accompanied by different letters are statistically different at P= 0.05.

Time	Trt	J_{tot}	$J_{f.D}$	J_{NF}	J_{NPQ}	J_{PSII}	J_{NC}	J_{CO2}	J_R	J_{AT}
		($\mu molm^{-2}s^{-1}$)								
10.00	HLS	765.14 a	138.62 a	20.14 ab	451.01 a	155.36 a	84.70 a	70.67 a	60.93 b	23.77 ab
	HLW	765.57 a	130.43 a	25.32 a	435.26 a	174.56 a	100.83 a	73.73 a	58.64 b	42.18 a
	LLS	446.39 b	91.12 b	10.27 b	180.09 b	164.91 a	85.84 a	79.07 a	78.12 a	7.72 b
	LLW	446.04 b	91.27 b	13.40 b	179.72 b	160.63 a	87.13 a	73.50 a	72.19 a	14.95 b
13.30	HLS	679.86 a	107.76 a	3.81 b	463.57 a	104.72 a	74.82 a	29.91 a	27.10 a	47.72 a
	HLW	679.58 a	113.80 a	13.00 a	438.52 a	114.25 a	73.45 a	40.80 a	34.02 a	39.43 a
	LLS	361.11 b	60.73 b	5.98 ab	192.82 b	101.57 a	68.70 a	32.87 a	34.54 a	34.17 a
	LLW	361.25 b	68.81 b	8.38 ab	180.38 b	105.67 a	68.73 a	36.93 a	37.92 a	30.81 a
16.30	HLS	85.64 a	17.87 a	1.00 a	20.59 a	46.18 a	29.80 a	16.38 a	18.56 a	11.23 a
	HLW	85.71 a	16.71 a	1.48 a	20.18 a	47.34 a	34.79 a	12.55 a	16.73 a	18.07 a
	LLS	42.50 b	9.43 b	0.33 b	6.28 b	26.46 b	19.12 b	7.34 a	13.45 a	5.67 a
	LLW	42.50 b	8.64 b	0.88 b	5.80 b	27.18 b	17.48 b	9.70 a	14.98 a	2.50 a

Tab.2. Estimated energy partitioning consumed via various utilization and dissipation pathways on plants in highlight full watered (HLS), highlight 50% watered (HLW), moderate low light full watered (LLW) and moderate low light 50% watered (LLW) in 3 different time of the day on east side of canopy. For each time of the day values accompanied by different letters are statistically different at P= 0.05.

Time	Trt	PAR	P_n	g_s	WUE	T_{air}
		($\mu molm^{-2}s^{-1}$)	($\mu molm^{-2}s^{-1}$)	(mol $m^{-2}s^{-1}$)	(µmol/mmol)	(°C)
10.00	HLS	151.00 a	4.71 a	0.11 a	2.05 a	27.14 a
	HLW	150.67 a	5.65 a	0.13 a	1.87 a	26.72 b
	LLS	100.89 b	4.11 a	0.08 a	2.30 a	27.39 a
	LLW	101.00 b	3.87 a	0.11 a	1.85 a	27.46 a
13.30	HLS	1450.67 a	17.00 a	0.19 a	2.69 a	33.02 a
	HLW	1450.33 a	13.02 a	0.19 a	2.35 a	32.83 a
	LLS	898.67 b	7.17 b	0.11 b	2.45 a	31.49 a
	LLW	901.00 b	15.97 a	0.22 a	2.41 a	32.07 a
16.30	HLS	1649.67 a	7.92 a	0.13 b	2.11 b	33.59 a
	HLW	1650.50 a	11.89 a	0.23 a	2.14 b	32.84 b
	LLS	800.25 b	5.89 a	0.10 b	3.18 a	30.03 c
	LLW	801.67 b	9.32 a	0.13 b	2.94 a	32.10 c

Tab.3. Incident irradiance (PPFD), net photosynthesis (P_n), stomatal conductance (g_s), water use efficiency (WUE) and air temperature (T_{air}) measured on plants in highlight full watered (HLS), highlight 50% watered (HLW), moderate low light full watered (LLW) and moderate low light 50% watered (LLW) in 3 different time of the day on west side of canopy. For each time of the day values accompanied by different letters are statistically different at P= 0.05

Time	Trt	J_{tot}	$J_{f,D}$	J_{NF}	J_{NPQ}	J_{PSII} ($\mu molm^{-2}s^{-1}$)	J_{CO2}	J_{NC}	J_R	J_{AT}
10.00	HLS	64.18 a	15.33 a	0.11 a	8.40 a	40.34 a	18.83 a	21.52 a	19.24 a	2.28 a
	HLW	64.03 a	14.48 a	0.54 a	8.90 a	40.11 a	22.61 a	17.50 ab	21.49 a	-3.99 a
	LLS	42.88 b	8.95 b	-0.01 a	5.11 b	28.83 b	16.43 a	12.40 b	18.60 a	-6.20 a
	LLW	42.93 b	9.11 b	0.20 a	5.20 b	28.41 b	15.46 a	12.95 b	18.07 a	-5.11 a
13.30	HLS	616.53 a	118.42 a	13.52 a	331.72 a	151.38 a	68.00 a	83.38 a	92.74 a	-9.36 b
	HLW	616.39 a	110.03 a	16.62 a	345.53 a	144.21 a	52.08 a	92.13 a	52.98 bc	39.15 a
	LLS	381.93 b	68.27 b	7.96 b	193.52 b	112.18 a	28.69 b	83.49 a	29.68 c	53.81 a
	LLW	382.93 b	75.66 b	5.30 b	163.01 b	138.96 a	63.87 a	75.09 a	69.31 ab	5.79 b
1630.	HLS	701.11 a	115.06 a	31.03 a	439.91 a	115.11 ab	31.67 a	83.44 a	31.01 a	52.43 a
	HLW	701.46 a	116.78 a	28.02 a	429.28 a	127.39 a	47.57 a	79.82 a	38.04 a	41.77 a
	LLS	340.11 b	59.66 b	6.91 b	182.89 b	90.64 b	23.55 a	67.09 a	22.84 a	44.25 a
	LLW	340.71 b	64.81 b	3.76 b	162.36 b	109.78 ab	37.27 a	72.51 a	35.97 a	36.55 a

Tab.4. Estimated energy partitioning consumed via various utilization and dissipation pathways on plants in highlight full watered (HLS), highlight 50% watered (HLW), moderate low light full watered (LLW) and moderate low light 50% watered (LLW) in 3 different time of the day on west side of canopy. For each time of the day values accompanied by different letters are statistically different at P= 0.05.

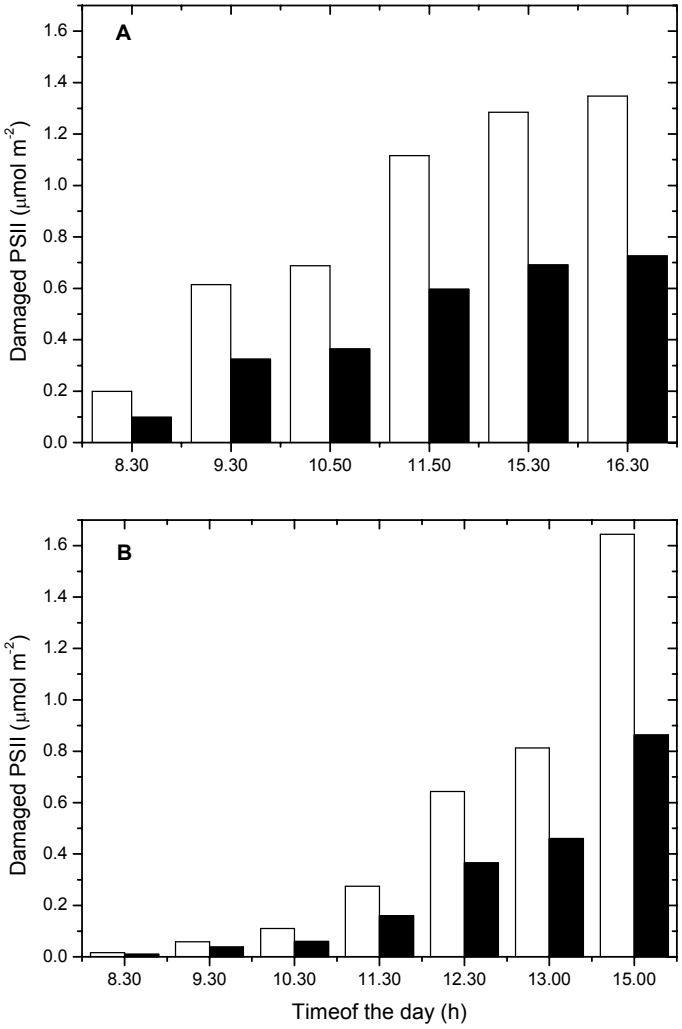

Fig. 7. Estimated PSII damage during the day of highlight (white bars) and shaded (black bars) samples on east (A) and west (B) side of canopy.

Chapter VI

GENERAL CONCLUSIONS

Using solar energy as fuel for life plant is intrinsically suicidal since the high constant photodamage risk. This dissertation would try to highlight the complex relation existing between plant, in particular peach, and light analysing the principal strategies plants developed to manage the incoming light for deriving the maximal benefits as possible minimizing the risks.

In the first instance the new method proposed for functional PSII determination based on P_{700} redox kinetics seems to be a valid, non intrusive, universal and field-applicable technique, even because it is able to measure in deep the whole leaf tissue rather than the first leaf layers as fluorescence. Fluorescence F_v/F_m parameter gives a good estimate of functional PSII but only when data obtained by ad-axial and ab-axial leaf surface are averaged. In addition to this method the energy quenching analysis proposed by Kornyeyev and Hendrickson (2007), combined with the photosynthesis model proposed by von Caemmerer (2000) is a forceful tool to analyse and study, even in the field, the relation between plant and environmental factors such as water, temperature but first of all light.

"Asymmetric" training system is a good way to study light energy, photosynthetic performance and water use relations in the field. At whole plant level net carboxylation increases with PPFD reaching a saturating point. Light excess rather than improve photosynthesis may emphasize water and thermal stress leading to stomatal limitation. Furthermore too much light does not promote net carboxylation improvement but PSII damage, in fact in the most light exposed plants about 50-60% of the total PSII is inactivated. At single leaf level, net carboxylation increases till

saturation point (1000 – 1200 μmolm^{-2}s^{-1}) and light excess is dissipated by non photochemical quenching and non net carboxylative transports. The latter follows a quite similar pattern of P_n/PPFD curve reaching the saturation point at almost the same photon flux density. At middle-low irradiance NPQ seems to be lumen pH limited because the incoming photon pressure is not enough to generate the optimum lumen pH for violaxanthin de-epoxidase (VDE) full activation. Peach leaves try to cope with the light excess increasing the non net carboxylative transports. While PPFD rises the xanthophyll cycle is more and more activated and the rate of non net carboxylative transports is reduced. Some of these alternative transports, such as the water-water cycle, the cyclic transport around the PSI and the glutathione-ascorbate cycle are able to generate additional H^+ in lumen in order to support the VDE activation when light can be limiting. Moreover the alternative transports seems to be involved as an important dissipative way when high temperature and sub-optimal conductance emphasize the photoinhibition risks.

In peach, a moderate water and light reduction does not determine net carboxylation decrease but, diminishing the incoming light and the environmental evapo-transpiration request, stomatal conductance decreases, improving water use efficiency. Therefore lowering light intensity till not limiting levels, water could be saved not compromising net photosynthesis. The quenching analysis is able to partition absorbed energy in the several utilization, photoprotection and photo-oxidation pathways. When recovery is permitted only few PSII remained un-repaired, although more net PSII damage is recorded in plants placed in full light. Even in this experiment, in over saturating light the main dissipation pathway is the non photochemical quenching; at middle-low irradiance it seems to be pH limited and other transports, such as photorespiration and alternative transports, are used to support photoprotection and to contribute for creating the optimal trans-thylakoidal ΔpH for violaxanthin de-epoxidase. These alternative pathways become the main quenching mechanisms at very low light environment.

Another aspect pointed out by this study is the role of NPQ as dissipative pathway when conductance becomes severely limiting.

The evidence that in nature a small amount of damaged PSII is seen indicates the presence of an effective and efficient recovery mechanism that masks the real photodamage occurring during the day. At single leaf level, when repair is not allowed leaves in full light are two fold more photoinhibited than the shaded ones. Therefore light in excess of the photosynthetic optima does not promote net carboxylation but increases water loss and PSII damage.

The more is photoinhibition the more must be the photosystems to be repaired and consequently the energy and dry matter to allocate in this essential activity. Since above the saturation point net photosynthesis is constant while photoinhibition increases it would be interesting to investigate how photodamage costs in terms of tree productivity. An other aspect of pivotal importance to be further widened is the combined influence of light and other environmental parameters, like water status, temperature and nutrition on peach light, water and phtosyntate management.

REFERENCES

Allen J.F., 1995. *Thylakoid protein phosphorylation, state 1-state 2 transitions, and photosystem stoichiometry adjustment: redox control at multiple levels of gene expression*. Physiol. Plant., 93: 196-205.

Anderson B., and Barber J., 1996. *Mechanisms of photodamage and protein degradation during photoinhibition of Photosystem II.* In: Photosynthesis and the environment. Baker NR. Ed. 1996: pp. 101-121.

Anderson J.M. and Aro E.M., 1994. *Grana stacking and protection in photosystem II in thylakoid membranes of higher plant leaves under sustained high irradiance: an hypothesis*. Photosynth. Res. 41: 315-326.

Anderson J.M., 1986. *Photoregulation of the composition, function and structure of thylakoid membranes*. Annu. Rev. Plant Physiol., 37: 93-136.

Anderson J.M., 2001. *Does functional Photosystem II complex have an oxygen channel?* FEBS Lett., 488: 1-4.

Anderson J.M., Park Y.-I. and W.S. Chow, 1997. *Photoinactivation and photoprotection of photosystem II in nature*. Physiol. Plant., 100: 214-223.

Anderson, J.M. and Chow, W.S., 2002. Structural and functional dynamics of plant Photosystem II. Phil. Trans. R. Soc. Lond. B 357: 1421-1430.

Anderson, J.M., 1999 I*nsights into the consequences of grana stacking in vascular plants: a personal perspective*. Aust. J. Plant Physiol. 26: 625-639.

Aro E.M., McCaffery S and Anderson J.M., 1994. *Recovery from photoinhibition in peas (Pisum sativus L.) acclimated to varying growth conditions*. Plant Physiol., 104: 1033-1041.

Aro E.M., McCaffery S. and Anderson J.M., 1994 *Recovery from photoinhibition in light- acclimated peas : role of D1 protein turnover*. Plant Physiol., 104: 1033-1041.

Aro E.M., Virgin I. and Anderson B., 1993. P*hotoinhibition of Photosystem II. Inactivation protein damage and turn over.* Biochim. Biophys. Acta, 1143: 113-134.

Artus N.N., Somerville S.C. and Somerville C.R., 1986. *The biochemistry and cell biology of photorespiration*. CRC Crit. Rev. Plant Sci., 4: 121-147.

Asada K., 1994. *Mechanisms for scavenging reactive molecules generated in chloroplasts under light stress.* In: Photoinhibition of Photosynthesis. Baker NR, Bowyer JR, eds. 1994.: pp. 129-142. From: Molecular Mechanisms to the Field. Oxford: BIOS Sci. Publ.

Asada K., 1999. *The water-water cycle*. Annu. Rev. Plant Physiol. Plant Mol. Biol. 50: 601-639.

Asada K., Heber U. and Schreiber U., 1992. *Pool size of electrons that can be donated to P_{700}^{+}, as determined in intact leaves: donation to P_{700}^{+} from stromal components via the intersystem chain*. Plant Cell Physiol., 33: 927-932.

Asada K., Heber U. and Schreiber U., 1993. *Electron flow to the intersystem chain from stromal components and cyclic electron flow in maize chloroplasts, as detected in intact leaves by monitoring redox changes of P_{700} and chlorophyll fluorescence*. Plant Cell Physiol., 34: 39-50.

Avenson T.J., Cruz J.A., and M. Kramer D., 2004. *Modulation of energy-dependent quenching of excitons in antennae of higher plants.* Proc. Natl. Acad. Sci., 101: 5530-5535.

Baker N.R. and Rosenqvist E., 2004. *Applications of chlorophyll fluorescence can improve crop production strategies: an examination of future possibilities*. J. Exp. Bot., Vol. 55, No 403: 1607-1621.

Barber J. and Andersson B., 1992. *Too much of a good thing: Light can be bad for photosynthesis.* Trends Biochem. Sci., 17: 61-66.

Barth C., Krause G.H. and Winter K., 2001. *Responses of photosystem I compared with photosystem II to high-light stress in tropical shade and sun leaves.* Pant, Cell and Environment, 24: 163-176.

Bertamini M. and Nedunchezhian N., 2004. *Photoinhibition and recovery of photosynthesis in leaves of Vitis berlandieri and Vitis Rupestris.* J. Plant Physiol., 161: 203-210.

Björkman O. and Demmig-Adams B., 1994. *Regulation of photosynthetic light energy capture, conversion, and dissipation in leaves of higher plants*. In Ecophysiology of Photosynthesis, ed. E.D. Schulze, MM Caldwell: pp. 17-47.

Blankership R.E. and Prince R.C., 1985. *Excited-state redox potential and the Z scheme of photosynthesis.* Trend. Biochem. Sci., 10: 382-383.

Bohning R.H. and Burnside C.A., 1956; *The effect of light intensity on rate of apparent photosynthesis in leaves of sun and shade plants*. Amer. J. of Bot., Vol. 43: 557-561.

Bohning R.H. and Burnside C.A., 1956; *The effect of light intensity on rate of apparent photosynthesis in leaves of sun and shade plants*. Amer. J. of Bot., Vol. 43:557-561.

Bottomley W., Spencer D. and Whitfeld P.R., 1974. *Protein synthesis in isolated spinach chloroplasts: comparison of light-driven and ATP-driven synthesis*. Archives of Biochemistry and Biophysics, 164: 106-117.

Bouvier F., D'Harlingue A., Hugueney P., Marin E., Marion-Poll A. and Camara B., 1996. *Xanthophyll biosynthesis: cloning, expression, functional reconstitution, and regulation of beta-cyclohexenyl carotenoid epoxidase from pepper (Capsicum annuum)*. J. Biol. Chem., 271: 28861-28867.

Bratt C.E., Arvidsson P.O., Carlsson M. and Åkerlund H.E., 1995. *Regulation of violaxanthin de-epoxidase activity by pH and ascorbate concentration*. Photosynth. Res., 45: 169-175.

Burrows F.J. and Milthorpe F.L., 1976. *Stomatal conductance in the control of gas exchange*. In Kozlowski T.T. (Ed.), Water Deficits and Plant Growth, vol. 4. Academic Press, New York.

Cailly A.L., Rizza F., Genty B. and Harbinson J., 1996 *Fate of excitation at PS II in leaves. The non-photochemical side*. Plant Physiol. Biochem. (special issue): 86.

Caruso T., Barone E. and Di Vaio C., 2000. *Factors affecting tree crop efficiency in young peach trees: rootstock vigour and training system*. Acta Hort., 557:193-197.

Chalmers D.J. and van den Ende B., 1989. *Tatura trellis peaches: productivity over fifteen years*. Acta Hort., 254: 303-306.

Cheng L. and Ma F., 2004. *Diurnal operation of the xanthophyll Cycle and the Antioxidant System in apple peel.* J. Amer. Soc. Hort. Sci., 129(3): 313-320.

Cheng L., Fuchigami L.H. and Breen P.J., 2000. *Light absorption and partitioning in relation to Nitrogen content in "Fuji" apple leaves*. J. Amer. Hort. Sci., 125(5): 581-587.

Cheng L., Fuchigami L.H. and Breen P.J., 2001; *The relationship between photosystem II efficiency and quantum yield for CO_2 assimilation is not affected by nitrogen content in apple leaves*. J. Exp. Bot., 52(362): 1865-1872.

Chow W. S**.**, Lee H.-Y., Park Y.-I., Park Y.-M., Hong Y.-N. and Anderson J. M., 2002. *The role of inactive photosystem II-mediated quenching in a last-ditch community defence against high-light stress* in vivo. Phil. Trans. Royal Soc., 357: 1441-1450.

Chow W.S., 1994. *Photoprotection and photoinhibitory damage*. In: Advances in Molecular and Cell Biology, ed. EE Bittar, J Barber, 10: 151-196.

Chow W.S., 2003. *Photosynthesis: from natural towards artificial*. J. Biol. Phys., 29: 447-459.

Chow W.S., Hope A.B. and Anderson J.M., 1989. O*xygen per flash from leaf disks quantifies photosystem II*. Biochim. Biophys. Acta, 973: 105-108.

Chow W.S., Hope A.B. and Anderson J.M., 1991. *Further studies on quantifying Photosystem II in vivo by flash-induced oxygen yield from leaf discs*. Aust. J. Plant Physiol., 18: 397-410.

Chow W.S., Lee H.-Y., He J., Hendrickson L., Hong Y.-N. and Matsubara S., 2005. *Photoinactivation of Photosystem II in leaves*. Photosynth. Res., 84: 35-41.

Chow WS, Hope AB (2004a) Electron fluxes through Photosystem I in cucumber leaf discs probed by far-red light. Photosynth. Res. 81: 77-89

Chow WS, Hope AB (2004b) Kinetics of reactions around the cytochrome *bf* complex studied in intact leaf disks. Photosynth. Res 81: 153-163

Chow WS, Hope AB, Anderson JM (1988) Variable stoichiometries of photosystem II to photosystem I reaction centres. Photosynth. Res 17: 277-281

Chow, W.S. and Aro, E.M.,2005 *Photoinactivation and Mechanisms of Recovery*. In: Photosystem II: The Light Driven Water/Plastoquinone OxidoReductase. T Wydrzynski and K Satoh (eds). pp 627-648.

Corelli Grappadelli L. and Magnanimi E., 1993. *A whole-tree system for gas-exchange studies*. HortScience., 28:41-45.

Corelli Grappadelli L., Giovannini D., and Ravaglia R., 1996. *Tipi di foglie e loro ruolo nella crescita dei frutti e nella produttività in pesci a diverso habitus vegetativo*. Proc. "Progetto Finalizzato Frutticoltura – Agro.Bio.Fruit". Cesena (Italy) 10-11 May: 148-149.

Corelli Grappadelli L., Sansavini S., Stefanelli D., Asinelli A. and Gaddoni M., 2000. F*orme di allevamento ed epoche di potatura del pesco per la bassa pianura padana*. Proc. XXIII Convegno Peschicola, Ravenna (Italy), 12 - 13 September 1997: 111-119.

Corelli Grappadelli, L. and Magnanini E., 1997. *Whole-tree gas exchanges: can we do it cheaper?* Acta Hort., 451:279-285.

Corelli-Grappadelli L. and Lakso A.N., 2007. *Is maximizing Orchard light interception always the best Choice?* Proceeding of the eight International Symposium on Canopy, Rootstocks and Environmental Physiology in Orchard Systems. Acta Hort., 732: 507-518.

Dau H., 1994. *Molecular mechanisms and quantitative models of variable photosystem II fluorescence*. Photochem. Photobiol., 60: 1-23.

Demmig-Adams B, Adams W.W. III, Barker D.H., Logan B.A., Bowling D.R. and Verhoeven A.S., 1996. *Using chlorophyll fluorescence to assess the fraction of absorbed light allocated to thermal dissipation of excess excitation*. Physiol. Plant., 98: 253-264.

Eaglesham A.R.J. and Ellis R.J., 1974. *Protein synthesis in chloroplasts II. Light-driven synthesis of membrane proteins by isolated pea chloroplasts*. Biochimica et Biophysica Acta, 335: 396-407.

Edwards G.E. and Baker N.R., 1993. *Can CO_2 assimilation in maize leaves be predicted accurately from chlorophyll fluorescence analysis?* Photosynth. Res., 37: 89-102.

Escalona J.M., Flexas J. and Medrano H., 1999; *Stomatal and non-stomatal limitations of photosynthesis under water stress in field-grown grapevines*. Aust. J. Plant Physiol. 26: 421-433.

Evans J.R., 1996. *Developmental constraints on photosynthesis: effects of light and nutrition*. In: *Photosynthesis and the environment*. N.R. Baker ed., Kluwer Academic Publishers, Dordrecht, The Nederlands: pp. 281-304.

Fan D.-Y., Hope A.B., Smith P.J., Jia H., Pace R.J., Anderson J.M. and Chow W.S., 2008. *The stoichiometry of the two photosystems in higher plants revisited*. Biochim. Biophys. Acta, in press.

Farquhar G.D. and Sharkey T.D., 1982. *Stomatal conductance and photosynthesis*. Ann. Rev. Plant Physiol., 33: 317-345.

Farquhar G.D., von Caemmerer S. and Berry J.A., 1980. *A byochemical model of photosynthetic CO_2 assimilation in leaves of C_3 species*. Planta, 149: 78-80.

Flexas J., Bota J., Escalona J.M., Sampol B.e Medrano H., 2002. *Effects of drought on photosynthesis in grapevines under field conditions: an evaluation of stomatal and mesophyll limitations*., Funct. Plant Biol., 29: 461-471.

Flexas J., Briantais J.M., Cerovic Z., Medrano H. and Moya I., 2000. *Steady-state and maximum chlorophyll fluorescence responses to water stress in grapevine leaves: a new remote sensing system*. Remote Sens. Environ., 73:283-297.

Flore J.A. and Lakso A.N., 1988. *Envirormental and physiological regulation of photosynthesis in fruit crops.* Hort. Rev, 11: 111-157.

Foyer C.H., 1995. *Free radical process in plants.* 65th Meeting held at the University of Aberden, 18-21 December 1995.

Foyer C.H: e Harbinson J., 1994. *Oxygen metabolism and the regulation of photosynthetic electron transport*. In: *Causes of photooxydative stress and amelioration of defence systems in plants.* Ed. CH. Foyer. PM. Mullineaux: pp. 1-42.

Galmés J., Abadia A., Cifre J., Medrano H. and Flexas J., 2007; *Photoprotection processes under water stress and recovery in Mediterranean plants with different growth forms and leaf habits*. Physiol. Plant. 130: 495-510.

Gaudillere J.P. and Moing A., 1992; *Photosynthesis of peach leaves: light adaptation, limiting factors and sugar content*. Proceeding of PEACH XXIII Acta Hort. 315: 103-109.

Genty B., Briantais J.M. and Baker N.R., 1989. *The relationship between the quantum yield of photosynthetic electron transport and quenching of chlorophyll fluorescence*. Biochem. Biophys. Acta., 990: 87-92.

Gilmore A.M., 1997. *Mechanistic aspects of xanthophyll cycle-dependent photoprotection in higher plant chloroplasts and leaves*. Physiol. Plant., 99: 197-209.

Gindaba J. and Wand S.J.E., 2007. *Climate-ameliorating measures influence photosynthetic gas exchange of apple tree*. Annals of Applied Biology, 150: 75-80.

Giuliani R., Magnanini E., Fragassa C., Nerozzi F., 2000. *Ground monitoring the light-shadow windows of a tree canopy to yield canopy light interception and morphological traits*.
Plant, Cell and Environment, 23 (8): 783-796.

Glenn D.M., Erez A., Puterka G.J. and Gundrum P., 2003. Particle films affect carbon assimilation and yield in "Empire" apple. J. Amer. Soc. Hort. Sci., 128(3): 356-362.

Glenn D.M., Puterka G.J., Drake S., Unruh T.R., Knight A.L., Baherle P., Prado E. and Baugher T., 2001. *Particle film application influences apple leaf physiology, fruit yield and fruit quality*. J. Amer. Soc. Hort. Sci., 126: 175-181.

Glenn D.M., Puterka G.J., vanderZwet T., Byers R.E. and Feldhake C., 1999. *Hydrophobic particle films: A new paradigm for suppression of arthropod pests and plant disease*. J. Econ. Entom., 92: 759-771.

Govindjee, 1995. *Sixty three years since Kautsky: chlorophyll a fluorescence.* Aust. J. Plant Physiol., 22: 131-160.

Greer D.H. and Halligan A.E., 2001; *Photosynthetic and fluorescence light responses for kiwifruit (Actinidia deliciosa) leaves at different stages of development on vines grown at two different photon flux densites*. Aust. J. Plant Physiol. 28: 373-382.

Greer D.H., 2001; *Photon flux density dependence of carbon acquisition and demand in relation to shoot growth of kiwifruit (Actinidia deliciosa) vines grown in controlled environments*. Aust. J. Plant Physiol. 28: 111-120.

Grossman Y.L. and DeJong T.M., 1998. *Training and pruning system effects on vegetative growth potential, light interception, and cropping efficiency in peach trees*. J. Amer. Soc. Hort. Sci,. 123(6): 1058-1064.

Guerriero R., Loreti F., Morini S. and Natali S., 1980. *Eight years of observations on a peach double-row planted orchard.* Acta Hort., 114:362-382.

Halliwell B. and Gutteridge J.M.C., 1984 *Oxygen toxicity, oxygen radicals, transition metals and disease*. Biochem. J., 219: 1-14.

Harbinson J. and Hedley C.L., 1989. *The kinetics of P_{700}^{+} reduction in leaves: a novel in situ probe of thylakoid functioning*. Plant, Cell and Environment. 12: 357-369.

Havaux M., Strasser R.J., Greppin H., 1991. *A theoretical and experimental analysis of the qP and qN coefficients of chlorophyll fluorescence quenching and their relation to photochemical and non photochemical events*. Photosynth. Res., 27: 41-55.

He J. and Chow W.S., 2003. *The rate coefficient of repair of Photosystem II after photoinactivation*. Physiol. Plant., 118: 297-304.

Heber U. and Walker D., 1992. *Concerning a dual function of coupled cyclic electron transport in leaves*. Plant Physiol., 100: 1621-1626.

Heber U., Bligny R., Streb P. and Douce R, 1996. *Photorespiration is essential for the protection of the photosynthetic apparatus of C3 plants against photoinactivation under sunlight*. Bot. Acta, 109:307-315.

Hendrickson L., Förster B., Pogson B.J. and Chow W.S., 2005. *A simple chlorophyll parameter that correlates with the rate coefficient of photoinactivation of Photosystem II*. Potosyn. Res., 84: 43-49.

Hendrickson L., Furbank R.T. and Chow W.S., 2004. *A simple alternative approach to assessing the fate of absorbed light energy using chlorophyll fluorescence*. Photosynth. Res., 82: 73-81.

Hikosaka K., Kato M. and Hirose T., 2004. *Photosynthetic rates and partitioning of absorbed light energy in photoinhibited leaves*. Physiol. Plant., 121: 699-708.

Horton P., Ruban A.V. and Walters R.G., 1996. *Regulation of light harvesting in green plants*. Ann. Rev. Plant Physiol. Plant Mol. Biol., 47: 655-684.

Hughes J.L., Smith P., Pace R. and Krausz E., 2006. *Charge separation in photosystem II core complexes induced by 690-730 nm excitation at 1.7 K*. Biochim. Biophys. Acta 1757: 841-851

Hutton R.J., Mc Fadyen L.M. and Lill W.J., 1987. *Relative productivity and yield efficiency of canning peach trees in three intensive growing systems*. HortScience, 22: 552-560.

Iacono F. and Sommer K.J., 1999; *The measurement of chlorophyll fluorescence as a tool to evaluate the photosynthetic performance of grapevine leaves*. Acta Hort. 493: 31-44.

Jarvis P.G., 1976. *The interpretation of the variations in leaf water potential and stomatal conductance found in canopies in the field*. Phil. Trans. R. Soc. Lond., B 273: 593-610.

Jifon J.L. and Syvertsen J.P., 2003. *Kaolin particle film application can increase photosynthesis and water use efficiency of "Ruby Red" grapefruit leaves.* J. Amer. Soc. Hort. Sci,. 128(1): 107-112.

Joliot P. and Joliot A., 2002. *Cyclic electron transfer in plant leaf*. Proc. Nat. Acad. Sci., 99: 10209-10214.

Jones L.W. and Kok B., 1966. *Photoinhibition of chloroplast reactions. Kinetics and action spectra*. Plant Physiol., 41: 1037-1043.

Kaiser W.M., 1979. *Reversible inhibition of the Calvin cycle and activation of oxidative pentose phosphate cycle in isolated intact chloroplasts by hydrogen peroxide.* Planta 145: 377-382.

Kappel F. and Flore J.A., 1983; *Effect of shade on photosynthesis, specific leaf weight, leaf chlorophyll content and morphology of young peach trees*. J. Amer. Soc. Hort. Sci. 108(4): 541-544.

Keren N., Gong H and Ohad I., 1995. *Oscillation of reaction center II-D1 protein degradation in vivo induced by repetitive light flashes*. J. Biol. Chem., 270: 806-814.

Kim S.-J., Lee C.-H., Hope A.B. and Chow W.S., 2001. *Inhibition of Photosystems I and II and enhanced back flow of Photosystem I electrons in cucumber leaf discs chilled in the light*. Plant Cell Physiol., 42: 842-848.

Kitajima M. and Butler W.L., 1975. *Quenching of chlorophyll fluorescence and primary photochemistry in chloroplasts by dibromothymoquinone*. Biochim. et Biophys. Acta, 376: 105-115.

Klughammer C. and Schreiber U., 1998. *Measuring P_{700} absorbance changes in the near infrared spectral region with a dual wavelength pulse modulation system*. In: Garab G (ed) Photosynthesis: Mechanisms and Effects, Vol. V. Kluwer Academic Publishers, Dordrecht, the Netherlands, pp 4357-4360.

Knox J.P. and Dodge A.D., 1985 *Singlet oxygen and plants*. Phytochemistry, 24: 889-896.

Koller, 1990. *Light-driven leaf movement.* Plant Cell and Environ., 13: 615-632.

Komenda J. and Barber J., 1995. *Comparison of psbO and psbH deletion mutants of Synechocystis PCC 6803 indicates that degradation of D1 protein is regulated by the Q_B site and dependent on protein synthesis*. Biochemistry, 34: 9625-9631.

Kornyeyev D. and Hendrickson L., 2007. *Energy partitioning in photosystem II complexes subjected to photoinhibitory treatment*. Funct. Plant Biol., 34: 214-220.

Krall, J.P. and Edwards G.E., 1992. *Relationship between photosystem II activity and CO_2 fixation in leaves*., Physiol. Plant., 86: 180-187.

Kramer D.M., Johnson G., Kiirats O. and Edwards G.E., 2004. *New fluorescence parameters for the determination of Q_A redox state and excitation energy fluxes*. Photosynth. Res., 79: 209-218.

Krause G.H. and Weis E., 1991. *Chlorophyll fluorescence and photosynthesis: the basics*. Annual Review of Plant Physiology and Plant Molecular Biology, 42: 313-349.

Krieger-Liszkay A., 2005. *Singlet oxygen production in photosynthesis*. Journal of Experimental Botany, Vol. 56, No. 411: 337-346.

Kühlbrandt W., Wang D.N. and Fujiyoshi Y., 1994. *Atomic model of plant light-harvesting complex by electron crystallography*. Nature, 367: 614-621.

Lakso A.N., 1994. *Apple*. In: Handbook of environmental physiology of fruit crops. B.S.Schaffer and P.C. Anderson (eds). CRC Press, Boca Raton. Volume 1: 3-42.

Lee H.Y., Chow W.S. and Hong Y.N., 1999. *Photoinactivation of Photosystem II in leaves of Capsicum annuum*. Physiol. Plant., 105: 377-384.

Lee H.-Y., Hong Y.-N., Chow W.S., 2001. *Photoinactivation of photosystem II complexes and photoprotection by non-functional neighbours in Capsicum annuum L. leaves*. Planta, 212: 332-342.

Lindahl M., Spetta C., Hundal T., Oppenheim A.B., Adam Z. and Andersson B., 2000. *The Thylakoid FtsH Protease Plays a Role in the Light-Induced Turnover of the Photosystem II D1 Protein*. The Plant Cell, 12: 419-431.

Long S.P., Humphries S. and Falkowski P.G.,1994. *Photoinhibition of photosynthesis in nature*. Annu. Rev. Plant Mol. Biol., 45: 633-662.

Loreti F., Massai R. and Morini S., 1989. *Further observations on high density nectarine plantings*. Acta Hort., 243:353-360.

Losciale P., Oguchi R., Hendrickson L. Hope, A. B. Corelli-Grappadelli L. and Chow W. S**.,** 2007. *A rapid, whole-tissue determination of the functional fraction of Photosystem II after photoinhibition of leaves based on flash-induced P_{700} redox kinetics*. Physiol. Plant., 132: 23-32.

Massonnet C., Costes E., Rambal S., Dreyer E. and Regnard J.L., 2007.*Stomatal regulation of photosynthesis in apple leaves: evidence for different water-use strategies between two cultivars*. Ann. of Bot., 100: 1347-1356.

Matsubara S. and Chow W.S., 2004. *Population of photoinactivated Photosystem II reaction centers characterized by chlorophyll a fluorescence lifetime in vivo*. Proc. Natl. Acad. Sci. USA, 101: 18234-18239.

Matsubara S., Naumann M., Martin R., Nichel C., Rascher U., Morosinotto T., Bassi R., and Osmond. B., 2004. *Slowly reversible de-epoxidation of lutein-epoxide in deep shade leaves of a tropical tree legume may 'lock-in' lutein-based photoprotection during acclimation to strong light*. J. Exp. Bot. Vol. 56, No. 411: 461-468.

Mattoo A.K. and Edelman M., 1987. *Intramembrane translocation and posttranslational palmitoylation of the chloroplast 32-kDa herbicide-binding protein*. Proc. Natl. Acad. Sci. USA, 84: 1497-1501.

Mattoo A.K., Hoffman-Falk H., Marder J.B. and Edelman M., 1984. *Regulation of protein metabolism: coupling of photosynthetic electron transport to in vivo degradation of the rapidly metabolized 32-kilodalton protein of the chloroplast membranes*. Proc. Natl. Acad. Sci. USA, 81: 1380-1384.

Maxwell K. and Johnson G.N., 2000. *Chlorophyll fluorescence: a practical guide*. J. Exp. Bot., Vol. 51 No 345: 659-668.

Melis M., Spangfort M. and Andersson B., 1987. *Light-absorption and electron transport balance between Photosystem II and Photosystem I in spinach chloroplasts*. Photochem. Photobiol., 45: 129-136.

Miller G.W., Huang I.J., Welkie G.W. e Pushnik J.C., 1995. *Functions of Iron in plants with special emphasis on chloroplasts and photosynthetic activity*. In: *Iron nutrition in soils and plants*. J.Abadià ed. Kluwer Accademic, Boston: pp. 19-28.

Monteith J.L., 1977. *Climate and the efficiency of crop production in Britain*. Phil. Trans. R. Soc. Lond. B., 281: 277-294.

Morosinotto T, Caffarri S, Dall'Osto L and Bassi R., 2003. *Mechanistic aspects of the xanthophyll dynamics in higher plant leaves.* Physiol. Plant., 119: 347-354.

Müller P., Li X. and Niyogi K.K., 2001. *Non-Photochemical Quenching. A Response to Excess Light Energy*. Plant Physiol., 125: 1558-1566.

Nagy L., Bálint E., Barber J., Ringler A., Cook K.M. and Maróti P., 1995. Photoinhibition and law of reciprocity in photosynthetic reaction of Synechocystis sp. PCC6803. J. Plant Physiol., 145: 419-415.

Naor A., Klein I. and Doron I., 1995. *Stem water potential and apple size*. J. Amer. Soc. Hort. Sci., 120: 577-582.

Nixon P.J., Barker M., Boehm M., de Vries R. and Komenda J., 2005. *FtsH-mediated repair of the photosystem II complex in response to light stress*. J. Exp. Bot., Vol. 56, No. 411: 357-363.

Niyogi K.K., 1999. *Photoprotection revisited: genetic and molecular approaches*. Ann. Rev. Physiol. Plant Mol. Biol., 50: 333-359.

Niyogi K.K., Li X., Rosenberg V. and Jung H., 2004. *Is PsbS the site of non-photochemical quenching in photosynthesis?* J. Exp. Bot., Vol. 56, No. 411: 375-382.

Nobel P.S., 1983. *Biophysical plant physiology and ecology*. W.H. Freeman and Company, N.Y (eds).

Noctor G. and Foyer C.H. 1998. *Ascorbate and glutathione: keeping active oxygen under contro.* Annu. Rev. Plant Physiol. Plant Mol. Biol., 49: 249-279.

Nuzzo V., Dichio B. and Xiloyannis C., 2002. *Canopy development and light interception in peach trees trained to Transverse Y and Delayed Vase in the first four years after planting*. Acta Hort., 592:405-412.

Oguchi R., Hikosaka K. and Hirose T., 2005; *Leaf anatomy as a constraint for photosynthetic acclimation: differential responses in leaf anatomy to increasing growth irradiance among three deciduous trees*. Plant Cell and Environment 28: 916-927.

Ohad I., Keren N., Zer H., Gong H. and Mor T.S., 1994. *Light-induced degradation of the photosystem II reaction centre D1 protein in vivo: an integrative approach.* In: Photoinhibition of Photosynthesis. Baker NR, Bowyer JR, eds. 1994.: pp. 161-167. From: Molecular Mechanisms to the Field. Oxford: BIOS Sci. Publ.

Öquist G. and Chow, W.S., 1992. *On the relationship between the quantum yield of Photosystem II electron transport, as determined by chlorophyll fluorescence and the quantum yield of CO_2-dependent O_2 evolution*. Photosynth. Res*.,* 33**:** 51-62.

Ort D., 2001. *When there is too much light.* Plant Physiol., 125: 29-32.

Osmond C.B., 1981. Photorespiration and photoinhibition: some implication for the energetics of photosynthesis. Biochim. Biophys. Acta, 639: 77-98.

Owens T.G., 1996. *Processing of excitation energy by antenna pigments.* In: Photosynthesis and the environment. Baker NR. Ed. 1996: pp. 1-23.

Palmer J.W., 1980; *Computed effects of spacing on light interception and distribution within hedgerow trees in relation to productivity*. Proceeding of Symposium on Research and Development on Orchard and Plantation Systems. Acta Hort., 114: 80-88.

Papageorgiou G.C., Govindjee (eds) (2004) Chlorophyll a Fluorescence. A Signature of Photosynthesis. Springer, Dordrecht, The Netherlands, ISBN: 1-4020-3217-X

Park Y.-I., Anderson J.M. and Chow W.S., 1996. *Photoinactivation of functional photosystem II and D1-protein synthesis in vivo are independent of the modulation of the photosynthetic apparatus by growth irradiance*. Planta, 198: 300-309.

Park Y.-I., Chow W.S. and Anderson J.M., 1995. *Light inactivation of functional PSII in leaves of peas grown in moderate light depends on photon exposure*. Planta, 196: 401-411.

Park Y.I., Chow W.S. and Anderson J.M., 1997. *Antenna size dependency of photoinactivation of Photosystem II in light-acclimated pea leaves*. Plant Physiol. 115: 151-157.

Pastenes C., Porter V., Baginsky C., Horton P. and Gonzalez J., 2003; *Paraheliotropism can protect water-stressed bean (Phaseolus vulgaris L.) plants against photoinhibition*. J. Plant Physiol. 161: 1315-1323.

Powles S.B., 1984; *Photoinhibition of photosynthesis induced by visible light*. Ann. Rev. Plant Physiol. 35: 15-44.

Raveh E., Choen S., Raz T, Yakir D., Grava A. e E.E. Goldschmidt, 2003. *Increased growth of young citrus trees under reduced radiation load in semi-arid climate*. J. of Exp. Bot., Vol 54, No 381: 365-373.

Roháček K., 2002. *Chlorophyll fluorescence parameters: the definitions, photosynthetic meaning, and mutual relationships*. Photosynthetica, 40: 13-29.

Sauer K., 1975. *Primary events and the trapping of energy.* In: Biogenetics of photosynthesis. Govindjee, ed.: pp.116-181.

Schatz G.H., Brock H. and Holzwarth A.R. 1988. *Kinetic and energetic model for the primary processes in Photosystem II*. Biophys J., 54: 397-405.

Schultz H.R., 1996. *Leaf absorptance of visible radiation in Vitis vinifera L: estimates of age and shade effects with a simple field method*. Sci. Hort., 66: 93-102.

Schulze E.D., 1986. *Carbon dioxide and water vapour exchange in response to drought in the atmosphere and the soil*. Ann. Rev. Plant Physiol., 37: 247-274.

Seaton G.G.R. and Walker D.A., 1990. *Chlorophyll fluorescence as a measure of photosynthetic carbon assimilation*. Proc. R. Soc. Lond., B 242: 29-35.

Smirnoff N., 1996. *The function and metabolism of ascorbic acid in plants*. Ann. Bot. 78: 661-669.

Sun Z.-L., Lee H.-L., Matsubara S., Hope A.B., Pogson B.J., Hong Y.-N. and Chow W.S., 2006. *Photoprotection of residual functional photosystem II units that survive illumination in the absence of repair, and their critical role in subsequent recovery*. Physiol. Plant., 128: 415-424.

Telfer A., Dhami S., Bishop S.M., Phillips D. and Barber J., 1994. *βcarotene quenches singlet oxygen formed by isolated photosystem II reaction centers*. Biochemistry, 33: 14469-14474.

Tyystjärvi E. and Aro E.M., 1996. *The rate constant of photoinhibition, measured in lincomycin-treated leaves, is directly proportional to light intensity*. Proc. Natl. Acad. Sci. USA, 93: 2213-2218.

von Caemmerer, 2000. *Biochemical models of leaf photosynthesis*. Techniques in plant sciences No 2. CSIRO Publishing (Australia). ISBN: 64306379X.

Walters R.G. and Horton P., 1993. T*heoretical assessment of alternative mechanisms for non-photochemical quenching of PSII fluorescence in barley leaves*. Photosynth. Res., 36:119-39.

Weis E. and Berry J.A., 1987. *Quantum efficiency of Photosystem II in relation to 'energy'-dependent quenching of chlorophyll fluorescence*. Biochim. Biophys. Acta, 894: 198-208.

Whitmarsh J., Samson G. and Poulson M., 1994. *Photoprotection in photosystem II: the role of cytochrome b559*., In: Photoinhibition of Photosynthesis. Baker NR, Bowyer JR, eds. 1994.: pp. 75-93. From: Molecular Mechanisms to the Field. Oxford: BIOS Sci. Publ.

Yamane Y., Shikanai T., Kashino Y., Koike H. and Satoh K., 2000. *Reduction of Q_A in the dark: Another cause of fluorescence Fo increased by high temperatures in higher plants*. Photosynth. Res., 63: 23-34.